

ELUCIDATING THE HIPPOCAMPAL DOPAMINERGIC SUBPROTEOME WITH
NOVEL BIOORTHOGONAL TECHNIQUES

Thesis by
Jennifer Jin Lee Hodas

In Partial Fulfillment of the Requirements
for the Degree of
Doctor of Philosophy

California Institute of Technology

Pasadena, California

2010

(Defended September 25, 2009)

© 2010

Jennifer J. L. Hodas

All Rights Reserved

ACKNOWLEDGEMENTS

First and foremost, I would like to thank my advisor, Professor Erin M. Schuman. I admire her infectious passion for science and her boundless curiosity and creativity. She has been more than my academic advisor—she has been such a fantastic role model for me, both inside and outside the lab. I used to always wonder if anyone could have a successful career, a family life, and be an interesting person all at the same time. Yup, that's Erin, and it's attainable. She could see beyond my odd sense of humor and encouraged me to explore whatever I found to be interesting. Wherever she would be in the world, she would always take the time to answer all of my questions and ensure that I had all of the resources I needed to be successful. I hope that I've made her proud and that she'll remember me for years to come. In the very least, I hope that the 4'x4' poster of her helps to remind her of my time in her lab!

I am so grateful to the members of my thesis committee: Professors Pamela J. Bjorkman, Raymond J. Deshaies, and Henry A. Lester. They have provided me with valuable guidance over the years and would suggest so many interesting directions where I could take my work. I would always wish after my annual meetings that I had a mini-lab of my own, a few more hands, or more hours in the day to explore everything. I guess the last alternative is to stay as graduate student, but... you know how that goes.

Next I have to thank Dr. Daniela Dieterich. I am so grateful that she took a leap of faith and agreed to take on a rotation student back in 2005. Little did I know at the time that my postdoc mentor would become one of my closest friends. Dani introduced me to the feline technologies that would impact my work, but also to all things German, every Trader Joe's product worth consuming, and the principle of dancing to the music when

times got tough. She challenged my scientific abilities, supported me through some difficult times, and would always be there to laugh and have fun. Even from halfway around the world, she continues to be such a dear and dedicated friend. I just wish she lived closer! (Maybe it'll happen when that big Californian earthquake occurs.)

Thanks to the past and present members of the Schuman Lab. Everyone has made these last few years a growing experience and I wish everyone the best on their future endeavors. There are a few individuals I couldn't have lived without. The espresso machine—it fueled me for years, giving me that extra pep to do that one more experiment, and has been the lab's central lifeline. Lin Chen—she provided not only gorgeous neuronal preps, taught me how to make them, and provided so much support and even more laughs, but also loves shoes as much as I do. Though I never accompanied her to pilates, she never held it against me and nevertheless ate lunch with me. Flora Hinz—my fellow food person of the purchased and homemade varieties. Dr. Iván Cajigas—another food fanatic who would correct my Spanish so patiently and would always be there to listen. Flora and Iván would always know what would make me happy... lunch at 11:30 am or earlier! Ana María Lust—she was always the quiet support I could count on. She's always been there for me and never hesitated to ask if she could help me with anything at all. Finally, I have to thank my lab mother, Alana Rathbun. She deserves a new paragraph.

Alana is another person who started as “just another” lab member, but became a dear, close friend whom I will have for the rest of my life. She is part amazing administrative assistant, part therapist, part lab mom, and 100% awesome. Alana and her

family have provided me with so many happy times and unconditional support. They've virtually adopted me as they have with so many, and I am so grateful that I met them.

Thank you to some other people around Caltech. Professor David A. Tirrell and folks in the Tirrell lab—Dr. Rebecca Connor, Dr. Jamie Link, Dr. Janek Szychowski, Dr. Stacey Maskarinec, and John Ngo—they provided me with so many useful suggestions, incredible knowledge, and endless support. My extended lunch crowd—Julie Cho, KJ Tiffany Chang, Oliver Losón, and Anh Pham. Ernie and his truck people—your tacos dorados and spinach quesadillas kept me going. All of the friends that I have made during my time here—I can't name all of you because I'm scared of missing someone, but you all know who you are.

Another big thank you goes out to Ruddock House. Becoming a Resident Associate was one of the best decisions I have made in my life. Somehow being an off-campus RA now doesn't measure up to the craziness and sleep-deprivation that drove me to be a more efficient person in the lab. All of you have made an impact on my life, and I cherish all of the laughs and tears that we have shared. Be good, don't burn the House down, and remember to take down those holiday lights.

Many thanks to the Hodas and Oken families. Since I first met them in March 2005, they have all been endless sources of personal and scientific support for me. I am so fortunate to have such a warm and loving family. I am especially grateful to David and Judy Hodas for their caring phone calls and emails and for encouraging their son to pursue science and find his way to Caltech.

An enormous thank you goes to my family for giving me the opportunities throughout my life that have shaped who I am today. My parents, Ted and Vicki Lee,

always knew that I liked science, but encouraged me to explore other interests so I wouldn't become a total geek. I like to think that I can blend into a crowd of "normal" people due to their efforts. My brother, Jeff Lee, for being supportive now that he's over that "torment my big sister" phase. They all obliged and let me run off to Yale for four years and welcomed me back to California when I decided to go to Caltech. I hope that I've made them proud so far and that I continue to make them proud in the future.

Even though she can't read this (or has never let on that she can), thank you to my cat, Lanikai. As she did as a kitten during my senior year of college, she has caringly/stubbornly sat between my keyboard and me as I wrote this thesis. She has never wavered in her love for me/her food and has made my life full of laughs and meows.

When I started graduate school, I never would have imagined that the experience would change my life. I expected to buckle down, keep my nose to the grindstone... forget about smelling all of those roses. Instead, I have met so many amazing people, had so many life-changing experiences, and, as a result, grown immensely as an individual. I have really grown up at Caltech—I met a guy, got engaged, got married, and now am expecting a baby. Had you told me that all of these major life events would have happened during my time here, I wouldn't have believed a word of it. This thesis is dedicated to this guy—Nathan O. Hodas. He's shown me so much love and support over the years and is the love of my life. I could go on and on, but in short: his sheer brilliance, strength, and quirkiness will keep me intrigued and happy for many, many years to come. I love you so much and thank you for putting up with my cooking.

ABSTRACT

Both synaptic and behavioral plasticity require *de novo* protein synthesis. Dopamine is a critical neuromodulator, and abnormalities in dopaminergic regulation underlie disorders like Parkinson's disease, Alzheimer's disease, and schizophrenia—diseases that impair the ability of the brain to perform complex processes, including the formation and retrieval of memories. The stimulation of D1/D5 dopaminergic receptors in the hippocampus is critical for protein synthesis-dependent long-term potentiation (LTP), a process important for long-term synaptic plasticity and memory. The proteins synthesized upon activation of dopaminergic pathways, the dopaminergic subproteome, however, remain unknown.

Here, we describe the development of two sister technologies that employ bioorthogonal chemistry to effectively and specifically identify and visualize a proteome in an unbiased, nontoxic manner. In both bioorthogonal noncanonical amino acid tagging (BONCAT) and fluorescent noncanonical amino acid tagging (FUNCAT), we utilize methionine surrogates, either azidohomoalanine (AHA) or homopropargylglycine (HPG), which are conjugated via [3+2] copper (I)-catalyzed cycloaddition to either a biotin or fluorescent molecule-bearing probe. We demonstrate the utility of these methods by showing that both AHA and HPG can be used to examine two temporally distinct protein populations. Furthermore, we visualize the dendrite-specific contribution to the neuronal proteome by taking advantage of the spatial control achievable by FUNCAT. We then combine these techniques to address the question of the identity of the proteins in the specifically dendritic subproteome of the hippocampus. We confirm that upon stimulation with a D1/D5 dopamine receptor-specific agonist, there are significantly

increased levels of protein synthesis in dendrites when compared to unstimulated dendrites. By utilizing a combination of these novel methods and more traditional techniques, we are able to provide the first comprehensive list of the dopaminergic dendritic subproteome of the hippocampus. These data suggest that the initial stages of D1/D5 receptor activation lead to the translation of proteins that may play a role in synaptic strengthening.

TABLE OF CONTENTS

ACKNOWLEDGEMENTS.....	iii
ABSTRACT	vii
TABLE OF CONTENTS	ix
LIST OF ILLUSTRATIONS.....	xi
ABBREVIATIONS USED.....	xiii
Chapter I	1
INTRODUCTION	1
Synaptic plasticity	2
Protein synthesis in learning and memory.....	3
Dopamine and its involvement in neurodegenerative disease	6
The development and use of bioorthogonal chemistry	11
Conclusion	16
Chapter II.....	18
DEVELOPMENT OF A NOVEL STRATEGY FOR THE IDENTIFICATION OF NEWLY SYNTHESIZED PROTEINS IN A COMPLEX MIXTURE.....	18
Review of proteomic sample preparations	19
The development of bioorthogonal noncanonical amino acid tagging	21
Mass spectrometry of BONCAT-prepared samples.....	24
BONCAT as a reliable method for studying the proteome	28
Chapter III.....	31
USING FLUORESCENT NONCANONICAL AMINO ACID TAGGING (FUNCAT) FOR THE VISUALIZATION OF LOCAL DENDRITIC PROTEIN SYNTHESIS.....	31
General uses of FUNCAT	34
Specificity of FUNCAT to visualize new protein synthesis.....	35
FUNCAT in different cell types.....	37
Exploring the possibility of labeling two different epochs of protein synthesis	39
Temporal sensitivity of FUNCAT	41
The effects of BDNF on neuronal proteome dynamics.....	43
Chapter IV	49
DEVELOPMENT OF DISULFIDE-BEARING PROBE FOR IMPROVING BONCAT	49
Synthesis and use of biotinylated disulfide alkyne and azide probes	52
Pre-alkylation abolishes background signal and prevents disulfide exchange	53
Click chemistry reaction of AHA and HPG with their respective disulfide-bearing probes is comparable	56
AHA and HPG are incorporated into proteins at similar rates	57
Chapter V.....	60
ELUCIDATING THE DENDRITIC DOPAMINERGIC SUBPROTEOME IN THE HIPPOCAMPUS USING BONCAT	60

SKF81297 produces an increase in dendritic protein synthesis in hippocampal neurons	62
Isolating the dendritic compartment.....	63
The use of ¹³ C –arginine instead of d ₁₀ -leucine in BONCAT	65
BONCAT for dendritic slices	66
Bioinformatics processing and criteria.....	67
The hippocampal dopaminergic subproteome.....	69
Chapter VI	72
DISCUSSION AND FUTURE DIRECTIONS.....	72
Use of bioorthogonal chemistry in biological applications	73
Development of a disulfide-bearing alkyne probe	75
AHA versus HPG for BONCAT experiments.....	76
Development of FUNCAT	77
Visualization of locally dendritic proteomes using FUNCAT	78
Elucidating the hippocampal dopaminergic subproteome.....	79
Future directions.....	80
Work Cited	82
APPENDIX.....	96
Materials and Methods	97
Publication (Dieterich et al., 2007)	107

LIST OF ILLUSTRATIONS

Figure 2.1. The BONCAT strategy for labeling, detection, and identification of newly synthesized proteins.	22/23
Figure 2.2. Structure of biotin-FLAG-alkyne probe and AHA-based modifications.....	24
Figure 2.3. Dot blot analysis of AHA versus methionine-treated samples.....	26
Figure 2.4. Western blot analysis of AHA versus Met-treated sample purification fractions.....	29
Figure 3.1. Chemical components and FUNCAT procedure.	33/34
Figure 3.2. Visualization of newly synthesized proteins with FUNCAT in dissociated primary hippocampal neurons.	36
Figure 3.3. Visualization of newly synthesized proteins with FUNCAT in organotypic hippocampal cultures.....	38/39
Figure 3.4. Sequential labeling of newly synthesized proteins with two metabolic markers.	40/41
Figure 3.5. Time-course for the detection of newly synthesized proteins in somata and dendrites.....	42/43
Figure 3.6. BDNF-induced increases in protein synthesis.....	44/45
Figure 3.7. The methionyl tRNA synthetase MetRS and the amino acid transporter LAT1 are present in dendrites.....	46
Figure 3.8. BDNF-induced increase in dendritic protein synthesis.....	47/48
Figure 4.1. Synthesis and application of disulfide-bearing tags for click chemistry.....	53
Figure 4.2. Alkylation prior to click chemistry reaction significantly reduces non-specific protein labeling.....	55
Figure 4.3. Click chemistry of AHA or HPG yield the similar reaction efficiencies..	56/57
Figure 4.4. E. coli incorporates azidohomoalanine and homopropargylglycine into newly synthesized protein at comparable rates.....	58

Figure 5.1. SKF81297 stimulation produced an increase in newly synthesized proteins in the distal dendrites.....	63
Figure 5.2. Transwell culture system for the isolation of the dendritic compartment.....	64
Figure 5.3. Microdissection of a dendritic segment from an acute hippocampal slice....	65
Figure 5.4. Schematic summary of three complete MudPIT experiments.....	69
Figure 5.5. Confirmation of candidate proteins via Western blot.....	71

ABBREVIATIONS USED

¹³C-Arg: ¹³C-arginine

β-Me: β-mercaptoethanol

aCSF: Artificial cerebrospinal fluid

AHA: Azidohomoalanine

ANL: Azidonorleucine

BDNF: Brain-derived neurotrophic factor

BONCAT: Bioorthogonal noncanonical amino acid tagging

cAMP: Cyclic adenosine monophosphate

d₁₀-Leu: d₁₀-leucine

DIV: Days *in vitro*

DST: Disulfide tag

EPSCs: Excitatory postsynaptic currents

FLA: 5'-carboxyfluorescein-PEO₈-azide

FUNCAT: Fluorescent noncanonical amino acid tagging

GFP: Green fluorescent protein

HA: Hemagglutinin

HAP1A: Huntingtin-associated protein 1A

HBS: HEPES-buffered saline

HEK: Human embryonic kidney

HibA: HibernateA media

HPG: Homopropargylglycine

ICAT: Isotope coded affinity tagging

LTP: Long-term potentiation

MAP2: Microtubule-associated protein 2

mEPSCs, or minis: Miniature excitatory postsynaptic currents

MudPIT: Multidimensional protein identification technique

ORF: Open reading frame

PBS: Phosphate-buffered saline

PEO: Polyethylene oxide

PKA: Protein kinase A

RNA: Ribonucleic acid

RT: Room temperature

SILAC: Stable isotope labeling by amino acids in cell culture

TPP: Trans-Proteomic Pipeline

TRA: TexasRed-PEO₂-alkyne

VTA: Ventral tegmental area

Chapter I

INTRODUCTION

Synaptic plasticity

Structural and functional changes in the brain are often the result of synaptic plasticity. Synaptic plasticity refers to the strengthening and weakening of synapses in response to stimuli, such as neurotransmitters and electrical impulses. The idea of synaptic plasticity was initially proposed by Donald Hebb. He stated that the repeated and persistent stimulation of the presynaptic cell resulting in firing of the postsynaptic cell would produce a lasting strengthening of the connection between them (Hebb, 1949). Since then, there have been many different terms for the types of synaptic plasticity that can occur. The primary form of plasticity that is thought to represent a cellular basis for learning and memory is long-term potentiation (LTP).

As the name implies, LTP describes a long-lasting increase in synaptic strength. This phenomenon was first observed by Terje Lømo in 1966 in the rabbit hippocampus, published in 1973 as “long-lasting potentiation” (Bliss and Lømo, 1973), and rebranded as long-term potentiation soon thereafter (Douglas and Goddard, 1975). It was first observed *in vivo*. Following high frequency stimulation, the excitatory postsynaptic potentials (EPSPs) elicited by stimulation of presynaptic axons were enhanced for periods of one hour to days. Since then, the link between LTP and learning has been established in a variety of species. Even in a simple system, such as the sea slug *Aplysia*, there is synaptic plasticity that takes place after long-term facilitation to enable basic learning (Montarolo et al., 1986). In mammals, the hippocampus has been implicated as a major structure in the establishment of learning and memory. This was demonstrated with spatial memory tasks in rats, in which the rats failed to exhibit long-term memory when LTP was blocked using a N-methyl-D-aspartate (NMDA) receptor antagonist

(Morris et al., 1986). The importance of the hippocampus has also been demonstrated in humans, particularly in studies involving the patient H.M. who had part of his temporal lobe removed in an attempt to alleviate seizures and then suffered severe anterograde amnesia (Milner, 1959; Corkin et al., 1997).

LTP continues to be a topic of interest in neuroscience, whether it is to determine its local influences on subcellular processes using modern techniques (e.g., Engert and Bonhoeffer, 1999) or to chart molecular effects on the makeup of the neuron. On a molecular level, it has been demonstrated that enduring LTP—required for the establishment of some types of long-term memory— is both transcription and translation dependent (Krug et al., 1984; Frey et al., 1988; Huang and Kandel, 1994; Nguyen et al., 1994). These observations prompted the investigation of RNA and proteins that may contribute to synaptic function and plasticity.

Protein synthesis in learning and memory

The hunt for the molecular basis of memory has brought the focus to the proteins that are synthesized within neurons, particularly in the hippocampus. The first evidence for a role of new protein synthesis in memory was the observation that the injection of the protein synthesis inhibitor puromycin in the temporal lobe of mice resulted in severe memory deficits in a spatial learning task (Flexner et al., 1963). Though this result could have been attributed to the nonspecific effects of the protein synthesis inhibitor, subsequent work shows that memory tasks in a variety of species are dependent upon protein synthesis

(reviewed in Davis and Squire, 1984). The question then turned to where these proteins were being synthesized in the neuron, and how they would find their way to the sites of synaptic contact. Though all protein translation was thought to take place in the soma, recent work has suggested the existence of local protein synthesis occurring in the dendrites.

The first evidence that suggested the existence of ribosomes outside of the soma came from electron micrograph images from monkey motoneuron preparations that showed ribosomal particles in the proximal region of the dendrites that featured synapse-like protrusions (Bodian, 1965). Later, other electron micrograph images revealed the presence of polyribosomes in the distal dendrites in neurons from the dentate gyrus (Steward and Levy, 1982). Even in biochemical preparations specific for isolating synapses, a number of groups saw the incorporation of radiolabeled amino acids into protein (Rao and Steward, 1991; Weiler and Greenough, 1991; Torre and Steward, 1992). In addition, ³H-leucine-labeled proteins were observed in hippocampal dendrites after just three minutes (Feig and Lipton, 1993), casting doubt on the idea that proteins are solely synthesized in the soma and trafficked to the most distal parts of the dendrites. This opened up the possibility that there could be a local protein translation response instead of a neuron-wide translation activation event that would require new protein trafficking from the cell body to the dendrites—a distance that can be up to 400 microns.

The evidence of polyribosomes centralized at synapses during synaptogenesis suggests that local protein synthesis might play a key role in synaptic expansion and growth (Steward and Falk, 1986). The first evidence causally bridging local protein

synthesis and long-term synaptic enhancement was shown in hippocampal slices stimulated with brain-derived neurotrophic factor (BDNF) (Kang and Schuman, 1996), a neurotrophin required for normal neuronal development (Ernfors et al., 1995). More recently, polyribosomes have been observed to redistribute from the base of synapses into the spines upon tetanic stimulation in rat hippocampal slices (Ostroff et al., 2002; Bourne et al., 2007). The presence of polyribosomes that become mobilized after LTP suggests their role in providing a relatively quick translational response at synapses. However, there still was doubt that there was translation and also mRNA strictly compartmentalized to the dendrites (and axons).

The ability for acute hippocampal slices to survive and maintain synaptic transmission after microdissection of the soma from the dendrites allowed for the demonstration of local dendritic protein synthesis. One of the first examples of this preparation showed the necessity of protein synthesis for CA3-CA1 transmission after cell bodies in the CA1 region in rat hippocampus were separated from dendrites (Kang and Schuman, 1996). Also, in some cases, there is a specific requirement for dendritic, but not somatic, protein synthesis in long-term depression (Huber et al., 2000). Furthermore, there is recent visual evidence of local dendritic protein synthesis. Using a two-surface cell culture system, Torre and Steward were able to observe, via autoradiographic analysis, the incorporation of isotope-labeled amino acid into protein selectively in the dendrites, even when the cell bodies were removed (Torre and Steward, 1992). This was followed by the visualization of GFP-tagged proteins, in both physically and optically isolated dendrites in culture that was inhibited by protein synthesis inhibitors (Aakalu et

al., 2001; Job and Eberwine, 2001). Finally, the local application of protein synthesis inhibitors in acute slices has also been shown to inhibit LTP (Bradshaw et al., 2003), thus showing the importance of the dendritic protein synthesis to synaptic function. Local protein synthesis is now believed to be one major mechanism by which synapses ensure the specificity of synaptic strength and acquire the necessary protein components for maintaining long-term synaptic plasticity (Kang et al., 1997; Schuman, 1999).

As a result, a new line of research into the regulation and identity of these dendritic proteins has emerged. This has extended into determining the mRNAs and proteins that are localized in synaptoneuroosomes and their relative concentrations (Miller et al., 2002; Zhong et al., 2006). There has also been work to determine the overall proteome of transgenic animals with compromised translational regulation or the proteome induced by a specific chemical stimulus (e.g., Liao et al., 2007; Liao et al., 2008), but none of these address the local proteome that is specifically synthesized in the dendrites. The work described below attempts to solve this problem by utilizing novel methodology coupled with the spatial specificity needed to elucidate the dendritic proteome within the hippocampus.

Dopamine and its involvement in neurodegenerative disease

Across a wide range of species, the neurochemicals responsible for signaling and synaptic function are conserved. One of these, dopamine, is a biogenic amine that came into its own a few decades ago. Prior to that time, dopamine was believed to simply be a precursor to norepinephrine and epinephrine, but it was Arvid Carlsson who established

its importance as a signaling molecule in 1957 (Carlsson et al., 1957). It has since been categorized as a catecholamine neurotransmitter and neuromodulator with innervation in a number of cerebral structures. As a neuromodulator, it exerts peripheral effects by either enhancing or depressing effects of other neurotransmitters. In this capacity, dopamine aids to modulate a myriad of functions, such as hormone secretion, renal function, and the release of other catecholamines.

Dopamine is primarily associated with reward and addiction mechanisms, but it is also important for the establishment of memories. First glimpses of dopaminergic innervation in the brain came with the advent of Falck fluorescence, which revealed dopamine-containing neurons to be in the brainstem with projections to the hypothalamus, limbic cortex, and striatum (Dahlstrom and Fuxe, 1964). Since then, dopamine has been found to innervate the human brain in four major pathways: (1) nigrostriatal, which extends from the substantia nigra to the striatum; (2) tubuloinfundibular, hypothalamus to pituitary gland; (3) mesocortical, ventral tegmental area to the cortex; and (4) mesolimbic, ventral tegmental area (VTA) to many parts of the limbic system, such as the hippocampus. Only recently has dopamine been directly implicated to play a major role in hippocampal function. There is a strong presence of dopaminergic fibers in particular substructures within the hippocampus, namely the subiculum, hilus, and stratum lacunosum moleculare (Gasbarri et al., 1994; Goldsmith and Joyce, 1994; Gasbarri et al., 1996). The physical connection from the VTA to the hippocampus was initially thought to be through the prefrontal cortex, but recent evidence suggests that the nucleus accumbens and ventral pallidum are actually the

structures involved (Floresco et al., 2001). Electrophysiology experiments in rats demonstrate that dopaminergic projections extend through the subiculum into the nucleus accumbens, which then stimulates the VTA (Legault et al., 2000). Furthermore, this projection pattern is confirmed by an observed increase in dopamine in the nucleus accumbens upon the presentation of novel stimuli (Ihalainen et al., 1999) or stimulation of the subiculum (Wood and Rebec, 2004). Even recent functional magnetic resonance imaging (fMRI) studies of the mesolimbic system note the connection between reward-mediated learning and memory formation, thus suggesting that this is a dopamine-dependent process (Adcock et al., 2006; Wittmann et al., 2005).

Since the hippocampus is the primary center for the establishment and maintenance of memories, a variety of learning tasks have been utilized to demonstrate a behavioral link to dopamine signaling. Evidence of dopamine's role has been demonstrated using conditioning and memory tasks in both simple and more advanced species. In the sea slug *Aplysia*, the application of dopamine to a neuron responsible for memory and reward behavior yielded the same result as after an operant conditioning task (Brembs et al., 2002). In aging rats, which have impaired long-term potentiation, there were significant improvements in spatial memory tasks when drugs specific for the dopamine signaling pathway were applied (Bach et al., 1999). Finally, the administration of dopamine pathway activating drugs in aging primates can improve their working memory abilities, even up to one year after the end of the drug treatment (Castner and Goldman-Rakic, 2004). In humans, impairments in dopamine signaling have also been suggested to be responsible for age-related cognitive decline (Volkow et al., 1998; Backman and Farde,

2001; Nieoullon, 2002).

Treatments for problems in dopamine signaling have also been important in the amelioration of a variety of neurological disorders with working memory deficits, such as schizophrenia (Goldberg et al., 1991; Abi-Dargham et al., 2002), Attention Deficit Hyperactivity Disorder (ADHD; Levy and Farrow, 2001; Nieoullon, 2002) and Parkinson's disease (Schmidt et al., 1985; Rinne et al., 2000; Cools et al., 2002; Madras et al., 2005; Smeyne and Jackson-Lewis, 2005). The cause and treatment of these disorders may be explained by molecular phenomena. For example, Bernabeu and colleagues (1997) found that the inhibition of D1/D5 dopamine receptors resulted in amnesia, while their activation enhanced memory consolidation in rats. Also, antagonists against these same types of dopamine receptors were shown to be effective antipsychotic drugs, potentially for the treatment of schizophrenia (Andersen et al., 1992).

There are currently five known classes of dopamine receptors, D1 through D5, all of which are seven-domain transmembrane proteins. They are divided into two major groups, D1-like and D2-like receptors, depending upon their G-protein-linked effector molecules. The D1-like receptor class consists of D1 and D5 (also known as D1b) receptors, while the D2-like receptor class is made up of D2, D3, and D4 receptors. These two classes serve alternate functions. The D1/D5 receptors are involved in the upregulation of the cAMP-regulated pathway via $G_s\alpha$, which has been linked to slow synaptic transmission (Greengard, 2001). D1/D5 receptors activation results in the activation of adenylate cyclase, which regulates the production of cAMP. A few of cAMP's downstream effectors are protein kinase A (PKA), cAMP-responsive element

binding protein (CREB), and the DARPP-32/PP-1 pathway. PKA and CREB have both been identified as contributors to synaptic plasticity (Lonze and Ginty, 2002; Nguyen and Woo, 2003; Waltereit and Weller, 2003). On the other hand, the D2-like receptor class downregulates the same pathway via $G_i/G_{o\alpha}$ and also controls calcium and potassium channels (Missale et al., 1998). Together, these dopaminergic receptors work to modulate the activity of the excitatory N-methyl-D-aspartate (NMDA) class of glutamatergic receptors, which are involved in the development of working memory (Wang, 1999). Interestingly, recent work has also suggested the D1-like dopaminergic receptors may influence NMDA receptor activity by direct protein-protein interactions (Lee et al., 2002).

D1/D5 receptors are present in the striatum, dentate gyrus, and the prefrontal cortex (Smiley et al., 1994; Bergson et al., 1995; Swanson-Park et al., 1999; Khan et al., 2000). The D1 receptor is the most abundant dopaminergic receptor in the mammalian brain. However, the D5 receptor, though less widespread than D1, is found in higher concentrations in select regions of the brain, such as the hippocampus (Tiberi et al., 1991; Meador-Woodruff et al., 1992; Laurier et al., 1994; Sokoloff and Schwartz, 1995). The D1 and D5 receptors share roughly 80% homology in their transmembrane domains and also feature two N-glycosylation sites and a serine- and threonine-rich C-terminus. An important cysteine residue is located in the beginning of the C-terminus and is crucial in G protein signaling (O'Dowd, 1993). G proteins allow for a cascade of signaling to occur, such as the glycosylation of CREB, a protein that has recently been implicated to be a key in regulating synaptic plasticity (Lamarre-Vincent and Hsieh- Wilson, 2003).

The requirement of D1/D5 receptor activity for L-LTP and L-LTD has been observed by a number of different groups (Frey et al., 1991; Frey et al., 1993; Huang and Kandel, 1995; Matthies et al., 1997; Swanson-Park et al., 1999; Sajikumar and Frey, 2004). While there is a clear link between dopamine signaling and memory, not much work has been done to elucidate the protein products of D1/D5 receptor activation. Previous work demonstrated the upregulation of surface expression of GluR1, an AMPA receptor subunit, following dopamine stimulation in cultured hippocampal neurons (Smith et al., 2005). Despite this, the identities of the proteins affected by the activation of the D1/D5 receptors in the hippocampus are still largely unknown.

The development and use of bioorthogonal chemistry

Many methods have been developed over the years to study the behavior of individual biomolecules in an identity-specific manner. The most notable breakthrough was the introduction of green fluorescent protein (GFP), which can be genetically encoded to produce a fusion protein to track a particular substrate of interest (Tsien, 1998; Lippincott-Schwartz and Patterson, 2003). Since the introduction of GFP, there has been an entire spectrum of fluorescent proteins developed (Zhang et al., 2002), allowing for the simultaneous visualization of different proteins. However, this method does not necessarily demonstrate endogenous protein activity, as it involves the overexpression of the proteins of interest, thus potentially altering protein synthesis and degradation pathways. The interactions among proteins are often tightly regulated and only occur when there is a critical concentration of them present in the environment. In addition, the

fusion of GFP can often alter the functionality, localization, and expression of the protein of interest, due to steric hindrance, protein misfolding, or sheer bulkiness. Finally, GFP and its siblings are solely limited to monitoring proteins. They cannot be used to observe the activity and expression of glycans, lipids, and nucleic acids, or post-translational modifications. Luckily, there are other methods that allow for the observation of these other biomolecules.

Another technique that is often used is antibody-based labeling. This approach can be customized for both the recognized epitope as well as for the overall experimental purpose, whether it is for visualization or purification. This method can be coupled with the previously described genetic modification of the protein of interest to be fused to GFP, a FLAG peptide, or poly-histidine. These options allow for the use of commercially available antibody products against these commonly used substrates. However, antibodies can also be generated to specifically recognize the protein of interest, thus ensuring that the endogenous protein population is solely being monitored. For the visualization aspect of this technique, the antibodies can be conjugated to a variety of different fluorescent molecules, such as fluorescent dyes (like the Alexa dye series) or quantum dots. Quantum dots have recently become more widely used particularly for single molecule tracking experiments because they are resistant to photobleaching and available in a wide spectrum of colors. Previously, there was an issue with their intermittent blinking which would make it difficult to measure the trajectories of individual molecules, but the recent development of a non-blinking dots has the potential to make this a more powerful tool (Wang et al., 2009). Though the quantum dot allows for the live imaging of surface molecules, its overall size (ranging from 5-50 nanometers

in diameter, depending upon the color) can limit its use for the monitoring of intracellular events as it is too large to cross the cell membrane. In addition, all of these various techniques are limited since they can only monitor a predetermined protein target, either for initial detection by an antibody-based method or genetic modification for establishment of a fusion protein, and the target epitope must be readily accessible. For a top-down experimental approach, a more inclusive method is necessary, particularly one that would have minimal perturbation to the cellular system for the study of endogenous processes.

Bioorthogonal chemistry incorporates noncanonical forms of various cellular building blocks that bear chemical groups that are not readily found in the system of interest. To visualize or biochemically purify these labeled biomolecules, the novel chemical handles are conjugated to probes that can bear fluorescent dyes, quantum dots, or small molecular probes, such as poly-histidine or biotin. The overall benefit of utilizing bioorthogonal chemistry is its ability to be incorporated into the biomolecules of the cell with minimal perturbation. While the previously described methods, such as GFP, have proven to be useful, they often introduce a steric hindrance problem or an increase in protein expression, which ultimately alters the cell's metabolism. By using bioorthogonal chemistry, we are able to obtain a more accurate representation of the various cellular processes.

A few chemical reporters have been established and utilized in different applications over the past couple of decades in both prokaryotes and eukaryotes alike, with further developments on the horizon. One early example of bioorthogonal chemistry is found in the use of selenomethionine to replace methionine, which revolutionized

protein crystallography (Hendrickson et al., 1990). The most widely used chemical reporters are aldehydes, ketones, azides, and alkynes. These techniques have been used to label proteins, glycans, and lipids with high specificity and minimal perturbation to the system being observed.

Aldehydes and ketones are reacted with hydrazides and aminoxy groups to form stable Schiff bases (Jencks, 1959; Rideout et al., 1990). Unfortunately, since aldehydes and ketones are both readily present in the cell as metabolites in processes like glycolysis, chemical reports must be used in endogenous environments that lack these groups. As a result, this particular type of chemistry is limited to studying molecules on the cell surface. Furthermore, the ligation reactions are ideally performed at pH 5-6, limiting its applicability for *in vivo* labeling. Overall, aldehyde and ketone chemistry is limited in their uses as truly bioorthogonal chemical reporters. Luckily, the tools available for bioorthogonal chemistry do not end here.

The azide functional group is not present in most species, making it an interesting possibility for bioorthogonal chemistry. Though azide-containing molecules are generally thought to be toxic, these are limited to particular classes such as aryl azides and azide anions. Organic azides, such as those incorporated into unnatural amino acids and nucleotides, are stable and are nontoxic to cells. These molecules can undergo three different reactions. One is the Staudinger ligation where an azide is reacted with a triarylphosphine. This technique has been demonstrated in labeling glycans (Saxon and Bertozzi, 2000; Agard et al., 2004; Bussink et al., 2007; Hangauer and Bertozzi, 2008) and immobilizing small molecules onto glass surfaces (Soellner et al., 2003). Another method involving azides is strain-promoted cycloaddition with cyclooctynes. Since this

does not require the presence of catalysts and proceeds at room temperature, it can be used for *in vivo* labeling for the visualization of surface azide-bearing glycans (Baskin et al., 2007) or receptors (Schuman lab, unpublished data). In addition, this can be used for the enrichment of peptides for proteomic experiments, as was demonstrated in *E. coli* (Nessen et al., 2009). Finally, the third method in which azides can be utilized involves its conjugation to alkynes (and vice versa) via copper-catalyzed [3+2] cycloaddition, also known as click chemistry. Though this method cannot be utilized *in vivo* due to the toxic nature of the copper catalyst, this catalyst allows for the reaction to proceed faster than otherwise (Rostovtsev et al., 2002; Tornøe et al., 2002) and at least 25 times faster than strain-promoted cycloaddition and the Staudinger ligation (Prescher and Bertozzi, 2005).

The applications of click chemistry have been numerous in the past decade or so. Click chemistry has been utilized for the visualization of DNA and RNA (Sylvers and Wower, 1993), by conjugating a terminal alkyne-bearing nucleotide to an azide probe (Salic and Mitchison, 2008; Jao and Salic, 2008). Different azide oligosaccharides have been developed to regioselectively label glycans in cultured cells (Prescher et al., 2004; Dube et al., 2006), and recent work has incorporated these noncanonical sugars into mice (Suckow et al., 2000). Finally, a number of azide or alkyne-bearing amino acids have been developed to exploit the cell's endogenous translational machinery. It is possible to metabolically label proteins in a site-specific manner by expressing a mutated aminoacyl-tRNA synthetase and selective tRNA (Wang and Schultz, 2004). This method is useful for the selective investigation of one particular protein of interest, as it utilizes a nonsense stop codon to exchange one specific amino acid residue into a noncanonical amino acid. This has been used to monitor specific proteins in *E. coli* (Zhang et al., 2003) as well as in

yeast (Deiters et al., 2003) for visualization and biochemical detection. More commonly, noncanonical amino acids are incorporated in a residue-specific manner. For example, azidohomoalanine and homopropargylglycine, which have an azide and alkyne, respectively, have been used as surrogates for methionine and are promiscuously charged onto the endogenous methionyl tRNA (van Hest et al., 2000; Kiick et al., 2002). These have been used to label surface molecules in *E. coli* (Link and Tirrell, 2003; Link et al., 2004) and in mammalian cells (Beatty et al., 2006). The azidohomoalanine has been used for complex mixture proteomics in mammalian cells (Dieterich et al., 2006) and, as is described later in the thesis, in acute hippocampal tissue to isolate a subfraction of the overall brain proteome. Furthermore, we also demonstrate how azidohomoalanine is incorporated into newly synthesized proteins for the visualization of the neuronal proteome. Overall with bioorthogonal chemistry, virtually all biomolecules—proteins, DNA, RNA, lipids, and glycans—are studied with minimal perturbation by utilizing the endogenous cellular machinery.

Conclusion

In this work, we first establish a streamlined method for the identification of newly synthesized proteins. We demonstrate the utility of this method in two different cellular preparations and has the potential to be applied to other systems as well. This technique, originally published in 2006 (Dieterich et al., 2006) is called bioorthogonal noncanonical amino acid tagging (BONCAT) and is unique in that it can, in principle, result in the identification of an entire proteome, thus providing a top-down approach. After that, we also describe a sister technique using the same bioorthogonal chemistry principles in

which newly synthesized proteins are visualized. We use this technique to observe local protein translation in cultured hippocampal neurons and also the overall proteome in organotypic hippocampal slices. In the following chapter, we present a new probe for the improvement of our original BONCAT methodology, in order to maximize our detection of low abundance proteins. Finally, we will discuss the application of this probe for the elucidation of the dopaminergic subproteome in the dendritic region of CA1 in the rat hippocampus. Overall, this work utilizes the invaluable resource provided by bioorthogonal chemistry to elucidate a subproteome that may prove important for treating numerous neurodegenerative disorders that involve dysregulation of dopamine signaling.

Chapter II

DEVELOPMENT OF A NOVEL STRATEGY FOR THE IDENTIFICATION OF NEWLY SYNTHESIZED PROTEINS IN A COMPLEX MIXTURE

Proteins are highly dynamic molecules and essential key players in all cells. The events leading to their translation, the locales of their translation and maturation, and the subsequent modification events that may occur are all topics of inquiry. Early protein research centered around the study of a single protein or a small family of proteins at a time, but with the sheer enormity of the proteome and the multitude of interdependent protein-protein interactions (i.e. signaling pathways), this may not be the most practical or efficient approach. With an estimated number of 10,000 unique proteins in a typical mammalian cell (Pandey and Mann, 2000), mass spectrometry has made the identification and characterization of a proteome a much more manageable task.

Review of proteomic sample preparations

There are a myriad of proteomic techniques that have been developed to tease out the differences between, for example, a stimulated versus non-stimulated cell or tumorigenic tissue compared to normal tissue. Due to advances in mass spectrometry techniques, it has become possible to study pathways involved in neurodegenerative disease (Zhang et al., 2005; Zhou et al., 2005), to discover new biomarkers (Geonborg et al., 2006; Pawlik et al., 2006; Vaughn et al., 2006), and even to identify the proteins that undergo posttranslational modification by phosphorylation (Chang et al., 2004; Garcia et al., 2005; Peters et al., 2004) and glycosylation (Hang et al., 2003; Kaji et al., 2003; Khidekel et al., 2004; Zhang et al., 2003). Perhaps one of best known protein isolation methods associated with subsequent mass spectrometric analysis is two-dimensional gel

electrophoresis (Freeman and Hemby, 2004; Lilley and Friedman, 2004). This allows for the immediate visualization of protein differences between samples and for the subsequent mass spectrometric analysis of protein spots that differ between treatments, rather than all protein spots. However, as 2-D gels separate proteins by molecular weight and isoelectric point, proteins at the extremes of these indices are not often analyzed. In addition, the sensitivity of detection also makes this a method biased against low abundance proteins.

Other methods are more focused on the relative or absolute quantification of proteins between samples. One that is widely used is isotope-coded affinity tagging (ICAT), where thiol-specific reactive groups are used to tag two different protein populations with isotopically distinguishable probes (Gygi et al., 1999). There is also isobaric tagging, which relies upon amine-reactive groups to tag proteins for mass spectrometry (Ross et al., 2004) and the possibility of growing cells in ^{14}N or ^{15}N media (Washburn et al., 2002; MacCoss et al., 2003). Finally, there is stable isotope labeling by amino acids in cell culture (SILAC) in which cells (Ong et al., 2002; Andersen et al., 2005; deGodoy et al., 2008) and later mice (Kruger et al., 2008) have been introduced to media or chow that has isotope-labeled amino acids, thus allowing for the quantification of proteins expressed in two different groups. Despite the powerful nature of these techniques, there still remains the detection problem for low abundance proteins. In addition, there is the possibility of a biased detection for proteins that contain the amino acid used, as in ICAT which labels cysteine residues, making it disadvantageous for proteins that lack or have a limited number of cysteine residues.

In order to provide an additional tool for proteomic analysis, we sought to develop a method that would not only be unbiased toward certain protein types, but also enriched for low abundance proteins. Furthermore, we wanted to harness the cell's endogenous metabolic capabilities so as to reduce perturbation of the cell and ultimately acquire an accurate depiction of the cell's protein readout after a stimulus or different condition. Our final consideration was that the new method be compatible with the nature of our laboratory's work. As we study neurons, it was important that the technique be compatible with work in post-mitotic cells.

The development of bioorthogonal noncanonical amino acid tagging

In 2006, our laboratory reported the development of bioorthogonal noncanonical amino acid tagging (BONCAT; Dieterich et al., 2006) and followed up a year later with a detailed protocol (Dieterich et al., 2007; Figure 2.1). In BONCAT, we take advantage of bioorthogonal chemistry between an azide and an alkyne in the form of copper(I)-catalyzed [3+2] cycloaddition, otherwise known as “click chemistry.” Newly synthesized proteins are selectively labeled using azidohomoalanine (AHA), a methionine surrogate that bears a terminal azide. The chemoselectivity of this amino acid makes this an attractive and truly bioorthogonal technique, since azides are not found in natural cellular environments. It is nontoxic and is readily recognized by methionyl-tRNA synthetase without any modifications to the system (Kiick et al., 2002; Link and Tirrell, 2003). To examine the utility of this approach in neurons, we used dissociated

hippocampal neurons infected with a form of GFP and examined their morphology after a two-hour incubation with either AHA or methionine. The neurons maintained healthy dendrites and their overall morphology was unaltered, thus making AHA a viable option for use not only in dissociated hippocampal neurons, but also potentially in acute hippocampal slices, as will be discussed in a later chapter. In addition, the levels of protein translation observed in either AHA or methionine-labeled human embryonic kidney (HEK) 293 cells (labeled with [35 S] cysteine) were comparable. In addition, the application of AHA did not stimulate the protein degradation pathway, as evidenced by unaltered levels of ubiquitinated protein in AHA- or methionine-labeled cell lysates.

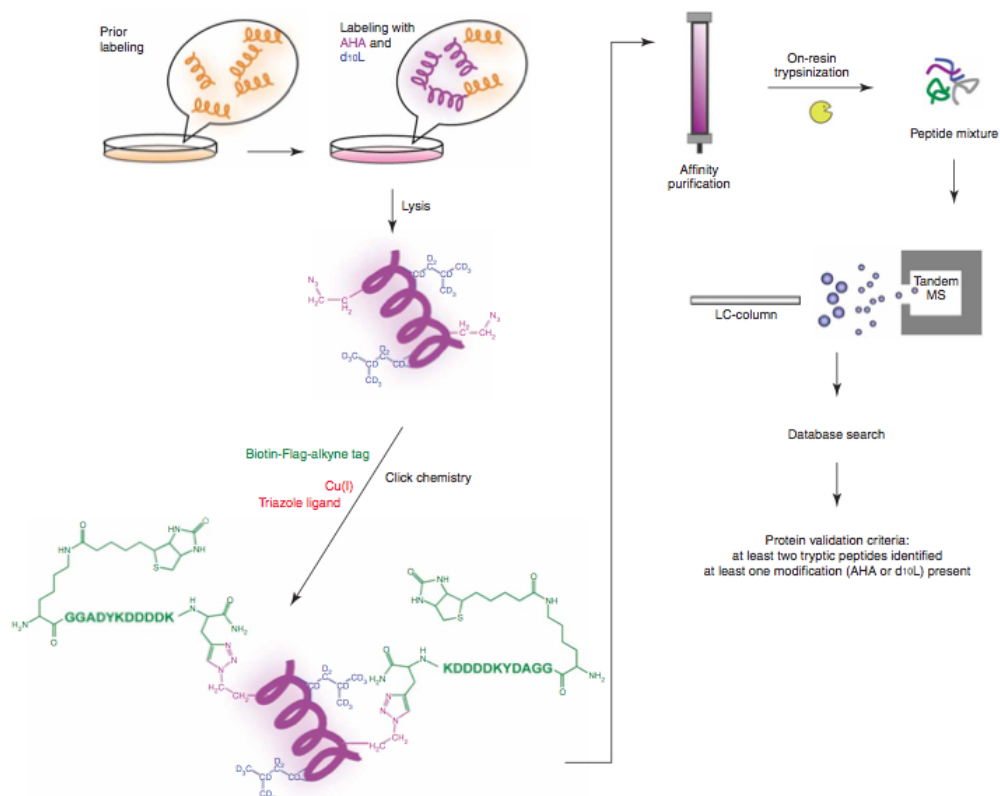


Figure 2.1. The BONCAT strategy for labeling, detection and identification of newly synthesized proteins. Cells are incubated with AHA and d_{10} Leu to allow protein synthesis with AHA and d_{10} Leu incorporation. After incubation, cells are lysed or undergo a subcellular fractionation for biochemical enrichment of specific cellular compartments subsequently followed by lysis. Lysates are then coupled to an alkyne-bearing affinity tag, followed by affinity chromatography, to enrich for AHA-labeled proteins. Purified proteins are digested with a protease and the resulting peptides are analyzed by tandem MS to obtain experimental spectra. Different search programs are used to match the acquired spectra to protein sequences.

For the isolation and enrichment of AHA-labeled proteins in this first version of BONCAT, we used a biotin-FLAG-alkyne tag (Figure 2.2). After cell lysis and conjugation to the alkyne tag, the newly synthesized proteins are purified using the biotin moiety to recognize an avidin-based gel-immobilized resin. The next component of the tag, the FLAG epitope, allows for trypsin to cleave the purified protein from the avidin affinity resin at two cleavage sites, while also providing a possibility for a second purification step, if necessary. This tag was designed such that, after trypsin cleavage, there is a mass difference between AHA and methionine, thus allowing for the AHA incorporation to be detected via mass spectrometry. In a successful cleavage event, where an AHA is clicked to the biotin-FLAG-alkyne tag, there is a mass increase of 107 atomic mass units above methionine. If unsuccessful tagging occurs, the tryptic cleavage does not occur properly and the tag is still attached to the AHA, resulting in a mass increase of 695.6 atomic mass units. Finally, in the instance of failed tagging, AHA is not properly clicked to the biotin-FLAG-alkyne tag and remains unligated, resulting in a mass loss of 5.1 atomic mass units when compared to methionine.

by band excision (deGodoy et al., 2006) is a possibility, this would again introduce a bias, this time against both high and low molecular weight proteins. We instead opted for the shotgun proteomic method: multidimensional protein identification technique (MudPIT; Link et al., 1999; Washburn et al., 2001). MudPIT provides a two-dimensional separation of peptides via liquid chromatography. Peptides are eluted off a triphasic column containing a hydrophobic reverse phase resin, a strong cation exchange resin, followed by another segment of hydrophobic resin before being sprayed directly into the mass spectrometer. Peptides are eluted slowly off the resin to achieve maximum separation, regardless of protein isoelectric point, molecular weight, abundance, and hydrophobicity.

For the initial demonstration of BONCAT, HEK293 cells were co-labeled with d_{10} -leucine (d_{10} -Leu) to provide an independent marker for newly synthesized proteins. This amino acid was selected since it is the most abundant in the mammalian proteome at 9.89% in the database used at the time of analysis. In addition, the HEK293 cells were transiently transfected with a hemagglutinin (HA)-tagged version of the brain-specific mammalian huntingtin-associated protein 1A (HAP1A) as a non-endogenous protein control to ensure that the combination of the BONCAT strategy and MudPIT worked in tandem. Also, since HA-HAP1A contains 14 methionine residues, it provided insight into the level of methionine exchange that could be expected in a two-hour incubation window with AHA.

In the next development of BONCAT, we demonstrated the technique to be compatible with dissociated hippocampal cultures, 21-28 days *in vitro* (DIV). In addition, we incorporated a means for quality control prior to the conclusion of the procedure,

since the entire protocol takes about three days prior to the mass spectrometry analysis. We included a dot blot analysis into the protocol after the click chemistry reaction. A dot blot is a simplified version of a one-dimensional gel, without any separation. A small aliquot of the click chemistry reaction is dotted onto a nitrocellulose membrane in duplicate, along with a series of biotinylated protein standards (Figure 2.3). In addition to providing a system to check for the fidelity of the ligation reaction, it also allows the researcher to estimate the amount of tagged newly synthesized protein present in the sample. The amount of immobilized avidin-based matrix can be adjusted accordingly for the subsequent affinity purification step.

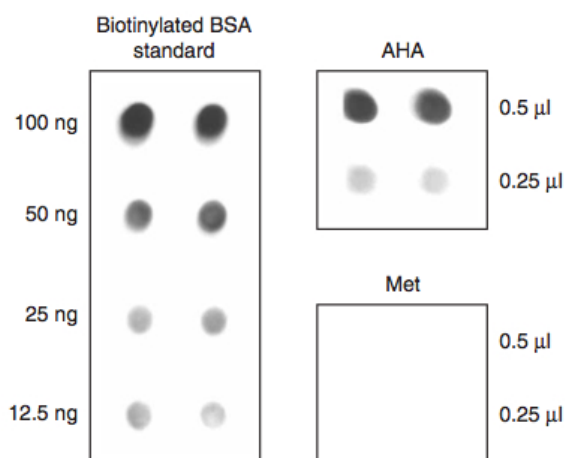


Figure 2.3. Dot blot analysis of AHA versus methionine-treated samples. Dot blot analysis provides a mid-procedure demonstration of proper copper(I)-catalyzed tagging as well as a crude estimate of the amount of tagged protein in the sample. Duplicates of each condition are shown. The Dot blot membrane was probed with an anti-biotin antibody.

The downstream instrumentation and analysis of the mass spectrometry data is primarily dependent upon the resources available at each proteomics facility. In the first

BONCAT experiments, we used a HP-1100 quaternary HPLC pump to generate the elution steps for MudPIT and an LCQ-DecaXP for the analysis itself (Graumann et al., 2004). Since then, we upgraded our setup to a LTQ and then a LTQ-Orbitrap. In a later chapter of this work, we will describe the most current version of our instrumentation, which includes the use of a LTQ-FT. The benefits of these instrumentation changes can include an increase in mass accuracy, sensitivity, and better dynamic range, all of which are critical for the analysis of complex mixtures.

From the mass spectrometry analysis, we attain the overall mass-to-charge ratio of the peptides as well as the individual amino acids. However, these are not assigned to any particular amino acid, nor have they been identified as certain proteins. For this, the proteomics community relies upon bioinformatics to make these assignments and determine the validity of the peptide and protein assignment results. The field of bioinformatics has evolved rapidly, which is reflected in the analysis that we have done. We currently have access to the SEQUEST (Eng et al., 1994), MASCOT (Perkins et al., 1999), and X!Tandem (Craig and Beavis, 2004) database search algorithms. One special consideration for analysis of BONCAT-identified proteins is the number of unique modifications that must be specified at the outset of the database search. There are three AHA-related modifications as well as one for the d_{10} -Leu. This is in conjunction with the alkylated lysine and cysteine modifications that occur in all samples (not specific to BONCAT). Also, the use of MudPIT for our complex mixture makes the size of the dataset very large, making the minimization of false positives a serious consideration. As a result, we have decided to rely on SEQUEST, which is what we started with in our

initial work and is the algorithm used by the J.R. Yates group, who originally developed MudPIT.

After the database search, the data undergoes a peptide validation and assignment via the Trans-Proteomic Pipeline (TPP; Keller et al., 2002; Nesvizhskii et al., 2003), an open-source software suite that is widely used by the proteomics community. The current form of SEQUEST that we have available is the SEQUEST Sorcerer, which allows for the TPP to be run immediately following the database search. This will be further discussed in a later chapter.

BONCAT as a reliable method for studying the proteome

There are additional concerns about various aspects of BONCAT that need to be addressed. First, there may be questions about the level of specificity of the purification procedure and whether proteins remained unaltered throughout the sample processing. Throughout sample preparation, the sample buffer contains a cocktail of protease inhibitors and many of the procedures are conducted at 4°C to further prevent protease activity. Also, regarding specificity, the azide-alkyne chemistry utilized in BONCAT is a truly bioorthogonal reaction that results in a covalent triazole ring. Moreover, the nature of the biotin-avidin affinity is widely known for its low dissociation constant K_d that is on the order of 10^{-15} mol/L (Laitinen et al., 2006), making it one of the strongest protein-ligand interactions found in nature. After the biotin-avidin binding reaction is completed, we remove using centrifugation the “binding supernatant” that consists of preexisting

proteins that do not have AHA incorporation and are thus not newly synthesized. Also, there are a series of wash steps using buffers that contain detergent, to encourage any possible nonspecifically bound proteins to dissociate from the immobilized avidin resin (Figure 2.4). Finally, we also recommend the use of Neutraavidin, which is a nonglycosylated form of avidin that retains its biotin affinity (Hiller et al., 1987) and has the least nonspecific binding of the various avidins that are available.

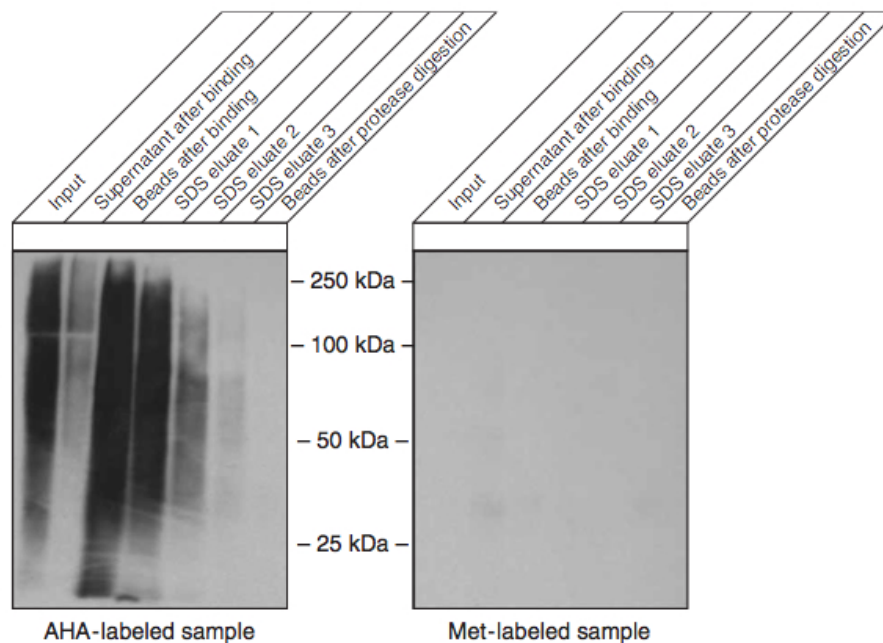


Figure 2.4. Western blot analysis of AHA versus Met-treated sample purification fractions. Upon completing the procedure, a western blot analysis of the various collected fractions will reflect the efficiency of the purification and subsequent trypsinization. The western blot membrane was probed with an anti-biotin antibody.

A second major concern with BONCAT is the use of methionine surrogates. In order to be identified, the proteins must contain at least one methionine. In the HEK293-derived samples that were incubated with AHA for two hours, there was a 2.40%

methionine content in proteins subsequently identified, whereas the entire protein reference database had a 2.13% overall methionine content, thus suggesting that BONCAT does not impose a significant bias toward methionine-rich proteins (Dieterich et al., 2006). There was also a wide range of isoelectric points, molecular weights, and cellular locales of the proteins identified by BONCAT. Another potential problem is the N-terminal methionine cleavage that occurs during the maturation of proteins. In the human database, 5.08% of the proteome possesses a single methionine residue that is also the initiating amino acid. However, the posttranslational processing and acetylation occurs for roughly 30% of all proteins (Meinzel et al., 2005), which does not necessarily exclude this entire subgroup of proteins. Finally, in the human database used for our initial analysis, 1.02% of the open reading frames (ORFs) did not contain any methionines and would be undetectable via BONCAT. However, these included very short proteins with fewer than 25 residues and also incomplete sequences. As a result, BONCAT is able to enrich a variety of newly synthesized proteins in a relatively unbiased manner.

As will be discussed in the following chapters, BONCAT is a versatile method that can be utilized for the study of not only cell lines, but also primary neuronal cultures and even tissue slices. It is a reliable technique that, in a two-hour AHA incubation, results in roughly 150-200 μg of newly synthesized protein from 1.8-2.1 mg of whole HEK293 cell lysate (Dieterich et al., 2007). Using bioorthogonal chemistry, BONCAT is a novel technique that combines high specificity and sensitivity for the isolation of newly synthesized proteins.

Chapter III

USING FLUORESCENT NONCANONICAL AMINO ACID TAGGING (FUNCAT) FOR THE VISUALIZATION OF LOCAL DENDRITIC PROTEIN SYNTHESIS

Following the establishment of BONCAT (Dieterich et al., 2006; Dieterich et al., 2007) for newly synthesized protein identification, we adapted the technology for the visualization of newly synthesized proteins, which we have named fluorescent noncanonical amino acid tagging (FUNCAT). In this technique, we utilize not only AHA, the chemoselective methionine surrogate, but we also introduce the use of another methionine analogue, homopropargylglycine (HPG). HPG is also incorporated using the cell's endogenous translational machinery (Kiick et al., 2002), but differs from AHA because it has a terminal alkyne that confers chemical functionality rather than an azide. As a result, HPG reacts with azide-bearing probes via the same copper (I)-catalyzed [3+2] cycloaddition ligation (Rostovtsev et al., 2002; Link et al., 2004). We used these two methionine surrogates to provide insight into the temporal and spatial control of protein synthesis utilizing local perfusion techniques and pulse-chase (AHA then HPG or vice versa) design experiments to image two distinct pools of newly synthesized proteins.

The reason for developing FUNCAT was to visualize newly synthesized proteins *in situ* using fluorescence microscopy. Previous work utilized a 3-azido-7-hydroxycoumarin for the visualization of HPG-labeled proteins (Beatty et al., 2006), but this particular dye bleaches quickly and is most easily excited using two-photon microscopy. Also, for the *in vivo* imaging of glycosylated surface molecules and receptors, others have used strain-promoted azide-alkyne cycloaddition (Baskin et al., 2007; Codelli et al., 2008; Laughlin et al., 2008; E.M. Schuman, unpublished results). However, we also had the additional goal of imaging intracellular proteins. As a result, we developed a Texas-Red alkyne tag to be clicked to the AHA-labeled proteins (TexasRed-

PEO₂-alkyne; TRA) and a fluorescein-based azide tag for conjugation to HPG-labeled proteins (5'-carboxyfluorescein-PEO₈-azide; FLA; Figure 3.1 A). Both probes are water-soluble due to their polyethylene oxide (PEO) linkers. This allows for straightforward synthesis, making it accessible to researchers without an organic synthesis background (Link and Tirrell, 2003), while also ensuring that the buffer washes after the click reaction can remove excess tag and hence reduce noise.

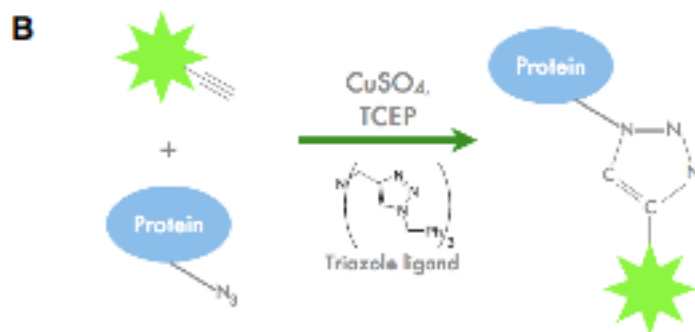
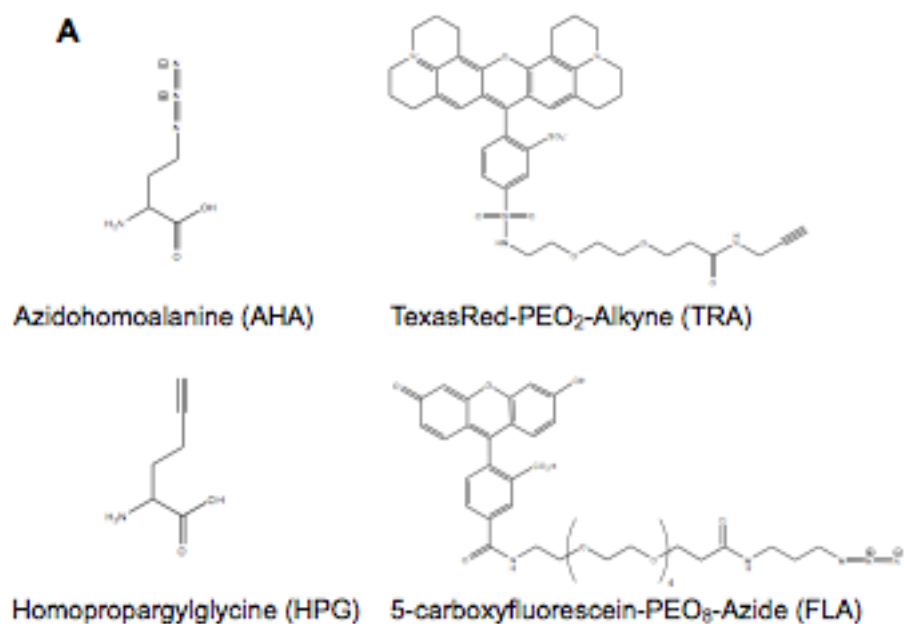


Figure 3.1. Chemical components and FUNCAT procedure. (A) Chemical structures of the modified amino acids Azidohomoalanine (AHA) and Homopropargylglycine (HPG), and the two fluorescent tags TexasRed-PEO2-Alkyne (TRA) and 5-carboxyfluorescein-PEO8-Azide (FLA) used in this study to visualize newly synthesized proteins. (B) Cartoon illustrating the Cu(I)-catalyzed [3+2] azide-alkyne cycloaddition (CuAAC) principle.

General uses of FUNCAT

The overall chemistry of FUNCAT is identical to that of BONCAT, but there are slight protocol differences introduced to effectively access the intracellular, endogenous population of newly synthesized proteins. Our initial experiments were conducted in dissociated, cultured hippocampal neurons. However, we later extended this method for use in organotypic and acute hippocampal slices, thus providing the potential for the visualization of newly synthesized proteins in the highly organized hippocampal network.

As in BONCAT, we initially incubated the dissociated hippocampal neurons in either HEPES-buffered saline (HBS) or HibernateA (HibA) media devoid of methionine, in order to deplete methionine from the system. Then AHA or HPG (in HBS or HibA) was added for the desired period of time. Immediately following incubation with AHA or HPG, cells were fixed and permeabilized using a detergent, such as Triton X-100, allowing access to the intracellular newly synthesized proteins. The click reaction is carried out overnight in the presence of a fluorescent probe, a copper catalyst, and a triazole ligand (Figure 3.1 B). At this point, the sample may be imaged, or subjected traditional immunocytochemistry without any decrease in TRA or FLA fluorescence intensity.

Initially, we incubated cells with varying concentrations of AHA and HPG ranging from 0.1 to 4 mM to determine the concentration at which there is saturation. We found that 2 mM of either AHA or HPG produces a saturation of incorporation, so this is the concentration that we used for subsequent experiments.

Specificity of FUNCAT to visualize new protein synthesis

To investigate the sensitivity of FUNCAT for monitoring protein synthesis, we tested the TRA and FLA probes for reactivity with methionine, AHA- or HPG-incubated cells. In methionine-treated cells, there was a near absence of a fluorescent signal. In addition, we incubated cells with AHA or HPG in the presence of the protein synthesis inhibitor anisomycin and observed a significant reduction in the fluorescent signal. Finally, we assembled the FUNCAT reaction without the copper catalyst, which yielded the same lack of fluorescence. These data indicate that FUNCAT yields specific protein-synthesis-dependent labeling of proteins (Figure 3.2 A).

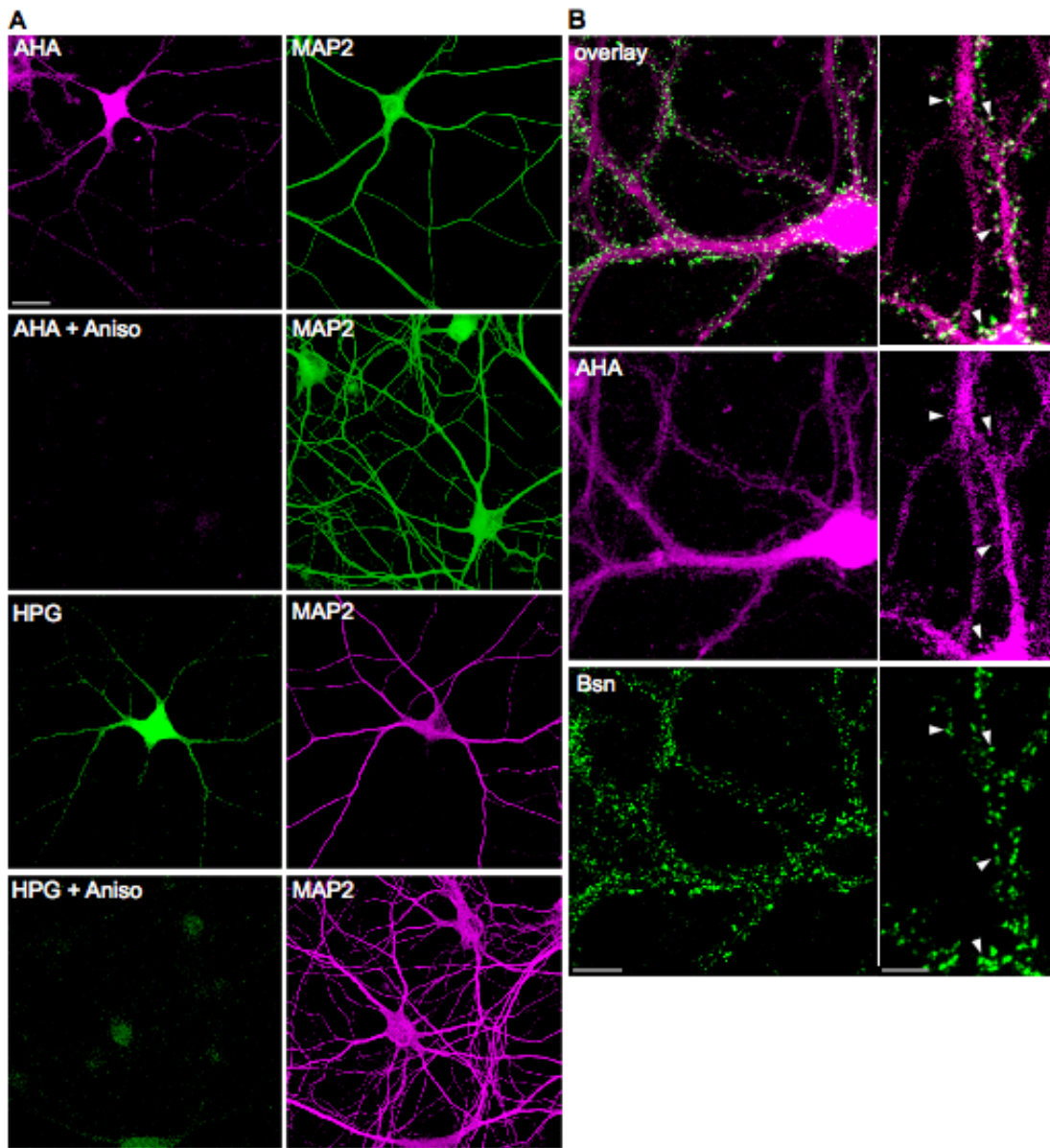


Figure 3.2. Visualization of newly synthesized proteins with FUNCAT in dissociated primary hippocampal neurons. (A) Dissociated hippocampal neurons (DIV 17) were incubated with either 2 mM AHA or 2 mM HPG in the presence or absence of 40 μ M anisomycin (Aniso) for 1 hour, tagged with 1 μ M TRA or FLA tag, and immunostained for the dendritic marker protein MAP2. Scalebar = 20 μ m. (B) Dissociated neurons were incubated with 2 mM AHA for 2 hours followed by tagging with 1 mM TRA tag and immunostaining for Bassoon as a synaptic marker. Arrowheads denote spine-like protrusions. Scalebar = 10 μ m in the left panel images, scalebar = 5 μ m in the blown-up images.

In previous experiments, we found that AHA was not toxic when present in the media of primary cultures of hippocampal neurons (Dieterich et al., 2006). Here we re-examined the morphology of dendrites and spines and examined the localization of the FUNCAT signal within these compartments. We coupled FUNCAT labeling with immunocytochemical labeling for synaptic proteins, such as the presynaptic protein Bassoon (tom Dieck et al., 2006). When the AHA or HPG incubation exceeded two hours, we were able to visualize newly synthesized proteins present at synapses. There was colocalization of the TRA or FLA signal with the presynaptic marker, Bassoon (Figure 3.2 B). In addition, following incubation with either AHA or HPG, we did not observe any changes in dendritic protrusions, overall cellular morphology, or changes in cell death, indicating that this technology can be used with relatively fragile cell populations.

FUNCAT in different cell types

Next, we sought to demonstrate FUNCAT in more intact tissue preparations. First, we tried using organotypic hippocampal slice cultures (21 DIV; Gogolla et al., 2006), which were initially 400 μm thick at preparation and ultimately 100 μm thick at use. These were incubated with AHA for 4 hours to ensure penetration of the amino acid through the depth of the slices. The fixation was performed in 4% paraformaldehyde in PBS for at least 30 minutes on ice and immediately washed thoroughly to remove all of the fixation solution prior to the FUNCAT reaction. We observed TRA signal in both the soma and

dendrites throughout all three dimensions of the slice (Figure 3.3). We then tested FUNCAT in acutely prepared hippocampal slices. First, we recovered the 500 μm slices in aCSF for 2 hours, followed by a 2.53-hour incubation in AHA-containing aCSF. After fixation and a series of washes, similar to those done for the organotypic slice cultures, the acute slices were resectioned to a 50 μm thickness because these slices retain their thickness whereas organotypic slices thin out during the culture period. In the resectioned hippocampal slices we observed that the TRA signal was present in both the soma and dendrites throughout the entire slice. Also, we found that a 2.5-hour incubation with AHA was sufficient to yield specific labeling of neurons located in the center of the 500 μm slice.

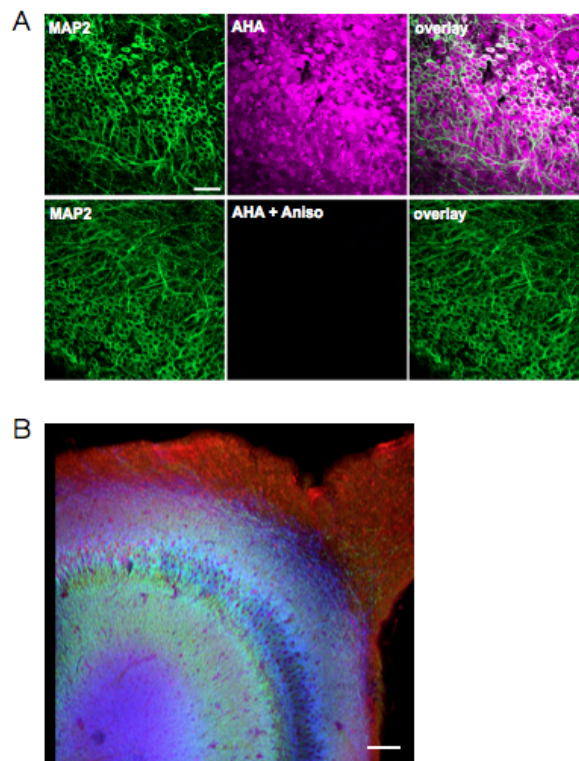


Figure 3.3. Visualization of newly synthesized proteins with FUNCAT in organotypic slice cultures and acute slices from the rat hippocampus. (A) Organotypic hippocampal cultures (DIV 21) were incubated in 2 mM AHA in the presence or absence of 40 mM anisomycin (Aniso) for 4 hours, and tagged with 1 μ M TRA overnight followed by MAP2 immunostaining. Scalebar = 50 μ m. (B) A 500 μ m-thick acute hippocampal slice was incubated for 2 hours with 4 mM AHA, fixed, and resectioned to 50 μ m in thickness. The slice was tagged with 1 μ M TRA overnight followed by immunostaining. Red = TRA, blue = GAD65, green = MAP2. Scalebar = 100 μ m.

Exploring the possibility of labeling two different epochs of protein synthesis

The availability of two different methionine surrogates and their respective fluorescent tags allows one, in principle, to label two temporally distinct protein pools using a pulse-chase type of experiment. We thus conducted a sequential labeling using AHA and HPG (1.5 hours AHA, then 1.5 hours HPG) followed by the click chemistry reactions using the TRA and FLA probes in dissociated neuronal cultures. We tested the various different sequential applications of the amino acid (first AHA then HPG, or first HPG then AHA) and also labeling order (TRA or FLA tagging). Since both AHA and HPG are incorporated into proteins via the same cellular mechanism, we would, for example, incubate the neurons first with AHA for 1.5 hours, wash the cells thoroughly, and then apply the HPG for 1.5 hours. After fixation, the neurons would be first exposed to the TRA tag and undergo a series of thorough wash steps prior to the assembly of the FLA tagging reaction. We found that incubating cells with HPG prior to AHA yields the best labeling result, since the charging rate of HPG onto the methionyl tRNA is slightly lower than that of AHA (Figure 3.4).

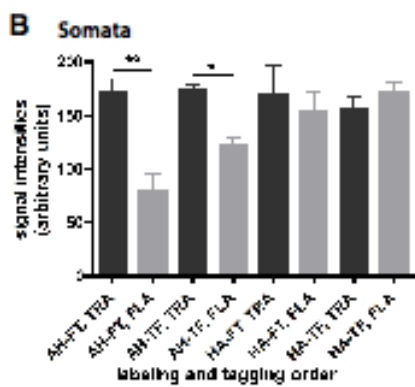
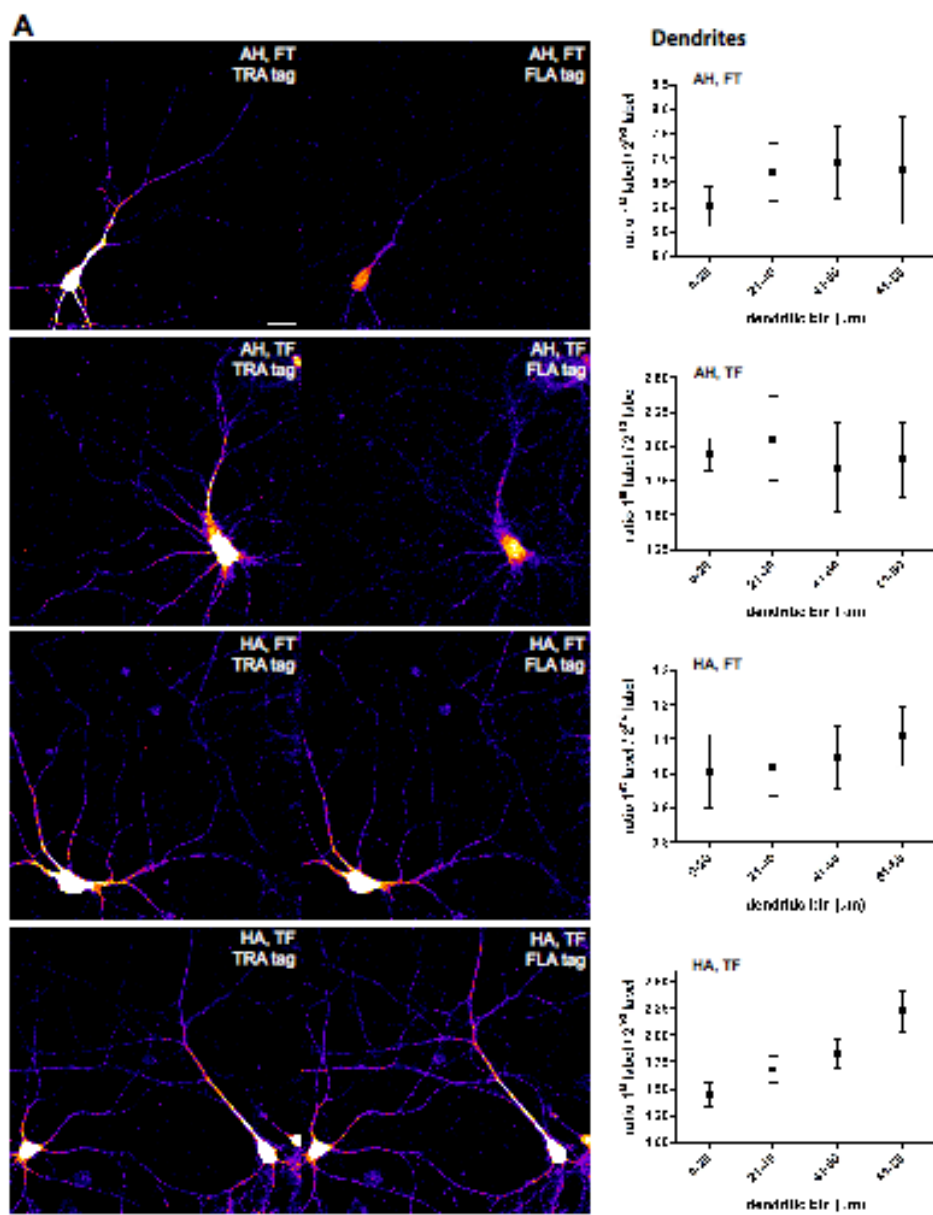


Figure 3.4. Sequential labeling of newly synthesized proteins with two metabolic markers. (A) Dissociated hippocampal neurons (DIV 16-18) were incubated in 2 mM AHA for 1.5 hours followed by 4 mM HPG for 1.5 hours and vice versa, and sequentially tagged with either 1 μ M TRA and 1 μ M FLA tag, or FLA tag followed by TRA tag for 12 hours each. Scalebar = 20 μ m. Labeling and detection sequences: AH, FT: first AHA then HPG, first FLA then TRA tag; AH, TF: first AHA then HPG, first TRA then FLA tag; HA, FT: first HPG then AHA, first FLA then TRA tag; HA, TF: first HPG then AHA, first TRA then FLA tag. Images were taken with same acquisition parameters on a Zeiss Meta 510 confocal microscope using a 40x objective, postprocessing and analysis were done with ImageJ. Graph (B) represents mean ratios of the first to second label (AHA or HPG) intensities with standard deviations of the dendrites in 20 μ m bins for the different detection sequences (TRA or FLA). n = 6-10. Graph (C) represents mean intensities of somata for the different labeling and detection sequences. P-values: ** p < 0.005; * p < 0.05.

Temporal sensitivity of FUNCAT

We next examined how quickly the FUNCAT signal can appear in cultured hippocampal neurons. For this, dissociated hippocampal neurons were incubated with AHA for 0, 10, 20, 30, 40, 50, or 60 minutes, processed via FUNCAT, and also immunostained for MAP2, a dendritic protein marker. We found that newly synthesized proteins were present in the soma of neurons as early as 10 minutes after AHA exposure (Figure 3.5). As the incubation times increased, there was more intense fluorescence in the soma, as well as the emergence of signal in the dendrites. In the proximal dendrites, we observed newly synthesized proteins following just 20 minutes of AHA incubation. This same experiment was done using HPG, and there was no difference in signal between AHA and HPG incubated neurons for time points greater than 30 minutes in duration. There is a slight discrepancy in early noncanonical amino acid incorporation, which suggests that AHA is incorporated into nascent proteins more quickly than HPG, as expected due to

different charging rates of AHA and HPG onto methionyl tRNA synthetases (Kiick et al., 2002).

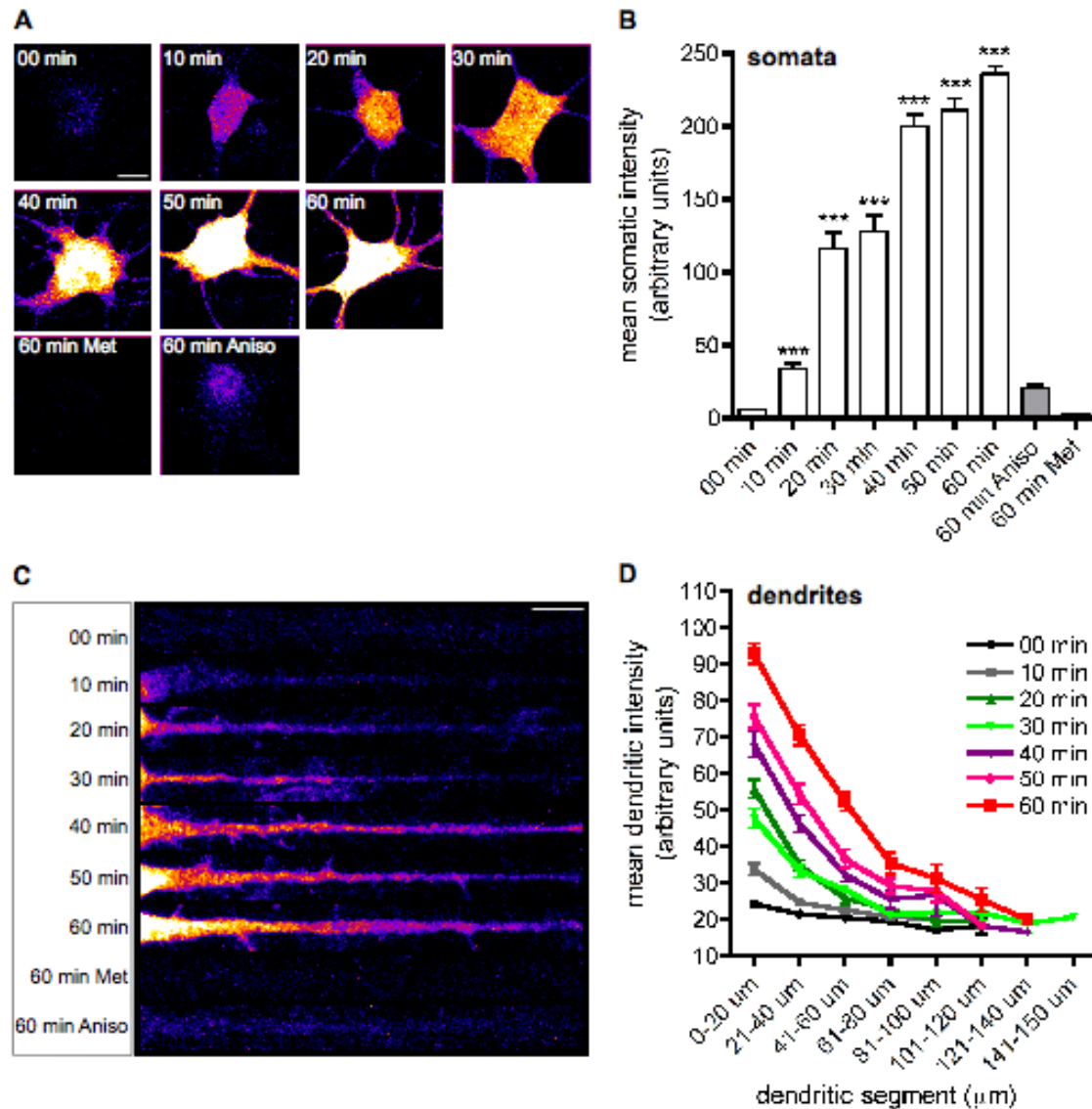


Figure 3.5. Time-course for the detection of newly synthesized proteins in somata and dendrites. (A) Cultures (DIV 16) were incubated for time points indicated with 2 mM HPG, 2 mM methionine (Met), or 2 mM HPG in the presence of 40 μ M anisomycin (Aniso). After cycloaddition with the fluorescent FLA tag, images were taken with same acquisition parameters on a Zeiss Meta 510 confocal microscope using a 63x objective. Scalebar = 5 μ m. Graph (B) represents mean intensities with standard deviation of the somata. Per time point, data from 20-50 cells were collected and analyzed using ImageJ.

Representative samples are shown in the right panel. (C) Representative straightened dendrites of neurons incubated with 2 mM HPG, 2 mM Methionine (Met), or HPG plus 40 μ M anisomycin (Aniso) for time points indicated. Color lookup table indicates fluorescence intensity. Left: proximal; right: distal. Scalebar = 10 μ m. Graph (D) represents mean intensities with standard deviation of the dendrites in 20 μ m bins. Per time point data from 30-70 dendrites were analyzed.

The effects of BDNF on neuronal proteome dynamics

Brain-derived neurotrophic factor (BDNF) is a neurotrophin that is part of the TrkB signaling pathway and is required for normal neuronal development. There is a requirement for BDNF in the maintenance of protein synthesis-dependent long-term potentiation (LTP) (Kang and Schuman, 1996; Kang et al., 1997refs), the mechanism that is responsible for the establishment and maintenance of memories. Furthermore, previous work in our group has demonstrated that BDNF stimulates local protein translation (Kang and Schuman, 1996; Aakalu et al., 2001). In bath application experiments, we sought to investigate the effects of synaptic stimulation on protein translation and on the localization of newly synthesized proteins. In the presence of BDNF and AHA for 1 hour, we found a 60 % increase in FUNCAT-derived fluorescence signal in the proximal dendrites when compared to control neurons that were only incubated with AHA (Figure 3.6).

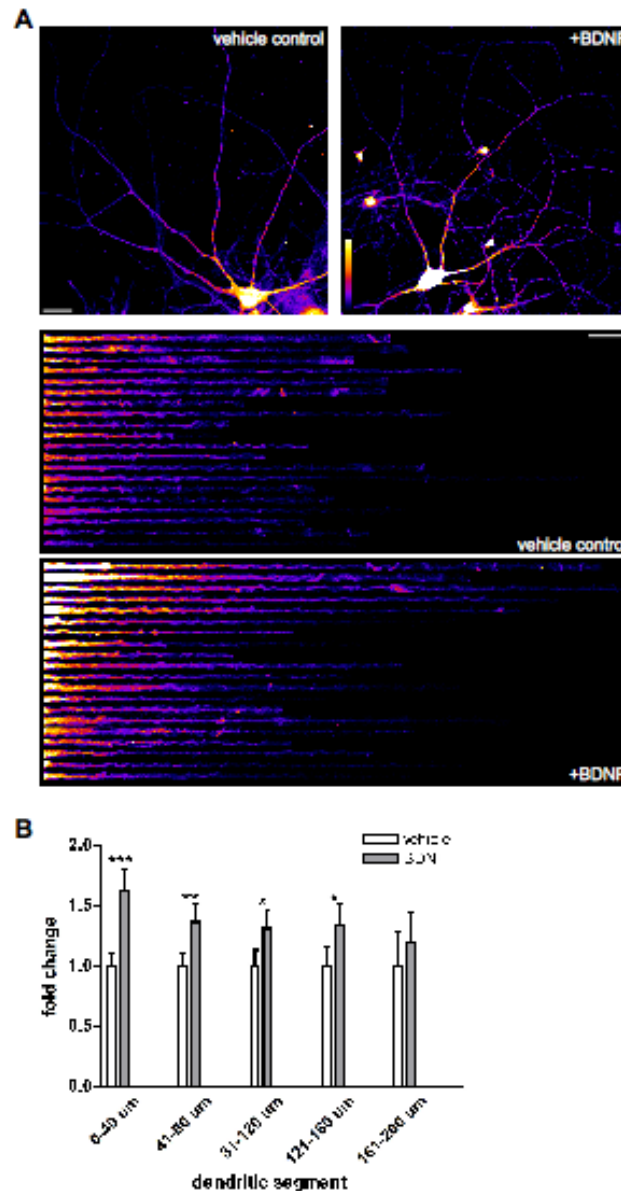


Figure 3.6. BDNF-induced increases in protein synthesis. (A) Hippocampal neurons (DIV 16) were incubated for 1 hour with 2 mM AHA (vehicle control) or with 2 mM AHA in the presence of 50 ng/ml BDNF. After a 15 min chase with 2 mM methionine, cells were fixed, tagged with 1 μ M fluorescent tag and immunostained for the dendritic marker protein MAP2. For quantitative analysis, dendrites of both groups were straightened and fluorescent intensities of binned 40 μ m segments were measured using ImageJ. Representative images for both groups are shown. Color lookup table indicates fluorescence intensity. Note the increase in signal intensity in both cell body and dendrites in BDNF-treated versus control cells. Left: proximal; right: distal. Scalebar = 20 μ m. (B) Graph shows the change of TRA-signal of BDNF-treated cells normalized to

controls (vehicle). Numbers of dendritic segments included in the analysis are specified at the bottom. P-values: *** $p < 0.000005$; ** $p < 0.005$; * $p < 0.05$.

Next, we employed a technique called local perfusion, in which we applied chemical stimuli and the noncanonical amino acids in a limited locale in the neuron—either over the cell body or a dendritic segment— using glass micropipettes. In order to ensure that AHA could be taken up across the dendritic membrane in the local perfusion experiments, we immunostained dissociated neuronal cultures for the localization of the amino acid transporter LAT1 as well as the methionyl tRNA synthetase. We found that both were distributed in the soma and dendrites— suggesting the ability to both take up amino acid and charge the tRNA in the dendrites (Figure 3.7). We then proceeded with the local perfusion experiments by locally applying anisomycin over the cell bodies while AHA was bath-applied with and without BDNF (Figure 3.8). By perfusing anisomycin, we are able to eliminate the somatic contribution to the neuronal proteome, thus allowing for the exclusive visualization of dendritic protein synthesis. The somatic perfusions of anisomycin were initiated 20 minutes prior to the bath application of AHA or AHA and BDNF so that we could decrease the translational contribution from the soma to a minimum. After that, the bath application proceeded for 30 minutes until fixation and FUNCAT processing. We found that there were comparable levels of newly synthesized proteins in the distal regions of the dendrites in both the anisomycin perfused and non-perfused neurons. This suggests a bona fide dendritic contribution to the neuronal proteome. Also, as was observed earlier, there was a statistically significant increase in

the amount of newly synthesized proteins in neurons simultaneously treated with BDNF.

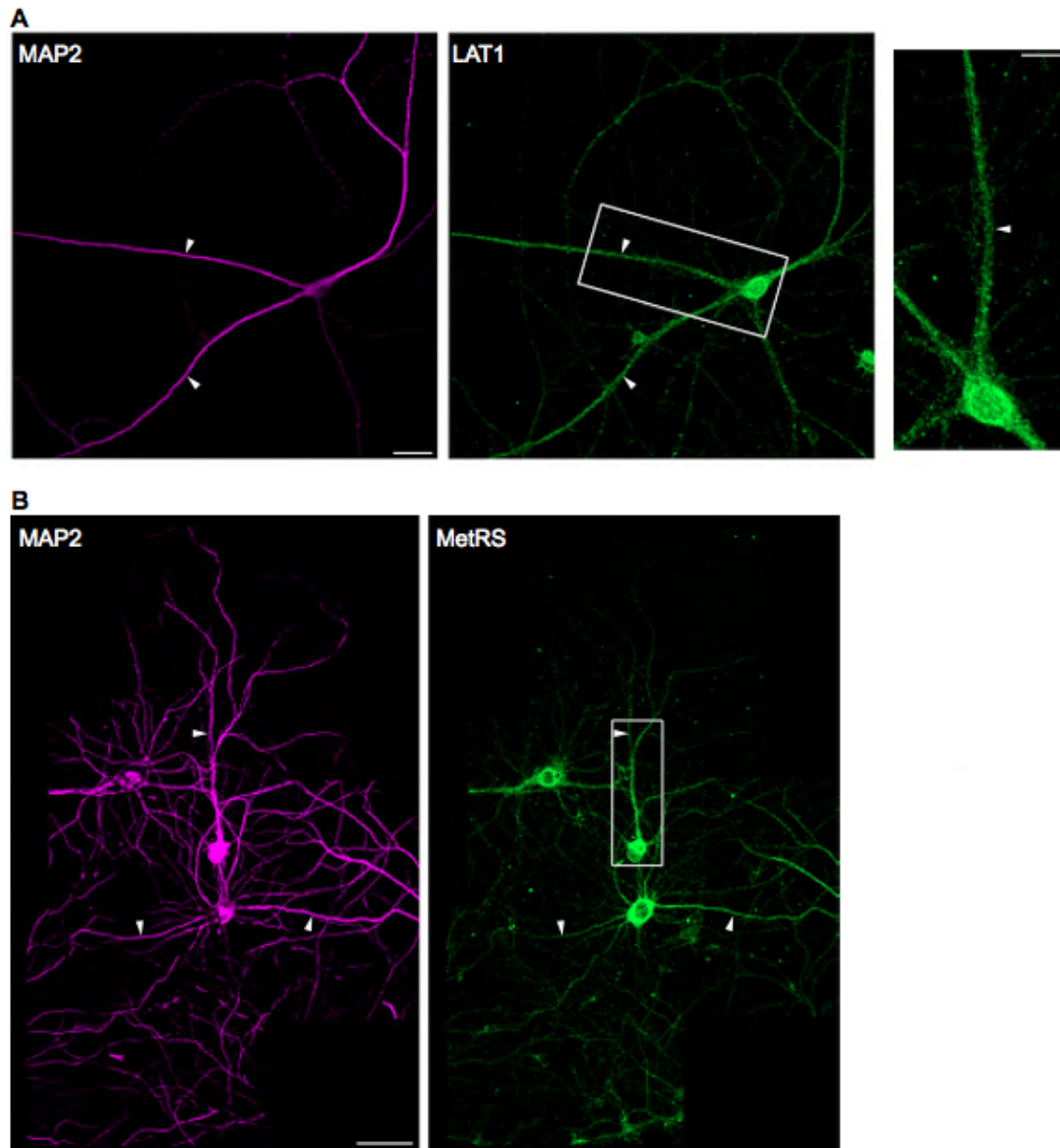


Figure 3.7. The methionyl tRNA synthetase MetRS and the amino acid transporter LAT1 are present in dendrites. Immunostaining of dissociated hippocampal neurons (DIV 17-20) for the dendritic marker protein MAP2 and the large amino acid transporter LAT1 (A), and methionyl tRNA synthetase (B). Arrowheads indicate dendritic processes. Scalebars = 20 μm (A) and 50 μm (B) in the overviews, scalebars = 10 μm in close-up images (A) and (B).

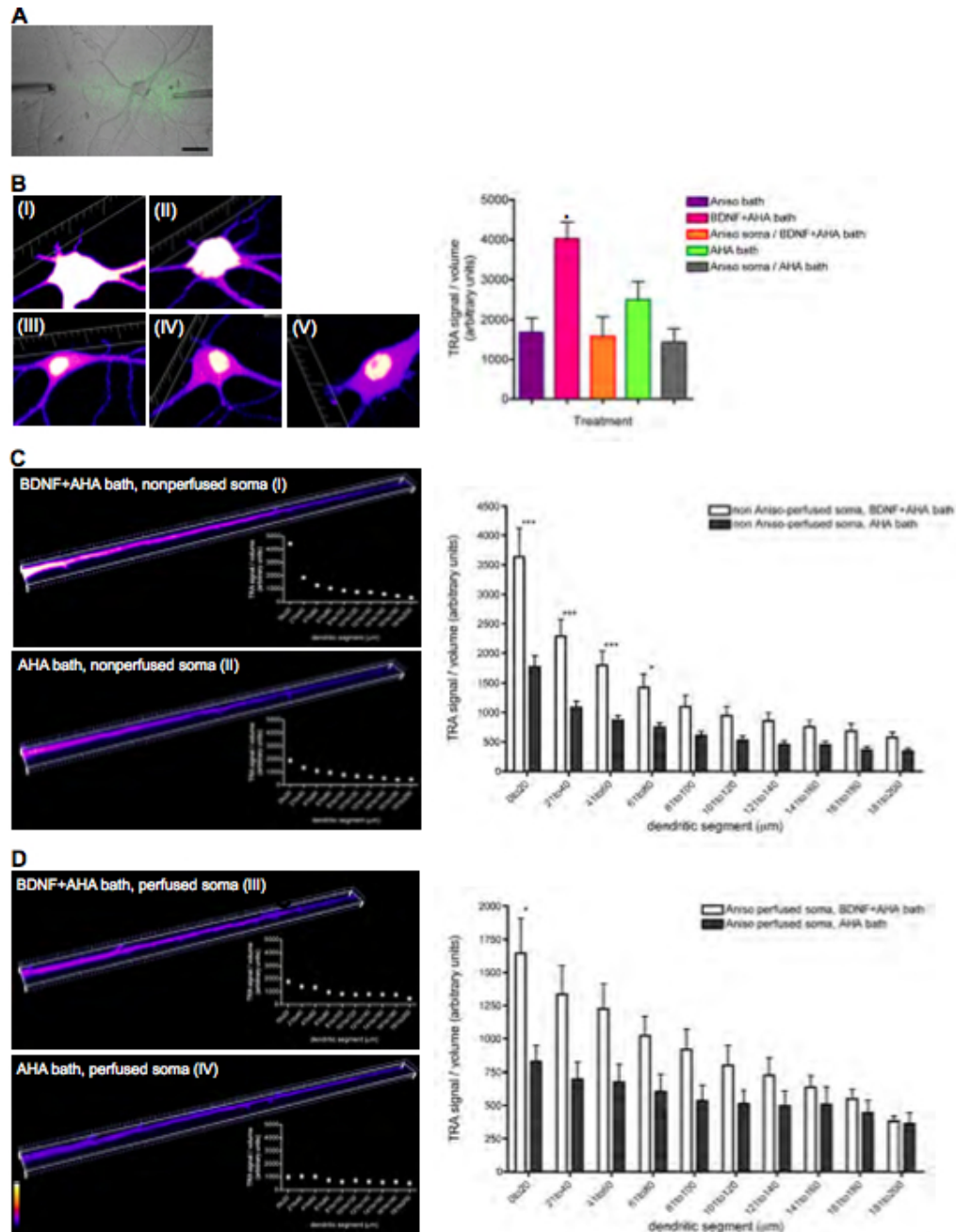


Figure 3.8. BDNF-induced increase in dendritic protein synthesis. (A) General local microperfusion set up showing a local perfusion stream (AlexaFluor 488 hydrazide in HibA) applied on the soma of a hippocampal neuron using a perfusion pipet (right) and a suction pipet (left). Scalebar = 50 μm . (B) Hippocampal neurons for somatic local perfusions were pre-incubated in HibA media without methionine for 10 min during which time the perfusion with 40 μM anisomycin plus 2 mM AHA in HibA was initiated. Twenty minutes after starting the perfusions, AHA (final concentration 2 mM), in combination with or without BDNF (final concentration 50 ng/ml), was added to the

dishes for another 30 min. After fixation, FUNCAT using 1 μ M TRA tag, and immunostaining for MAP2 was performed. Newly synthesized proteins of non-anisomycin-perfused (I, AHA plus BDNF; II, AHA) and anisomycin-perfused (III, AHA plus BDNF; IV, AHA) cells from same dishes, as well as anisomycin-bath applied dishes, (V) were imaged with a Zeiss Meta 510 confocal microscope using a 40x objective, postprocessing and analysis were done with Imaris software. Images in (B) show TRA signals of representative somata from groups I-V in 3D. $n = 6-9$. Large grid tick marks = 20 μ m. Graph on the right shows TRA-signal to volume ratios (based on MAP2 staining) for the different groups. (C and D) Analysis of newly synthesized proteins in dendrites originating from cells of treatment groups I-IV. Images on the left show the TRA signal intensity of representative dendrites. Left, proximal; right, distal. For quantitative analysis dendrites were first straightened with ImageJ and then analyzed using Imaris. Graphs in each image display the individual TRA signal / volume profile along the dendrite). Summary graphs shows TRA-signal to volume ratios (based on MAP2 staining) for the different groups; BDNF plus AHA, white boxes; AHA, dark boxes. Color lookup table indicates fluorescence intensity. Large grid tick marks = 10 μ m. $n = 6-9$. P-values: *** $p < 0.0005$; ** $p < 0.005$; * $p < 0.05$ using 2-way ANOVA statistical analysis.

In summary, we have established FUNCAT as a sensitive method to visualize newly synthesized proteins in both neuronal somata and dendrites.

Chapter IV

DEVELOPMENT OF DISULFIDE-BEARING PROBE FOR IMPROVING BONCAT

Recent developments in bioorthogonal chemistry have allowed the investigation of specific cell biological events with minimal perturbation, thus giving a more accurate picture of what is occurring within the cell. Though the use of small biomolecules, such as green fluorescent protein and FLAG and histidine epitopes, are effective tools, they can add significant size to the molecules of interest. On the other hand, small molecules that can be metabolically incorporated into proteins, RNA, and DNA are not as large. Such small molecules are generally noncanonical amino acids or unnatural nucleotides that bear novel chemical handles that allow for their selective isolation or visualization following incorporation into DNA, RNA or protein.

In this study, we sought a chemical functional group that was not readily found in organisms. This led us to pursue an azide-containing species (Kiick et al., 2002), which can undergo three major different types of chemical reactions, all with varying degrees of specificity. In the Staudinger ligation, an azide is reacted with a triphenylphosphine to form an amine bond (Saxon and Bertozzi, 2000). Although this reaction fulfills the specificity and bioorthogonality requirements, the reaction kinetics are slow compared to other chemical reactions. In copper-catalyzed [3+2] cycloaddition, or click chemistry, azides and alkynes are reacted to form a triazole (Kolb and Sharpless, 2003). This same principle also occurs in strain-promoted cycloaddition, in which azides are reacted to cyclooctynes in a copper catalyst-free environment for *in vivo* labeling in cells (Agard et al., 2004; Baskin et al., 2007). However, we preferred the faster reaction rate found in click chemistry and the opportunity for having our substrates of interest bear either an azide or alkyne was appealing as cyclooctynes provided some unwanted properties such as rapid degradation in our hands (Dieterich, Hodas, Schuman, unpublished results).

In order to identify and visualize newly synthesized proteins, we used an azide-bearing noncanonical methionine surrogate, azidohomoalanine (AHA). Previous work demonstrated cell surface labeling in *E. coli*, in which newly synthesized proteins were detected using a biotin alkyne probe (Link et al., 2004). This showed that AHA could be readily incorporated into the prokaryotic proteome. In our initial experiments we attempted to obtain labeling in a eukaryotic system followed by identification of newly synthesized proteins with mass spectrometry. The resulting technology, bioorthogonal noncanonical amino acid tagging (BONCAT), demonstrated the ability to enrich for and identify a complex mixture of proteins in an unbiased manner. In the initial experiments, following incubation of HEK293 cells with AHA, a diverse set of proteins were detected (Dieterich et al., 2006).

In the first demonstration of BONCAT, we used a biotinylated FLAG peptide alkyne probe to purify newly synthesized protein using an avidin resin. Upon trypsin digestion, tryptic peptides, comprising those derived from the newly synthesized proteins as well as avidin, were released (Dieterich et al., 2006; Dieterich et al., 2007). In subsequent proteomic experiments, we found that the removal of the avidin-derived peptides increased the number of novel peptide spectra detected, resulting in the identification of more low-abundant proteins. As a result, we sought to develop a chemically cleavable probe that would reduce the number of avidin-derived peptides present in the sample, allowing for better identification of complex protein mixtures. Moreover, with the ongoing expansion of the noncanonical amino acid library, it is clear that the incorporation of several distinct noncanonical amino acids into a system would be a powerful tool for evaluating different protein populations over time. For example,

the introduction of another methionine surrogate, azidonorleucine (ANL), was recently shown to be useful for the differential labeling of two distinct cell types (Ngo et al., 2009). Therefore, we compared the utility and biocompatibility of the alkyne-bearing tag we developed to an identical tag that bears an azide group.

Synthesis and use of biotinylated disulfide alkyne and azide probes

We developed a biotinylated probe that features a disulfide bond in the center, using a commercially available NHS ester conjugated to a biotin with propargylamine (Figure 4.1 A). This alkyne probe utilizes [3+2] copper-catalyzed cycloaddition to covalently bind to the azide of azidohomoalanine. Using a similar strategy, the alkyne of homopropargylglycine can be linked to a similar disulfide-bearing azide probe (Szychowski et al., 2009, submitted). We refer to these probes as “disulfide tag-alkyne” (DST-alkyne) and “disulfide tag- azide” (DST-azide), respectively. Both amino acid and probe combinations (AHA+ DST-alkyne or HPG + DST-azide) can be distinguished from methionine in mass spectrometry experiments, as there is a triazole modification that lends a mass increase to either AHA- or HPG-bearing peptides (Figure 4.1 B).

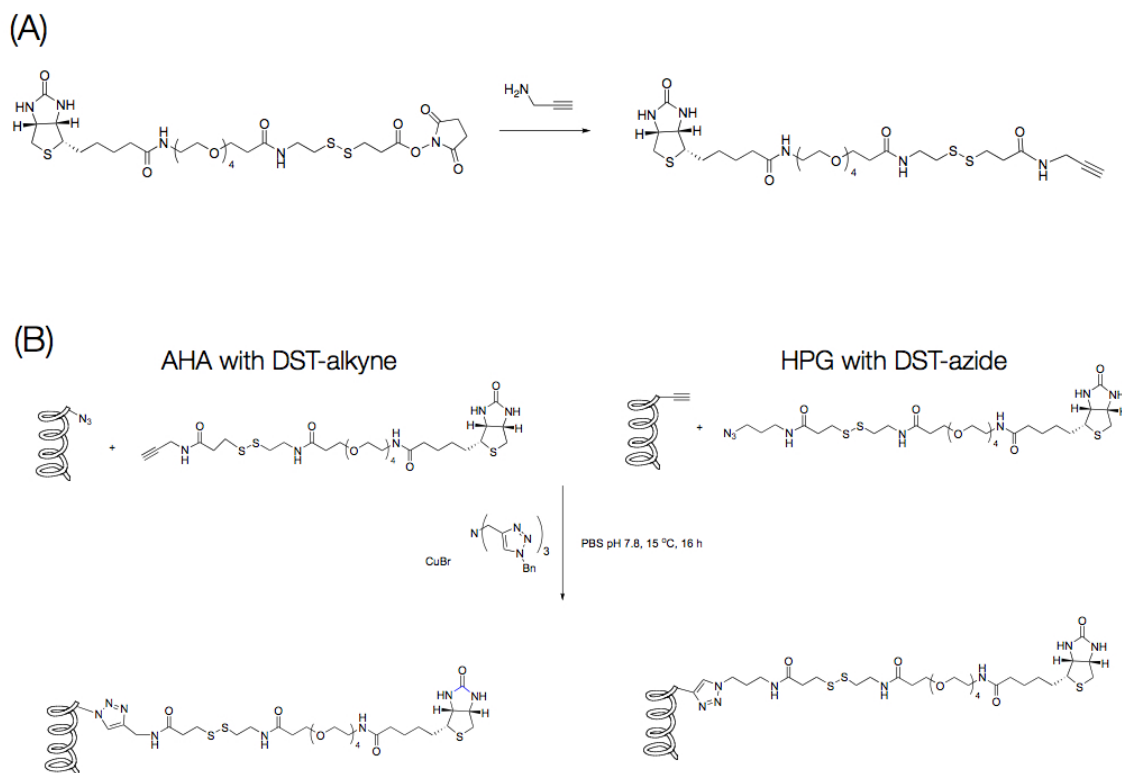


Figure 4.1. Synthesis and application of disulfide-bearing tags for click chemistry. (A) An alkyne-bearing amine is reacted with a biotinylated disulfide ester in the presence of diethyl ether. (B) The alkyne- and azide-bearing disulfide tags (DST) undergo copper-catalyzed [3+2] cycloaddition with the methionine surrogates azidohomoalanine (AHA) and homopropargylglycine (HPG), respectively.

Pre-alkylation abolishes background signal and prevents disulfide exchange

With the introduction of the DST-azide and –alkyne probes, we were aware of the potential nonspecific disulfide exchange that might occur between the probes' disulfide bond and any exposed cysteine residues of non-labeled proteins. This problem would lead to the purification of some preexisting proteins instead of exclusively newly synthesized proteins. In addition, the resulting alkyne probe product might react with

AHA residues during the click chemistry, if not removed (Figure 4.2 A). We sought to use an alkylation method that would be compatible with currently used mass spectrometry techniques, so as to limit the number of modification searches that would be needed for peptide and protein identification. Prior to alkylation, we reduced all disulfide bonds with 2% β -mercaptoethanol. [Note: though TCEP is widely used in proteomic sample preparation, the presence of the triphenylphosphine could convert the azide of AHA to an amine (Scriven and Turnbull, 1988) and thus interfere with the click chemistry]. Following reduction with β -mercaptoethanol, the reducing agent was removed by performing an acetone precipitation. After that, samples were alkylated with 11mM iodoacetamide, which was also subsequently removed using acetone precipitation. Using Western blot analysis, we compared the biotinylation signal from COS7 cell lysates incubated for 2 hours in either methionine or AHA (4 mM) and then alkylated or not prior to click chemistry with the DST-alkyne probe. The addition of the alkylation step resulted in a dramatic reduction of the biotin signal in the tagged, alkylated methionine sample, when compared to the tagged, non-alkylated methionine lysate. The biotinylation signal from the AHA signal was not changed by the alkylation step suggesting that most, if not all, of the biotinylation signal in AHA samples is derived from linkage with AHA-containing peptides (Figure 4.2 B).

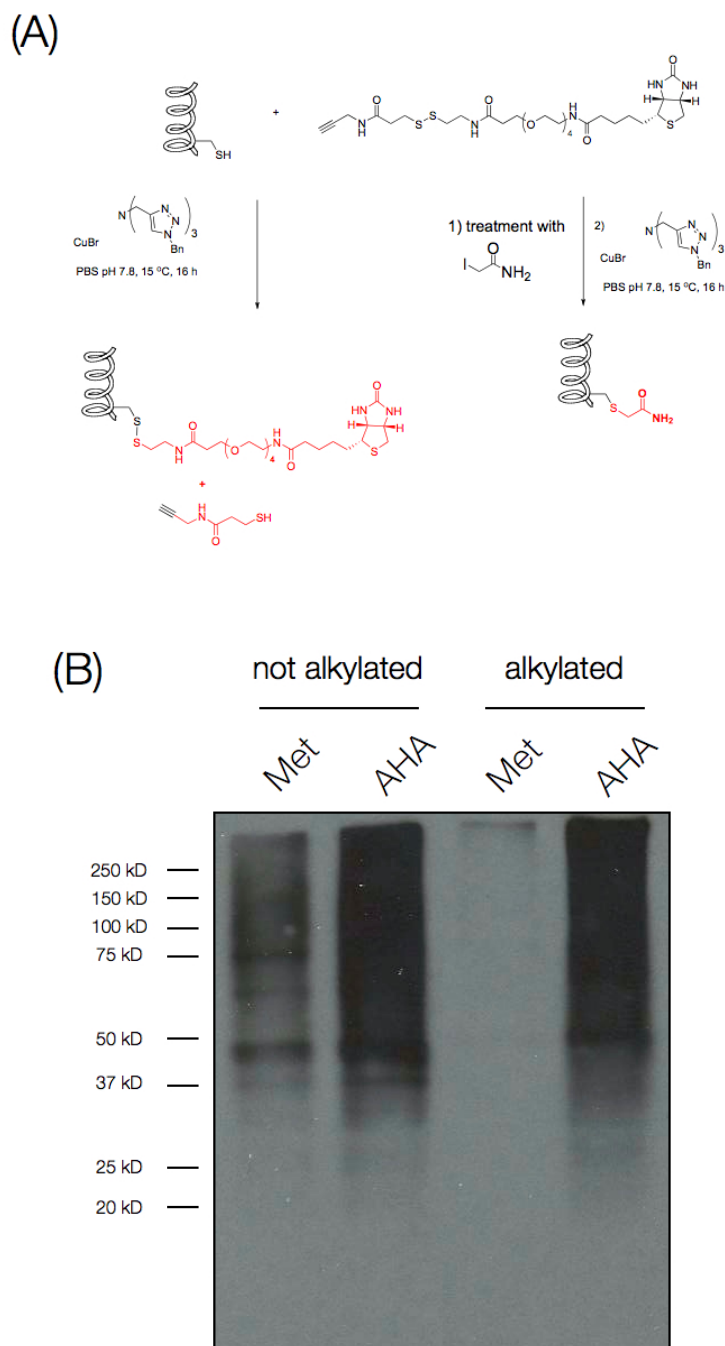
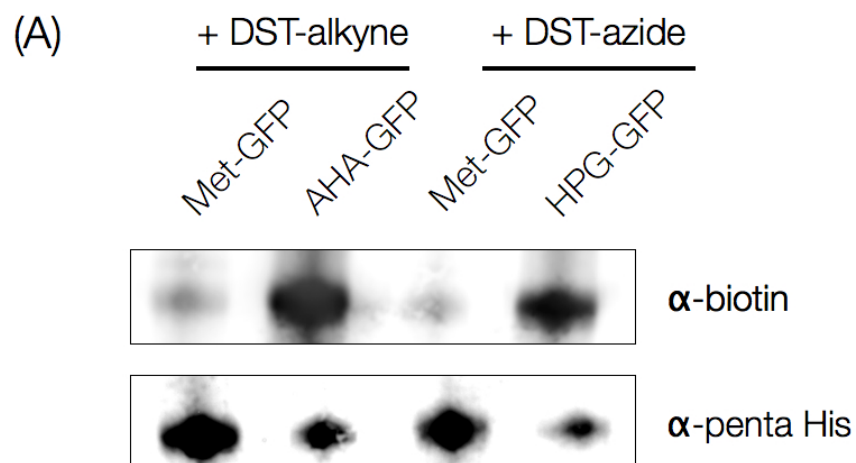


Figure 4.2. Alkylation prior to click chemistry reaction significantly reduces non-specific protein labeling. (A) Disulfide bonds from cysteines are first reduced and then protected using iodoacetamide, preventing possible disulfide exchange with the disulfide alkyne or azide tag. (B) COS7 cells that were incubated in either 4mM methionine or 4mM AHA were lysed and either not alkylated or alkylated prior to reaction with the DST-alkyne. They were analyzed via Western blot using an antibody against biotin.

Click chemistry reaction of AHA and HPG with their respective disulfide-bearing probes is comparable

With the development of these two novel disulfide-bearing probes, we aimed to determine the relative efficiency of the click chemistry reaction for azide- or alkyne-bearing proteins. In order to evaluate these probes and their AHA or HPG-labeled proteins, we generated a purified green fluorescent protein (GFP modified to contain a single N-terminal methionine codon followed by a histidine tag). We incubated E.coli constitutively expressing this construct with either AHA or HPG for 4 hours and then purified GFP from cell lysates. We conjugated the AHA or HPG protein with their respective alkyne or azide probes and compared the total amount of GFP protein with the level of biotin signal resulting from the probe conjugation. In comparing the two, we found that AHA and HPG yield comparable levels of reactivity to their respective probes (Figure 4.3).



(B)

Probe	Relative selectivity (arbitrary units)	Relative yield of click reaction (arbitrary units)
AHA + DST-alkyne	1.0	1.9
HPG + DST-azide	1.0	1.0

Figure 4.3. Click chemistry of AHA or HPG yield similar reaction efficiencies. (A) Methionine, AHA, or HPG-labeled GFP was reacted with either the DST-alkyne or DST-azide probe. The same Western blot was probed simultaneously for successfully labeled GFP (α -biotin) and total GFP (α -penta His). (B) Each probe's efficacy was assessed by normalizing the AHA- or HPG-GFP biotin signal to the Met-GFP signal for each probe.

AHA and HPG are incorporated into proteins at similar rates

The complimentary chemistry of AHA and HPG could, in principle, allow for two protein populations to be labeled in a pulse-chase type of experiment, allowing one to monitor proteome dynamics over time. In order to interpret such an experiment, we determined whether AHA and HPG affect cellular growth and protein synthesis similarly. First, we compared the growth rates of bacteria exposed to media containing either AHA or HPG. We used *E. coli* with IPTG-inducible expression of GFP containing one methionine residue at the initiator codon (same construct as above). These auxotrophic bacteria were then exposed to synthetic M9 medium supplemented with methionine, AHA, or HPG as well as the 19 other essential amino acids. The proliferation rates of these three groups were monitored over the course of 5 hours at 20-minute intervals. We found that the *E. coli* incubated in AHA and HPG grew at statistically indistinguishable rates. As expected, *E. coli* grew over 90% faster in the presence of methionine (Figure

4.4 A). We also explored the incorporation of the amino acids into protein by monitoring the GFP fluorescence over the same period of time. AHA and HPG produced near-equal levels of GFP fluorescence, while methionine-labeled cells had a 65% higher level of fluorescence (Figure 4.4 B). Taken together, these results indicate that AHA and HPG support cell growth and protein synthesis at similar rates.

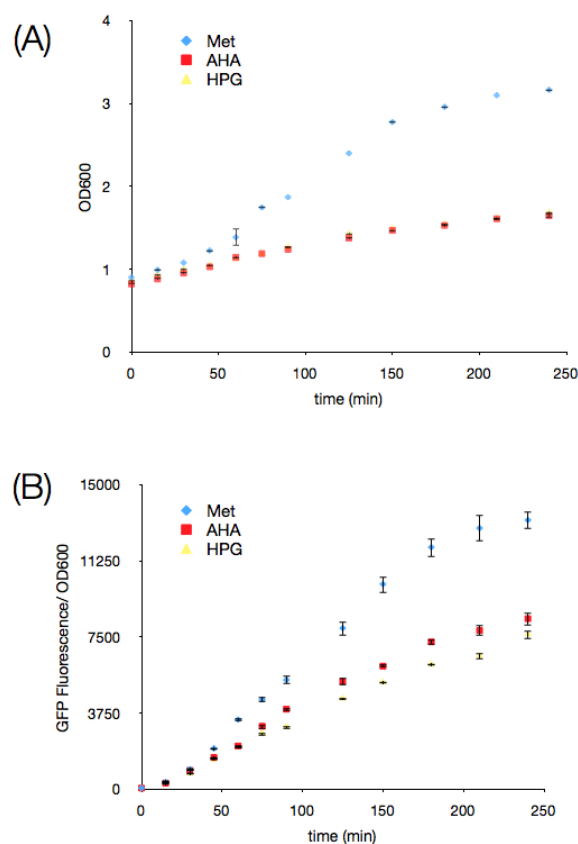


Figure 4.4. *E. coli* incorporates azidohomoalanine and homopropargylglycine into newly synthesized protein at comparable rates. *E. coli* expressing GFP bearing a single methionine residue were incubated in media containing 19 amino acids plus either methionine, AHA, or HPG for 4 hours after IPTG induction. (A) Methionine-incubated bacteria grow at a significantly higher rate, while AHA- and HPG-incubated bacteria grow at near-identical rates. (B) The level of GFP fluorescence depends upon whether methionine, AHA, or HPG is present in the media. Less GFP is synthesized in the presence of the non-canonical amino acids.

Bioorthogonal chemistry, which utilizes endogenous cellular machinery, has allowed for the exploration of protein translation *in situ*. With the establishment of BONCAT (Dieterich et al., 2006), the non-canonical amino acid AHA coupled with [3+2] copper-catalyzed cycloaddition allowed for the identification of a complex mixture of newly synthesized proteins in an unbiased manner. In an effort to improve the method, we sought to improve the detection of low-abundance proteins by developing a novel probe with a protocol that is compatible with proteomic sample preparation. In addition, we did a side-by-side comparison of AHA with another widely used methionine surrogate, HPG, to observe their effects on cell growth and protein expression.

Chapter V

**ELUCIDATING THE DENDRITIC DOPAMINERGIC SUBPROTEOME IN THE
HIPPOCAMPUS USING BONCAT**

The importance of the dendritic contribution to the neuronal proteome and learning and memory has been well established, whether by electron microscopy (Ostroff et al., 2002), local perfusion (Aakalu et al., 2001), or microdissections coupled with electrophysiology (Kang and Schuman, 1996). In addition, there have been efforts to characterize the synaptic proteome by using biochemical fractions containing synaptoneurosomes in which ribosomal particles have been identified. However, it is difficult to resolve just the dendrites, as there are no biochemical preparations that selectively isolate a single neuronal compartment.

We decided to investigate the effects of the D1/D5 dopamine receptor agonist SKF81297 on the hippocampal dendritic proteome. Stimulation of the D1-like dopaminergic receptors has been shown to be necessary and sufficient for the maintenance of L-LTP (Frey et al., 1991; Frey et al., 1993; Huang and Kandel, 1995; Matthies et al., 1997; Swanson-Park et al., 1999), which is a protein synthesis-dependent process. Previous work by Smith and colleagues (2005) demonstrated an increase in dendritic protein synthesis after the application of a D1/D5 dopamine receptor agonist, SKF81297. They also observed the upregulation in surface expression of GluR1, an AMPA receptor subunit. This, in turn, resulted in the increased frequency of miniature excitatory postsynaptic currents (mEPSCs, or minis), which are able to regulate local protein synthesis (Sutton et al., 2004). In this study we sought to determine the proteins that are rapidly synthesized in the dendrites of the hippocampus.

Using BONCAT, we were able to purify and enrich for newly synthesized proteins. The initial demonstration of this technique was done in HEK293 cells labeled with AHA (Dieterich et al., 2006). We later demonstrated this to be an effective

technique for studying more sensitive cell preparations— first in primary hippocampal neurons, organotypic slice cultures, and finally in acute hippocampal slices. Likewise, with the development of FUNCAT, we also showed the possibility of visualizing these AHA-labeled proteomes with a high degree of sensitivity and specificity. In order to study the dopaminergic hippocampal subproteome, we decided to first visualize the newly synthesized proteome using FUNCAT to assess whether a change in the amount of newly synthesized proteins could be detected in dendrites after stimulation of the D1-like dopaminergic receptors using SKF81297.

SKF81297 produces an increase in dendritic protein synthesis in hippocampal neurons

Primary hippocampal cultures were first incubated with methionine-free media for 30 minutes and then incubated with AHA for 1 hour, with and without SKF81297. This incubation was immediately chased with a methionine incubation for 10 minutes to terminate the charging of AHA onto tRNAs. Then, the neurons were immediately fixed, tagged with a fluorescent probe using click chemistry, and immunostained for MAP2, a dendritic protein marker. In dissociated hippocampal cultures treated with the D1 agonist, there was a 25-60% increase in FUNCAT fluorescence in the distal dendrites (Figure 5.1).

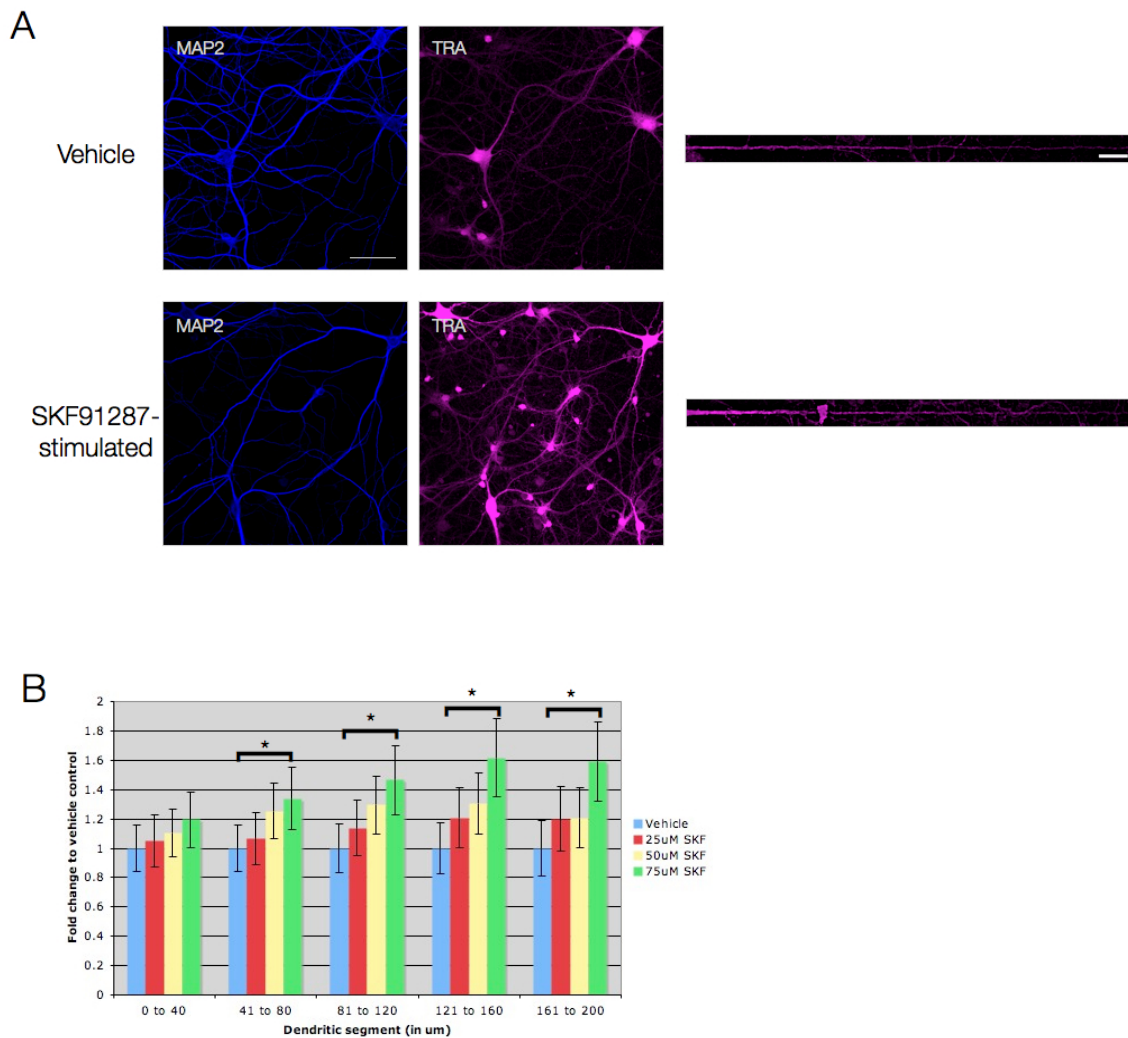


Figure 5.1. SKF81297 stimulation produced an increase in newly synthesized proteins in the distal dendrites. (A) Representative images from dissociated hippocampal cultures (DIV 21) incubated with 4 mM AHA in HBS for 1 hour and stimulated with 40 μ M SKF81297 as applicable. Straightened representative dendrites are shown to the right for each condition. Scalebar = 10 μ m. (B) Dissociated hippocampal cultures were incubated with varying concentrations (25 μ M, 50 μ M, 75 μ M) SKF81297 for 1 hour in 4 mM AHA in HBS. * denotes $p < 0.05$.

Isolating the dendritic compartment

In order to isolate the dendritic proteome, we first attempted to use a Transwell culture system to separate cell bodies from their processes. These cultures utilize a polycarbonate

mesh with a diameter wide enough to permit dendrites, but not cell bodies, to extend through the mesh. We first labeled these cultures with AHA and processed them using FUNCAT to visualize the extent of separation between the somatic and dendritic compartments (Figure 5.2). We found that the majority of dendrites remained on the somatic side of the membrane with minimal extension to the other side. For our mass spectrometry experiments, this preparation would not yield enough material, so we sought another method for the isolation of the dendrites.

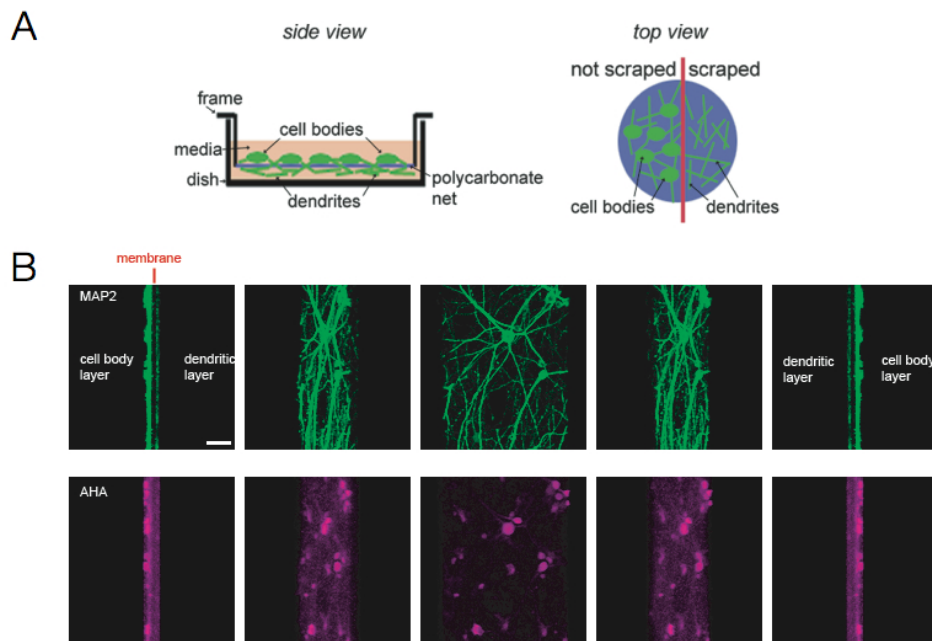


Figure 5.2. Transwell culture system for the isolation of the dendritic compartment. (A) Top and side views of the Transwell culture system. (B) Hippocampal neurons (DIV 14) were incubated with 4 mM AHA for 1.5 hours, processed via FUNCAT, and stained for MAP2. The polycarbonate membrane separating the somatic and dendritic layers is 3 μm thick. Scalebar = 20 μm .

We proceeded to try microdissections in acute hippocampal slices. In Kang and Schuman (1996), dendrites were physically separated from the cell bodies by a

transection along the separation between the stratum pyramidalis and stratum radiatum in the CA1 region of the hippocampus. Using this preparation for our proteomic studies would ensure that the proteins observed would originate dendrites and axons. To modify this preparation for our purposes, we made three additional cuts to completely isolate a chunk of tissue that includes the synaptic neuropil of stratum radiatum, but no principal cell bodies. (Figure 5.3).

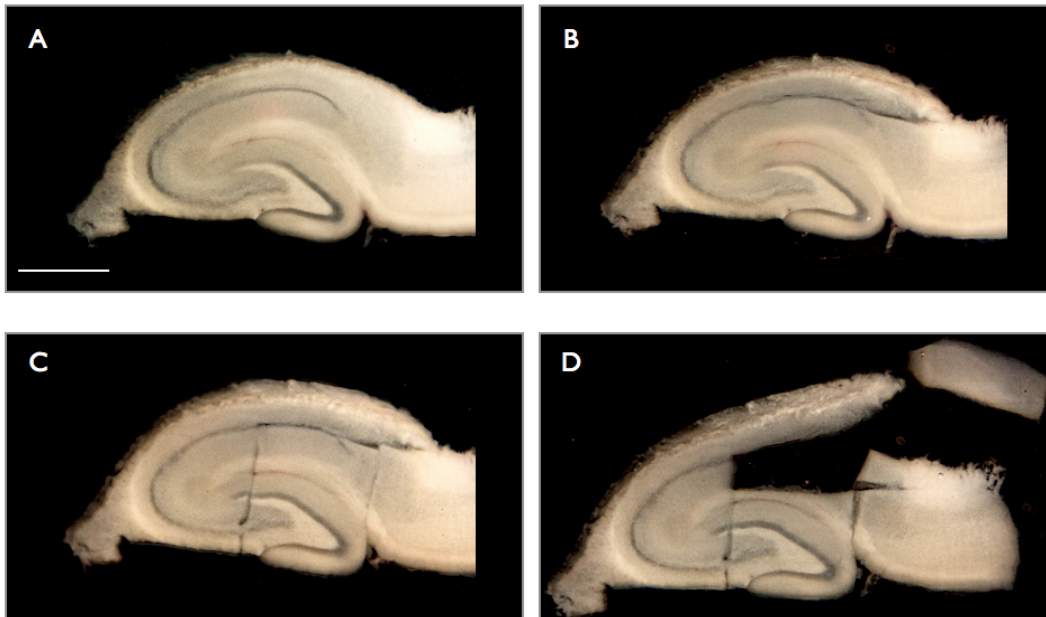


Figure 5.3. Microdissection of a dendritic segment from an acute hippocampal slice. 500 μm -thick acute hippocampal slices isolated from Sprague-Dawley rats (P24-26) are microdissected under a microscope in sequence, from panels A to D. The dissected stratum radiatum is shown in the top right of (D). Scalebar = 1 mm.

The use of ^{13}C -arginine instead of d_{10} -leucine in BONCAT

In our initial experiments, we determined that each condition (control/vehicle and SKF81297-treated) would require the sacrifice of one to two rats to ensure sufficient

material for the mass spectrometry analysis and also for the subsequent candidate confirmation experiments. Dendritic slices (500 μm -thick) were recovered on aCSF for 2 hours prior to noncanonical amino acid incubation and SKF81297 stimulation. In our previous applications of BONCAT, we co-incubated the cells with d_{10} -Leu to provide an additional indication of whether detected proteins were newly synthesized. We initially opted for leucine since it is the most abundant amino acid in the mammalian proteome. In these experiments, we used a different isotopic amino acid, ^{13}C -arginine (^{13}C -Arg). The use of ^{13}C -Arg limits the arginine content of each trypsin-digested peptide to 2, thus reducing the number of potentially modified peptides and the search time during the analysis.

BONCAT for dendritic slices

After recovery on aCSF for 2 hours, the dendritic slices were incubated with 4 mM AHA and 4 mM ^{13}C -Arg in aCSF with and without 40 μM SKF81297 for 2.5 hours before they were harvested and flash-frozen until further processing. Much of the original BONCAT procedure is the same as previously described (Dieterich et al., 2006; Dieterich et al., 2007) until the release of the enriched newly synthesized proteins from the NeutrAvidin agarose resin. For these experiments, we used the DST-alkyne probe to minimize avidin contamination that would result from on-resin trypsination. This allowed for the reduction of the newly synthesized proteins off the resin using β -Me. We found that the mass differences resulting from this probe were detectable via the LTQ-FT and matched when analyzed by the SEQUEST Sorcerer. In the instance of a failed tagging event, there was still a 5.08 atomic mass unit loss compared to methionine. Since the

chemical reduction of the disulfide bond in the DST-alkyne is a reliable event, we do not search for a failed cleavage event, which is an additional benefit to using the DST-alkyne probe instead of the biotin-FLAG-alkyne probe. For a successful cleavage event, there is a 195.18 atomic mass unit gain over methionine. In addition to these modifications, we still search for lysine alkylation, cysteine alkylation, and methionine oxidation, which are standard for proteomics experiments due to the reduction and alkylation of all peptides prior to trypsin digestion.

After trypsin digestion, we also desalt our samples using an HPLC coupled to a reverse-phase resin peptide macrotrap column to remove the urea that is necessary for the denaturation of the proteins. In a MudPIT experiment, the urea can often precipitate and result in clogging of the spray tip, which can often be remedied easily, but can also equally cause a premature termination of the experiment. Though this additional step can potentially cause peptide loss from the extra manipulation and the lack of an in-line delivery system to the LTQ-FT, the advantage consistency between experiments outweighs the disadvantage of potential sample loss.

Bioinformatics processing and criteria

To analyze our data for peptide assignment and protein validation in the past, we conducted post-processing of the data using one of many different types of software bundles that are available to the proteomics community. We primarily used SEQUEST Sorcerer, which automatically processes our data through the Trans-Proteomic Pipeline (TPP), an open-source software package made available by the Institute for Systems Biology. The two components that provide peptide and protein probabilities are

PeptideProphet and ProteinProphet, respectively. After this processing, we assess our data in two different groups: (1) 80% peptide and protein probabilities, doubly tryptic, and at least one peptide for each protein identification; and (2) 90% peptide and 95% protein probabilities, doubly tryptic, and at least two peptides for each protein identification. This allows us to assess both medium and high stringency data sets.

We have completed three complete sets of experiments, each with one vehicle and one SKF81297-treated groups. Ultimately, we only consider the proteins that are present in at least two sample groups by comparing the low-confidence protein lists and the high-confidence protein lists amongst themselves, and also the low and high lists to one another. We have found that there are very few protein identifications from the low-confidence lists that yield interesting protein candidates. In order to compare these lists, we utilize two different programs. The first is Scaffold, a program that is distributed by Proteome Software and is compatible with a number of different database search algorithm output formats (Keller et al., 2002; Nesvizhskii et al., 2003). Scaffold not only allows for the comparison of different datasets side-by-side but also makes it possible to see the different protein identifications with their various modifications and determine the amount of sequence coverage from the various datasets. We also use Cytoscape, which is an open-source software platform that allows for the visualization of proteomic data in a graphical manner (Shannon et al., 2003). It also makes it possible to see the data in the context of molecular interaction networks.

The hippocampal dopaminergic subproteome

Across the three complete datasets that we acquired on the LTQ-FT using MudPIT, we identified a total of 819 unique proteins with 526 of them present in at least two samples (Figure 5.4). One hundred and eleven proteins were common to both the vehicle and SKF81297-treated samples, but there were 177 proteins that were unique to the vehicle group and 179 that were found only in the agonist-treated sample. This difference suggests that either the proteins were in very low abundance and could not be detected even with the enrichment that occurs in BONCAT, or these proteins were selectively expressed or suppressed due to the stimulation of the D1/D5 receptors in the dendrites of the hippocampus.

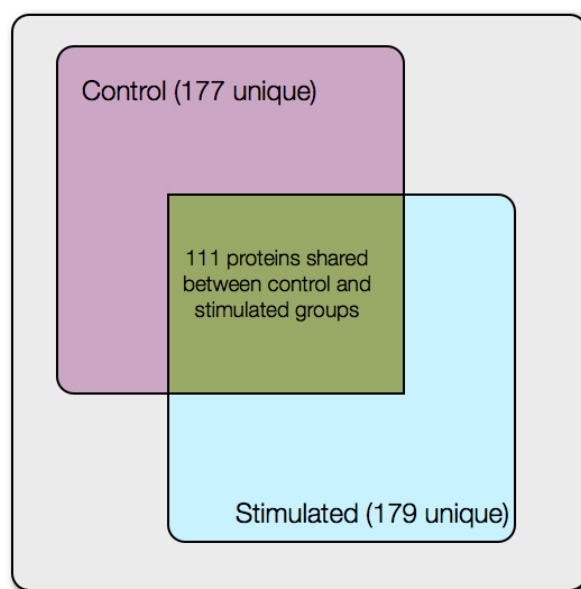


Figure 5.4. Schematic summary of three complete MudPIT experiments. The large gray box represents the 819 unique proteins that were found in the three experiments. The 177 proteins that were found solely in the control group are represented in pink, the 170 proteins unique to the SKF 81297-stimulated group in blue, and the 111 proteins found in both groups in green.

This list of proteins encompasses a variety of different categories. In addition to standard housekeeping proteins, such as those found in glycolysis, there are a number of proteins specific to LTP induction, such as those relevant for excitatory response. A candidate protein that was identified in previous work (Smith et al., 2005), GluR1, was also present in this data as a protein that is expressed in both conditions, but with greater sequence coverage in the agonist-treated sample. In addition, we identified many ribosomal subunits specifically in the D1/D5 agonist-treated sample, with an emphasis on the 60S larger subunit. This, along with the identification of some translation elongation and initiation factors, confirms the dendritic protein synthesis-dependent response of dopaminergic signaling that we observed using FUNCAT (Figure 5.1). Though cytoskeletal proteins are widely abundant, we noticed a marked increase in the number of identified structural proteins, perhaps to accommodate an increase of synaptic contacts induced by the stimulation of the D1/D5 receptors. The more interesting proteins that we observed were from the presynaptic terminal or for cell adhesion. We confirmed some candidates using Western blots. Samples were prepared in the same manner as they were for the proteomic analysis, but in the end they had the additional step of being precipitated so that all of the material could be used for a single blot to maximize detection. Using this approach, we confirmed the upregulation or selective expression of not only GluR1, but also synapsin I, β -catenin, and N-cadherin (Figure 5.5). A number of other proteins were specific to SKF81297-stimulation, such as PKA and CREB, both to be expected due to the D1-like receptors' role in the cAMP pathway. Interestingly, there were also proteins involved in synaptic plasticity, such as the presynaptic proteins bassoon and piccolo, as well as those involved in protein translation, Eef1/2 and Eif4b/e.

In addition, we detected the selective translation of a FMR1-interacting protein (Schenck et al., 2001). This work confirms previous work that there is an upregulation in dendritic protein translation upon the activation of the D1/D5 dopaminergic receptors in the hippocampus. Furthermore, the candidates that we have identified provide greater insight into the wide range of proteins that are potentially involved not only in the maintenance of L-LTP, but also possibly integral to dopaminergic signaling and the treatment of neurodegenerative disease.

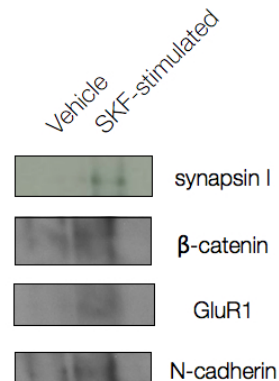


Figure 5.5. Confirmation of candidate proteins via Western blot. Newly synthesized proteins were isolated from dendritic segments incubated with aCSF and 4 mM AHA with and without 40 μ M SKF81297 stimulation for 2.5 hours and Western blotted. The same blot was probed with antibodies against synapsin I, β -catenin, GluR1, and N-cadherin.

Chapter VI

DISCUSSION AND FUTURE DIRECTIONS

The dopaminergic pathway in the hippocampus is thought to participate in the manifestation of neurodegenerative diseases that are characterized by symptoms of memory loss. By utilizing a combination of bioorthogonal chemistry, proteomics, and traditional molecular biology techniques, we have examined two important questions: how much dendritic protein synthesis contributes to the overall neuronal proteome and what is the identity of the proteins influenced by the D1/D5 dopaminergic receptors. Moreover, we have streamlined and improved BONCAT, a method that can be used for proteomic analysis in cell lines as well as in dissociated neuronal cultures and acute hippocampal slices. We also describe the development of FUNCAT for the visualization of newly synthesized proteomes and provide further evidence for local dendritic protein synthesis.

Use of bioorthogonal chemistry in biological applications

There are a number of different methods available that allow researchers to gain further insight into cellular mechanisms, but these often involve genetic manipulation. This not only can produce technical issues of toxicity, but also perturbations to the system under investigation. For example, GFP and other genetically encoded fluorescent proteins need to be overexpressed in a cell, thus upsetting the metabolic balance of the cell. In addition, they are often bulky and can hinder the trafficking or functionality of the protein being studied. Finally, this particular technique is limited to the study of proteins and cannot extend to nucleic acids or posttranslational modifications. There are other options, such as quantum dots, that do not require genetic manipulation, but these present other challenges that do not provide a clear window into the inner workings of the cell.

The concept of bioorthogonal chemistry provides an alternative to these methods since it lends novel chemical functionality to molecules using chemical groups that are not readily found living organisms. Azide-alkyne chemistry has recently come to the forefront due to its specific reactivity and reliability. It has been used to study surface proteins in *E. coli* (Link and Tirrell, 2003; Link et al., 2004), enzymatic reactions (Speers and Cravatt, 2004), protein glycosylation (Agard et al., 2004), and also nucleic acids (Jao and Salic, 2008; Salic and Mitchison, 2008). In addition, a similar type of chemistry that is independent of copper-mediated catalysis, strain-promoted cycloaddition (Baskin et al., 2007), has added to the azide-alkyne arsenal allowing *in vivo* labeling of surface molecules. The widespread interest in azide-alkyne chemistry is primarily due to the nontoxic nature of the azide and alkyne-containing molecules that are introduced to the cell. These noncanonical sugars, amino acids, lipids, metabolites, and nucleic acids do not sterically hinder regular cellular processes, thus providing a more accurate readout of the system under investigation.

With BONCAT, we demonstrated the labeling of mammalian cells with AHA to selectively label newly synthesized proteins (Dieterich et al., 2006; Dieterich et al., 2007). This technique allows for the enrichment of proteins in an unbiased manner, regardless of their molecular weight, relative abundance, and isoelectric point. In Chapter Two, we described the applicability of BONCAT to analyze proteomes in dissociated neuronal cultures and later in organotypic slice cultures and acute hippocampal slices. Then, in Chapter Five, we utilized BONCAT to selectively identify dendritic proteins after a microdissection preparation from acute hippocampal slices. Some protein-labeling techniques are incompatible for use in post-mitotic cells, such as neurons, but since

BONCAT utilizes the endogenous translational machinery this is not an issue. Since the first demonstration of BONCAT, we have established a streamlined protocol that is accessible for different applications (Dieterich et al., 2007). We also have incorporated a mid-protocol control to ensure that the click chemistry reaction worked prior to the affinity purification procedure in which newly synthesized proteins are enriched and isolated for subsequent analysis.

Though the final output of this method can be for Western blot analysis, it is designed to produce a complex sample to be analyzed via mass spectrometry in a top-down approach. To provide the optimal amount of separation of our sample, we use MudPIT (Link et al., 1999; Washburn et al., 2001). MudPIT is preferable to the other options used in the proteomic community (e.g., one-dimensional in-gel trypsination) because it provides the additional benefit of maximum peptide recovery and good resolution for low-abundance proteins. As a result, BONCAT is an excellent technique for the identification of proteins in a complex sample in an unbiased, bioorthogonal manner.

Development of a disulfide-bearing alkyne probe

In Chapter Four, we described the development of a new probe for use with the BONCAT strategy, as an alternative to the biotin-FLAG-alkyne tag. The original biotin-FLAG-alkyne tag was designed to provide two different methods for the purification of the newly synthesized proteins, either using the biotin against an avidin matrix or an antibody-based approach against the FLAG epitope. We found that a second purification step following purification via biotin was unnecessary. In addition, we discovered that

there were a large number of avidin peptides in our proteomics analysis due to the on-resin trypsination step. As a result, we developed a disulfide-bearing alkyne probe that utilizes the biotin-avidin purification as previously described, but allows for the release of the newly synthesized protein from the avidin matrix via chemical reduction by β -Me.

Though in our preliminary experiments there appeared to be no disulfide exchange between cysteines of preexisting or methionine-labeled proteins and the DST-alkyne, we proceeded to develop a strategy to ensure that the high specificity of the azide-alkyne reaction was retained. This revised strategy involved the reduction and subsequent alkylation of cysteine residues prior to the click chemistry reaction. As a result, the cysteines are protected in a manner compatible with proteomic analysis and are not reactive with the DST-alkyne. This improves the ability of BONCAT to be used in the study of complex mixtures, due to the increased chance of identifying low abundance proteins from the removal of the previously confounding and abundant avidin peptides.

AHA versus HPG for BONCAT experiments

Though our experiments have focused on the use of AHA for the labeling of newly synthesized proteomes, there is the possibility of labeling a second protein population with HPG, another methionine surrogate with a terminal alkyne. Previous work suggested that HPG might be at a relative disadvantage in being charged onto the endogenous methionyl tRNA (Kiick et al., 2002). In Chapter Four, we compared the click chemistry reactions of AHA and HPG, side-by-side, using their respective DST probes and observed that there was virtually no difference in incorporation (Figure 4.3). In addition, we found that AHA and HPG application had similar effects on growth rates

(Figure 4.4). Therefore, labeling two protein populations in a pulse-chase style of experiment is a possibility and would provide a powerful tool for investigating the changes that a stimulus can effect upon a proteome.

Development of FUNCAT

We used the same biorthogonal chemistry of BONCAT to develop FUNCAT for the visualization of newly synthesized proteins. We developed a fluorescent alkyne probe, TRA, for the ligation to AHA-labeled proteins. Though there was previous work describing the visualization of Chinese hamster ovary cells labeled with HPG (Beatty et al., 2007), two-photon microscopy is necessary to visualize the 3-azido-7-hydroxycoumarin tag that is used, which eliminates the possibility for *in vivo* imaging. In addition, there is a high degree of background signal, owing to the stickiness of the coumarin molecule, which makes it more difficult to use. To overcome these issues, we developed a different fluorescent tag that could be imaged using conventional fluorescence microscopy, while having greater photostability and significantly lower background.

In Chapter Three, we described FUNCAT and its application for the visualization of the neuronal proteome. In addition, we demonstrated the temporal resolution of FUNCAT. We observed that there are newly synthesized proteins in the soma as early as 10 minutes after AHA application, and in the dendrites after 20 minutes (Figure 3.5). With longer incubations, we could clearly resolve newly synthesized proteins in the distal dendrites. Initial experiments were performed in dissociated neuronal cultures, but we also applied FUNCAT to organotypic slice cultures.

We also extended FUNCAT to include another fluorescent tag that could be conjugated to HPG-labeled proteins, resulting in the ability to image proteins in two different colors, both with high specificity and high signal-to-noise. With these two methionine surrogates and respective fluorescent tags available, we proceeded to investigate the possibility of visualizing two distinct proteomes. We show that HPG labeling prior to AHA incubation yields the best results, and that the ligation of the TRA tag prior to the FLA tag is preferable (Figure 3.4). With FUNCAT, we have developed a method for the visualization of newly synthesized proteomes with temporal resolution.

Visualization of locally dendritic proteomes using FUNCAT

In order to explore the spatial resolution of FUNCAT, we decided to utilize local perfusion techniques to locally apply chemical stimuli as well as AHA to demonstrate dendritic protein synthesis. For this, we explored the effects of the BDNF, a neurotrophic factor that has been demonstrated to be critical for LTP and for the stimulation of local protein translation (Kang and Schuman, 1996; Aakalu et al., 2001). Our initial experiments displayed a 60% increase of FUNCAT-derived protein synthesis signal in the distal regions of the dendrites (Figure 3.6), thus setting the stage for our local perfusion experiments.

By locally perfusing the protein synthesis inhibitor anisomycin over the cell body, we effectively prevented the somatic contribution to the dendritic proteome. We applied AHA with and without BDNF in the bath of dissociated hippocampal neurons to discern whether BDNF would produce a change in the distal regions of the dendrites. In comparing the neurons that were perfused, we observed a significant increase in the

levels of protein synthesis in BDNF-stimulated dendrites (Figure 3.8). As a result, we demonstrated the ability to use FUNCAT to resolve a localized region of the neuron and the phenomenon of dendritic translation. This provides evidence for the quick translational response that is necessary for synaptic plasticity.

Elucidating the hippocampal dopaminergic subproteome

With the ability to identify and visualize newly synthesized proteomes, we decided to explore the dendritic hippocampal proteome under the effects of D1/D5 dopaminergic receptor stimulation. As described in Chapter Five, we used FUNCAT to visualize a dendrite-specific increase in protein synthesis upon the application of the D1-like receptor agonist SKF81297 (Figure 5.1), which confirmed previous observations (Smith et al., 2005). In order to specifically identify these dendritically synthesized proteins, we performed microdissections of the stratum radiatum in the CA1 of rat hippocampi. The tissue was then subjected to stimulation by SKF81297 concurrently applied with AHA and ^{13}C -Arg for labeling of the newly synthesized proteins. The SKF81297-stimulated and control samples were processed via BONCAT and analyzed by mass spectrometry. We found nearly 200 proteins that were unique to either the control or stimulated samples, with just over 100 proteins that were shared between the two groups. Strikingly, we identified a total of 819 unique proteins over three independent experiments.

This work represents the first full demonstration of the modified BONCAT strategy with the incorporation of the ^{13}C -Arg as an internal control as well as the use of the DST-alkyne probe, which prevents no avidin contamination. Previously published BONCAT-related work describes the HEK293 proteome (Dieterich et al., 2006), but we

have shown the technique's applicability in acute hippocampal slices. Furthermore, this is the first proteomic glimpse into the dendrite-specific contribution to the overall neuronal proteome. With just over 800 unique proteins synthesized over the course of 2.5 hours, we bolster the importance of the immediate translational response in the dendrites. Finally, we also provide a series of new candidates that are separate from the previously identified PKA/cAMP pathway that is implicated in D1-like receptor signaling. From our preliminary observations, stimulation of the D1/D5 receptors results in the synthesis of presynaptic proteins and cell adhesion molecules.

Future directions

With the exciting development of BONCAT and FUNCAT, this work reveals a few of the applications in which they can increase the experimental reach of more limited traditional techniques. One major improvement would be to adapt BONCAT for the quantification of proteins to supplement the identification that is already possible. We utilize one reagent that is commonly used in SILAC in this work, ^{13}C -Arg, but due to the post-mitotic state of neurons, it is a very expensive endeavor to achieve the required complete amino acid exchange. Perhaps a similar strategy to ICAT could be used for the labeling of the proteins, but it would need to be compatible with the alkylation protocol that should be used in conjunction with the DST probes. The quantification of proteins would provide a more precise view of the effects of stimuli.

FUNCAT can also benefit from additional developments, especially for *in vivo* intracellular imaging. Though there is progress with the difluorinated cyclooctyne probes (Baskin et al., 2007), these are currently limited to the visualization of surface molecules,

such as receptors, and cannot access the intracellular space. In addition, the cyclooctynes, due to their ring strain, are highly reactive and could result in greater background signal. Perhaps a patch-pipette delivery of a modified, copper catalysis-independent fluorescent probe would provide the access that is necessary. Permeabilization using detergents can often be deleterious to cellular health and result in poor molecular trafficking that is not indicative of endogenous states. The development of an intracellular, *in vivo* version of FUNCAT coupled with local perfusion would allow for the investigation of the fates of a local proteome.

Aside from technique development, it would be interesting to further study the effects of D1/D5 dopaminergic receptors on learning and memory by combining BONCAT with behavioral studies. Transgenic mice with modifications to the receptors and fed with AHA-containing chow (as well as those lacking this receptor class) would yield interesting information about their proteomes. This series of experiments would provide information that cannot be obtained otherwise by chemical stimuli, which is a more transient change. After this initial baseline assessment of the proteome, behavioral tasks would presumably induce small changes in the proteome that perhaps could be captured with BONCAT. It would be interesting to harvest tissue from the different regions of the murine brain to examine protein synthesis in other brain areas during learning. This sort of work would give insight into the overall plasticity of the brain to adapt to deficiencies in signaling and also the different mechanisms for memory formation and storage.

Work Cited

- Aakalu, G., Smith, W.B., Nguyen, N., Jiang, C., and Schuman, E.M. (2001). Dynamic visualization of local protein synthesis in hippocampal neurons. *Neuron* *30*, 489-502.
- Abi-Dargham, A., Mawlawi, O., Lombardo, I., Gil, R., Martinez, D., Huang, Y., Hwang, D.R., Kelip, J., Kochan, L., Van Heertum, R., Gorman, J.M., and Laruelle, M. (2002). Prefrontal dopamine D1 receptors and working memory in schizophrenia. *J Neurosci.* *22*, 3708-3719.
- Adcock, R.A., Thangavel, A., Whitfield-Gabrieli, S., Knutson, B., and Gabrieli, J.D. (2006). Reward-motivated learning: mesolimbic activation precedes memory formation. *50*, 507-517.
- Agard, N.J., Prescher, J.A., and Bertozzi, C.R. (2004). A strain-promoted [3 + 2] azide-alkyne cycloaddition for covalent modification of biomolecules in living systems. *J Am Chem Soc* *126*, 15046-15047.
- Andersen, P.H., Gronvald, F.C., Hohlweg, R., Hansen, L.B., Guddal, E., Braestrup, C., and Nielsen, E.B. (1992). NNC-112, NNC-687 and NNC-756, new selective and highly potent dopamine D1 receptor antagonists. *Eur J Pharmacol.* *219*, 45-52.
- Andersen, J.S., Lam, Y.W., Leung, A.K., Ong, S.E., Lyon, C.E., Lamond, A.I., and Mann, M. (2005). Nucleolar proteome dynamics. *Nature* *433*, 77-83.
- Bach, M.E., Barad, M., Son, H., Zhuo, M., Lu, Y.F., Shih, R., Mansuy, I., Hawkins, R.D., and Kandel, E.R. (1999). Age-related defects in spatial memory are correlated with defects in the late phase of hippocampal long-term potentiation in vitro and are attenuated by drugs that enhance the cAMP signaling pathway. *Proc Natl Acad Sci USA* *96*, 5280-5285.
- Backman, L., and Farde, L. (2001). Dopamine and cognitive functioning: brain imaging findings in Huntington's disease and normal aging. *Scand J Psychol.* *42*, 287-296.
- Baskin, J.M., Prescher, J.A., Laughlin, S.T., Agard, N.J., Chang, P.V., Miller, I.A., Lo, A., Codelli, J.A., and Bertozzi, C.R. (2007). Copper-free click chemistry for dynamic in vivo imaging. *Proc Natl Acad Sci USA* *104*, 16793-16797.
- Beatty, K.E., Liu, J.C., Xie, F., Dieterich, D.C., Schuman, E.M., Wang, Q., and Tirrell, D.A. (2006). Fluorescence visualization of newly synthesized proteins in Mammalian cells. *Angew Chem Int Ed Engl* *45*, 7364-7367.
- Bergson, C., Mrzljak, L., Smiley, J.F., Pappy, M., Levenson, R., and Goldman-Rakic, P.S. (1995). Regional, cellular, and subcellular variations in the distribution of D1 and D5 dopamine receptors in primate brain. *J Neurosci* *15*, 7821-7836.

- Bernabeu, R., Bevilaqua, L., Ardenghi, P., Bromberg, E., Schmitz, P., Bianchin, M., Izquierdo, I., and Medina, J.H. (1997). Involvement of hippocampal cAMP/cAMP-dependent protein kinase signaling pathways in a late memory consolidation phase of aversively motivated learning in rats. *Proc Natl Acad Sci USA* *94*, 7041-7046.
- Bliss, T.V., and Lomo, T. (1973). Long-lasting potentiation of synaptic transmission in the dentate area of the anaesthetized rabbit following stimulation of the perforant path. *J. Physiol.* *232*, 331-356.
- Bodian, D. (1965). A suggestive relationship of nerve cell RNA with specific synaptic sites. *Proc Natl Acad Sci USA*. *53*, 418-425.
- Bourne, J.N., Sorra, K.E., Hurlburt, J., and Harris, K.M. (2007). Polyribosomes are increased in spines of CA1 dendrites 2 h after the induction of LTP in mature rat hippocampal slices. *Hippocampus* *17*, 1-4.
- Bradshaw, K.D., Emptage, N.J., and Bliss, T.V. (2003). A role for dendritic protein synthesis in hippocampal late LTP. *Eur J Neurosci* *18*, 3150-3152.
- Brembs, B., Lorenzetti, F.D., Reyes, F.D., Baxter, D.A., and Byrne, J.H. (2002). Operant reward learning in *Aplysia*: neuronal correlates and mechanisms. *Science* *296*, 1706-1709.
- Bussink, A.P., Van Swieten, P.F., Ghauharali, K., Scheij, S., Van Eijk, M., Wennekes, T., Van Der Marel, G.A., Boot, R.G., Aerts, J.M.F.G., and Overkleeft, H.S. (2007). N-Azidoacetylmannosamine-mediated chemical tagging of gangliosides. *The Journal of Lipid Research* *48*, 1417-1421.
- Carboni, B., Benalil, A., and Vaultier, M. (1993). Aliphatic amino azides as key building blocks for efficient polyamine syntheses. *J Org Chem* *58*, 3736-3741.
- Castner, S.A., and Goldman-Rakic, P.S. (2004). Enhancement of working memory in aged monkeys by a sensitizing regimen of dopamine D1 receptor stimulation. *J Neurosci* *24*, 1446-1450.
- Chang, E.J., Archambault, V., McLachlin, D.T., Krutchinsky, A.N., and Chait, B.T. (2004). Analysis of protein phosphorylation by hypothesis-driven multiple-stage mass spectrometry. *Anal Chem.* *76*, 4472-4483.
- Codelli, J.A., Baskin, J.M., Agard, N.J., and Bertozzi, C.R. (2008). Second-generation difluorinated cyclooctynes for copper-free click chemistry. *J Am Chem Soc* *130*, 11486-11493.

- Corkin, S., Amaral, D.G., González, R.G., Johnson, K.A., and Hyman, B.T. (1997). H.M.'s medial temporal lobe lesion: findings from magnetic resonance imaging. *J Neurosci.* *17*, 3964-3979.
- Craig, R., and Beavis, R.C. (2004). TANDEM: matching proteins with tandem mass spectra. *Bioinformatics.* *20*, 1466-1467.
- Dahlstrom, A., and Fuxe, K. (1964). Localization of monoamines in the lower brain stem. *Experientia.* *20*, 398-399.
- Davis, H.P., and Squire, L.R. (1984). Protein synthesis and memory: a review. *Psych Bull.* *96*, 518-559.
- de Godoy, L.M.F., Olsen, J.V., Cox, J., Nielsen, M.L., Hubner, N.C., Fröhlich, F., Walther, T.C., and Mann, M. (2008). Comprehensive mass-spectrometry-based proteome quantification of haploid versus diploid yeast. *Nature* *455*, 1251-1254.
- de Godoy, L.M.F., Olsen, J.V., de Souza, G.A., Li, G., Mortensen, P., and Mann, M. (2006). Status of complete proteome analysis by mass spectrometry: SILAC labeled yeast as a model system. *Genome Biol* *7*, R50.
- Deiters, A., Cropp, T.A., Mukherji, M., Chin, J.W., Anderson, J.C., and Schultz, P.G. (2003). Adding amino acids with the novel reactivity to the genetic code of *Saccharomyces cerevisiae*. *J Am Chem Soc.* *125*, 11782-11783.
- Dieterich, D.C., Lee, J.J., Link, A.J., Graumann, J., Tirrell, D.A., and Schuman, E.M. (2007). Labeling, detection and identification of newly synthesized proteomes with bioorthogonal non-canonical amino-acid tagging. *Nature protocols* *2*, 532-540.
- Dieterich, D.C., Link, A.J., Graumann, J., Tirrell, D.A., and Schuman, E.M. (2006). Selective identification of newly synthesized proteins in mammalian cells using bioorthogonal noncanonical amino acid tagging (BONCAT). *Proc Natl Acad Sci U S A* *103*, 9482-9487.
- Douglas, R.M., and Goddard, G.V. (1975). Long-term potentiation of the perforant path-granule cell synapse in the rat hippocampus. *Brain Res.* *86*, 205-215.
- Dube, D.H., Prescher, J.A., Quang, C.N., and Bertozzi, C.R. (2006). Probing mucin-type O-linked glycosylation in living animals. *Proc Natl Acad Sci U S A* *103*, 4819-4824.
- Eng, J., McCormack, A.L., and Yates, A.J. (1994). An approach to correlate tandem mass spectral data of peptides with amino acid sequences in a protein database. *J Am Soc Mass Spectrom* *5*, 976-989.
- Engert, F., and Bonhoeffer, T. (1999). Dendritic spine changes associated with hippocampal long-term synaptic plasticity. *Nature.* *399*, 66-70.

Ernfors, P., Kucera, J., Lee, K.F., Loring, J., and Jaenisch, R. (1995). Studies on the physiological role of brain-derived neurotrophic factor and neurotrophin-3 in knockout mice. *Int J Dev Biol.* *39*, 799-807.

Feig, S., and Lipton, P. (1993). Pairing the cholinergic agonist carbachol with patterned Schaffer collateral stimulation initiates protein synthesis in hippocampal CA1 pyramidal cell dendrites via a muscarinic, NMDA-dependent mechanism. *J Neurosci.* *13*, 1010-1021.

Flexner, J.B., Flexner, L.B., and Stellar, E. (1963). Memory in mice as affected by intracerebral puromycin. *Science.* *141*, 57-59.

Floresco, S.B., Todd, C.L., and Grace, A.A. (2001). Glutamatergic afferents from the hippocampus to the nucleus accumbens regulate activity of ventral tegmental area dopamine neurons. *J Neurosci* *21*, 4915-4922.

Freeman, W.M., and Hemby, S.E. (2004). Proteomics for protein expression profiling in neuroscience. *Neurochem Res* *29*, 1065-1081.

Frey, U., Huang, Y.Y., and Kandel, E.R. (1993). Effects of cAMP simulate a late stage of LTP in hippocampal CA1 neurons. *Science* *260*, 1661-1664.

Frey, U., Krug, M., Reymann, K.G., and Matthies, H. (1988). Anisomycin, an inhibitor of protein synthesis, blocks late phases of LTP phenomena in the hippocampal CA1 region in vitro. *Brain Res.* *452*, 57-65.

Frey, U., Matthies, H., and Reymann, K.G. (1991). The effect of dopaminergic D1 receptor blockade during tetanization on the expression of long-term potentiation in the rat CA1 region in vitro. *Neurosci Lett* *129*, 111-114.

Garcia, B.A., Shabanowitz, J., and Hunt, D.F. (2005). Analysis of protein phosphorylation by mass spectrometry. *Methods.* *35*, 256-264.

Gasbarri, A., Packard, M.G., Campana, E., and Pacitti, C. (1994). Anterograde and retrograde tracing of projections from the ventral tegmental area to the hippocampal formation in the rat. *Brain Res Bull.* *33*, 445-452.

Gasbarri, A., Sulli, A., Innocenzi, R., Pacitti, C., and Brioni, J.D. (1996). Spatial memory impairment induced by lesion of the mesohippocampal dopaminergic system in the rat. *Neuroscience.* *74*, 1037-1044.

Gogolla, N., Galimberti, I., DePaola, V., and Caroni, P. (2006). Preparation of organotypic hippocampal slice cultures for long-term live imaging. *Nat Protoc.* *1*, 1165-1171.

- Goldberg, T.E., Bigelow, L.B., Weinberger, D.R., Daniel, D.G., and Kleinman, J.E. (1991). Cognitive and behavioral effects of the coadministration of dextroamphetamine and haloperidol in schizophrenia. *Am J Psychiatry*. *148*, 78-84.
- Goldsmith, S.K., and Joyce, J.N. (1994). Dopamine D2 receptor expression in hippocampus and parahippocampal cortex of rat, cat, and human in relation to tyrosine hydroxylase-immunoreactive fibers. *Hippocampus*. *4*, 354-373.
- Graumann, J., Dunipace, L.A., Seol, J.H., McDonald, W.H., Yates, J.R., 3rd, Wold, B.J., and Deshaies, R.J. (2004). Applicability of tandem affinity purification MudPIT to pathway proteomics in yeast. *Mol Cell Proteomics* *3*, 226-237.
- Greengard, P. (2001). The neurobiology of slow synaptic transmission. *Science* *294*, 1024-1030.
- Gronberg, M., Kristiansen, T.Z., Iwahori, A., Chang, R., Reddy, R., Sato, N., Molina, H., Jensen, O.N., Hruban, R.H., Goggins, M.G., et al. (2006). Biomarker discovery from pancreatic cancer secretome using a differential proteomic approach. *Mol Cell Proteomics*, *5*, 157-171.
- Gygi, S.P., Rist, B., Gerber, S.A., Turecek, F., Gelb, M.H., and Aebersold, R. (1999). Quantitative analysis of complex protein mixtures using isotope-coded affinity tags. *Nat Biotechnol* *17*, 994-999.
- Hang, H.C., Yu, C., Kato, D.L., and Bertozzi, C.R. (2003). A metabolic labeling approach toward proteomic analysis of mucin-type O-linked glycosylation. *Proc Natl Acad Sci USA*. *100*, 14846-14851.
- Hangauer, M.J., and Bertozzi, C.R. (2008). A FRET-Based Fluorogenic Phosphine for Live-Cell Imaging with the Staudinger Ligation. *Angew. Chem. Int. Ed.* *47*, 2394-2397.
- Hebb, D.O. (1949). *The Organization of Behavior: A Neuropsychological Theory* (New York: John Wiley & Sons).
- Hendrickson, W.A., Horton, J.R., and LeMaster, D.M. (1990). Selenomethionyl proteins produced for analysis by multiwavelength anomalous diffraction (MAD): a vehicle for direct determination of three-dimensional structure. *EMBO J.* *9*, 1665-1672.
- Hiller, YI, Gershoni, J.M., Bayer, E.A., and Wilchek, M. (1987). Biotin binding to avidin. Oligosaccharide side chain not required for ligand association. *Biochem J.* *248*, 167-171.
- Huang, Y.Y., and Kandel, E.R. (1994). Recruitment of long-lasting and protein kinase A-dependent long-term potentiation in the CA1 region of hippocampus requires repeated tetanization. *Learn Mem.* *1*, 74-82.

- Huang, Y.Y., and Kandel, E.R. (1995). D1/D5 receptor agonists induce a protein synthesis-dependent late potentiation in the CA1 region of the hippocampus. *Proc Natl Acad Sci USA* *92*, 2446-2450.
- Huber, K.M., Kayser, M.S., and Bear, M.F. (2000). Role for rapid dendritic protein synthesis in hippocampal mGluR-dependent long-term depression. *Science* *288*, 1254-1257.
- Ihalainen, J.A., Riekkinen, P. Jr., and Feenstra, M.G. (1999). Comparison of dopamine and noradrenaline release in mouse prefrontal cortex, striatum and hippocampus using microdialysis. *Neurosci Lett.* *277*, 71-74.
- Jao, C.Y., and Salic, A. (2008). Exploring RNA transcription and turnover in vivo by using click chemistry. *Proc Natl Acad Sci USA* *105*, 15779-15784.
- Jencks, W.P. (1959). Studies on the mechanism of oxime and semicarbazone formation. *J Am Chem Soc.* *81*, 475-481.
- Job, C., and Eberwine, J. (2001). Identification of sites for exponential translation in living dendrites. *Proc Natl Acad Sci U S A* *98*, 13037-13042.
- Kaji, H., Saito, H., Yamauchi, Y., Shinkawa, T., Taoka, M., Hirabayashi, J., Kasai, K., Takahashi, N., and Isobe, T. (2003). Lectin affinity capture, isotope-coded tagging and mass spectrometry to identify N-linked glycoproteins. *Nat Biotechnol.* *21*, 667-672.
- Kang, H., and Schuman, E.M., (1996). A requirement for local protein synthesis in neurotrophin-induced hippocampal synaptic plasticity. *Science.* *273*, 1402-1406.
- Kang, H., Welcher, A.A., Shelton, D., and Schuman, E.M. (1997). Neurotrophins and time: different roles for TrkB signaling in hippocampal long-term potentiation. *Neuron* *19*, 653-664.
- Keller, A., Nesvizhskii, A.I., Kolker, E., and Aebersold, R. (2002). Empirical statistical model to estimate the accuracy of peptide identifications made by MS/MS and database search. *Anal Chem.* *74*, 5383-5392.
- Khan, Z.U., Gutierrez, A., Martin, R., Penafiel, A., Rivera, A., and de la Calle, A. (2000). Dopamine D5 receptors of rat and human brain. *Neuroscience.* *100*, 689-699.
- Khidekel, N., Ficarro, S.B., Peters, E.C., and Hsieh-Wilson, L.C. (2004). Exploring the O-GlcNAc proteome: direct identification of O-GlcNAc-modified proteins from the brain. *Proc Natl Acad Sci U S A* *101*, 13132-13137.
- Kiick, K.L., Saxon, E., Tirrell, D.A., and Bertozzi, C.R. (2002). Incorporation of azides into recombinant proteins for chemoselective modification by the Staudinger ligation. *Proc Natl Acad Sci U S A* *99*, 19-24.

Kolb, H.C., and Sharpless, K.B. (2003). The growing impact of click chemistry on drug discovery. *Drug Discov Today*. 8, 1128-1137.

Krug, M., Lossner, B., and Ott, T. (1984). Anisomycin blocks the late phase of long-term potentiation in the dentate gyrus of freely moving rats. *Brain Res Bull*. 13, 39-42.

Kruger, M., Moser, M., Ussar, S., Thievensen, I., Lubner, C., Forner, F., Schmidt, S., Zanivan, S., Fassler, R., and Mann, M. (2008). SILAC Mouse for Quantitative Proteomics Uncovers Kindlin-3 as an Essential Factor for Red Blood Cell Function. *Cell* 134, 353-364.

Laitinen, O.H., Hytonen, V.P., Nordlund, H.R., and Kulomaa, M.S. (2006). Genetically engineered avidins and streptavidins. *Cell Mol Life Sci*. 63, 2992-3017.

Lamarre-Vincent, N., and Hsieh-Wilson, L.C. (2003). Dynamic glycosylation of the transcription factor CREB: A potential role in gene regulation. *J Am Chem Soc* 125, 6612-6613.

Laughlin, S.T., Baskin, J.M., Amacher, S.L., and Bertozzi, C.R. (2008). In vivo imaging of membrane-associated glycans in developing zebrafish. *Science* 320, 664-667.

Laurier, L.G., O'Dowd, B.F., and George, S.R. (1994). Heterogeneous tissue-specific transcription of dopamine receptor subtype messenger RNA in rat brain. *Brain Res Mol Brain Res*. 25, 344-350.

Lee, F.J., Xue, S., Pei, L., Vukusic, B., Chery, N., Wang, Y., Wang, Y.T., Niznik, H.B., Yu, X.M., and Liu, F. (2002). Dual regulation of NMDA receptor functions by direct protein-protein interacts with the dopamine D1 receptor. *Cell* 111, 219-230.

Legault, M., Rompré, P.P., and Wise, R.A. (2000). Chemical stimulation of the ventral hippocampus elevates nucleus accumbens dopamine by activating dopaminergic neurons of the ventral tegmental area. *J Neurosci* 20, 1635-1642.

Levy, F., and Farrow, M. (2001). Working memory in ADHD: prefrontal/parietal connections. *Curr Drug Targets*. 2, 347-352.

Liao, L., Park, S.K., Xu, T., Vanderklish, P., and Yates, J.R. (2008). Quantitative proteomic analysis of primary neurons reveals diverse changes in synaptic protein content in *fmr1* knockout mice. *Proc Natl Acad Sci USA* 105, 15281-15286.

Liao, L., Pilotte, J., Xu, T., Wong, C., Edelman, G., Vanderklish, P., and Yates, J.R. (2007). BDNF Induces Widespread Changes in Synaptic Protein Content and Up-Regulates Components of the Translation Machinery: An Analysis Using High-Throughput Proteomics. *J. Proteome Res*. 6, 1059-1071.

- Lilley, K.S., and Friedman, D.B. (2004). All about DIGE: quantification technology for differential-display 2D-gel proteomics. *Expert Rev Proteomics* *1*, 401-409.
- Link, A.J., Eng, J., Schieltz, D.M., Carmack, E., Mize, G.J., Morris, D.R., Garvik, B.M., and Yates, J.R., 3rd (1999). Direct analysis of protein complexes using mass spectrometry. *Nat Biotechnol* *17*, 676-682.
- Link, A.J., and Tirrell, D.A. (2003). Cell surface labeling of *Escherichia coli* via copper(I)-catalyzed [3+2] cycloaddition. *J Am Chem Soc* *125*, 11164-11165.
- Link, A.J., Vink, M.K., and Tirrell, D.A. (2004). Presentation and detection of azide functionality in bacterial cell surface proteins. *J Am Chem Soc* *126*, 10598-10602.
- Link, A.J., Vink, M.K.S., and Tirrell, D.A. (2007). Preparation of the functionalizable methionine surrogate azidohomoalanine via copper-catalyzed diazo transfer. *Nature Protocols* *2*, 1879-1883.
- Lippincott-Schwartz, J., and Patterson, G.H. (2003). Development and use of fluorescent protein markers in living cells. *Science* *300*, 87-91.
- Lonze, B.E., and Ginty, D.D. (2002). Function and regulation of CREB family transcription factors in the nervous system. *Neuron* *35*, 605-623.
- MacCoss, M.J., Wu, C.C., Liu, H., Sadygov, R., and Yates, J.R., 3rd (2003). A correlation algorithm for the automated quantitative analysis of shotgun proteomics data. *Anal Chem* *75*, 6912-6921.
- Madras, B.K., Miller, G.M., and Fischman, A.J. (2005). The dopamine transporter and attention-deficit/hyperactivity disorder. *Biol Psychiatry* *57*, 1397-1409.
- Malgaroli, A., and Tsien, R.W. (1992). Glutamate-induced long-term potentiation of the frequency of miniature synaptic currents in cultured hippocampal neurons. *Nature*. *357*, 134-139.
- Matthies, H., Becker, A., Schroeder, H., Kraus, J., Holtt, V., and Krug, M. (1997). Dopamine D1-deficient mutant mice do not express the late phase of hippocampal long-term potentiation. *Neuroreport* *8*, 3533-3535.
- Meador-Woodruff, J.H., Mansour, A., Grandy, D.K., Damask, S.P., Civelli, O., and Watson, S.J. Jr. (1992). Distribution of D5 dopamine receptor mRNA in rat brain. *Neurosci Lett*. *145*, 209-212.
- Meinzel, T., Peynot, P., and Giglione, C. (2005). Processed N-termini of mature proteins in higher eukaryotes and their major contribution to dynamic proteomics. *Biochimie*. *87*, 701-712.

- Miller, S., Yasuda, M., Coats, J.K., Jones, Y., Martone, M.E., and Mayford, M. (2002). Disruption of dendritic translation of CaMKIIalpha impairs stabilization of synaptic plasticity and memory consolidation. *Neuron* 36, 507-519.
- Milner, B. (1959). The memory defect in bilateral hippocampal lesions. *Psych Res Rep* 11, 43-58.
- Missale, C., Nash, S.R., Robinson, S.W., Jaber, M., and Caron, M.G. (1998). Dopamine receptors: from structure to function. *Physiol Rev* 78, 189-225.
- Montarolo, P.G., Goelet, P., Castellucci, V.F., Morgan, J., Kandel, E.R., and Schacher, S. (1986). A critical period for macromolecular synthesis in long-term heterosynaptic facilitation in *Aplysia*. *Science* 234, 1249-1254.
- Morris, R.G., Anderson, E., Lynch, G.S., and Baudry, M. (1986). Selective impairment of learning and blockade of long-term potentiation by an N-methyl-D-aspartate receptor antagonist, AP5. *Nature* 319, 774-776.
- Nessen, M.A., Kramer, G., Back, J., Baskin, J.M., Smeenk, L.E., de Koning, I.J., van Maarseveen, J.H., de Jong, L., Bertozzi, C.R., Hiemstra, H., and de Koster, C.G. (2009). Selective enrichment of azide-containing peptides from complex mixtures. *J Proteome Res* 8, 3702-3711.
- Nesvizhskii, A.I., Keller, A., Kolker, E., and Aebersold, R. (2003). Statistical model for identifying proteins by tandem mass spectrometry. *Anal Chem* 75, 4646-4658.
- Ngo, J.T., Champion, J.A., Mahdavi, A., Tanrikulu, I.C., Beatty, K.E., Connor, R.E., Yoo, T.H., Dieterich, D.C., Schuman, E.M., and Tirrell, D.A. (2009). Cell-selective metabolic labeling of proteins. *Nature Chem Biol* 5, 715-717.
- Nguyen, P.V., Abel, T., and Kandel, E.R. (1994). Requirement of a critical period of transcription for induction of a late phase of LTP. *Science* 265, 1104-1107.
- Nguyen, P.V., and Woo, N.H. (2003). Regulation of hippocampal synaptic plasticity by cyclic AMP-dependent protein kinases. *Prog Neurobiol* 71, 401-437.
- Nieouillon, A. (2002). Dopamine and the regulation of cognition and attention. *Prog Neurobiol* 67, 53-83.
- O'Dowd, B.F. (1993). Structure of dopamine receptors. *J Neurochem* 60, 804-816.
- Ong, S.-E., Blagoev, B., Kratchmarova, I., Kristensen, D.B., Steen, H., Pandey, A., and Mann, M. (2002). Stable isotope labeling by amino acids in cell culture, SILAC, as a simple and accurate approach to expression proteomics. *Mol Cell Proteomics* 1, 376-386.

- Ostroff, L.E., Fiala, J.C., Allwardt, B., and Harris, K.M. (2002). Polyribosomes redistribute from dendritic shafts into spines with enlarged synapses during LTP in developing rat hippocampal slices. *Neuron* 35, 535-545.
- Pandey, A., and Mann, M. (2000). Proteomics to study genes and genomes. *Nature* 405, 837-846.
- Pawlik, T.M., Hawke, D.H., Liu, Y., Krishnamurthy, S., Fritsche, H., Hunt, K.K., and Kuerer, H.M. (2006). Proteomic analysis of nipple aspirate fluid from women with early-stage breast cancer using isotope-coded affinity tags and tandem mass spectrometry reveals differential expression of vitamin D binding protein. *BMC Cancer*. 6, 68.
- Perkin, D.N., Pappin, D.J., Creasy, D.M., and Cottrell, J.S. (1999). Probability-based protein identification by searching sequence databases using mass spectrometry data. *Electrophoresis*. 20, 3551-3567.
- Peters, E.C., Brock, A., and Ficarro, S.B. (2004). Exploring the phosphoproteome with mass spectrometry. *Mini Rev Med Chem* 4, 313-324.
- Prescher, J.A., and Bertozzi, C.R. (2005). Chemistry in living systems. *Nat Chem Biol* 1, 13-21.
- Prescher, J.A., Dube, D.H., and Bertozzi, C.R. (2004). Chemical remodelling of cell surfaces in living animals. *Nature* 430, 873-877.
- Rao, A., and Steward, O. (1991). Evidence that protein constituents of postsynaptic membrane specializations are locally synthesized: analysis of proteins synthesized within synaptosomes. *J Neurosci*. 11, 2881-2895.
- Rideout, D., Calogeropoulou, T., Jaworski, J., and McCarthy, M. (1990). Synergism through direct covalent bonding between agents: a strategy for rational design of chemotherapeutic combinations. *Biopolymers*. 29, 247-262.
- Rinne, J.O., Portin, R., Ruottinen, H., Nurmi, E., Bergman, J., Haaparanta, M., and Solin, O. (2000). Cognitive impairment and the brain dopaminergic system in Parkinson disease: [18F]fluorodopa positron emission tomographic study. *Arch Neurol*. 57, 470-475.
- Ross, P.L., Huang, Y.N., Marchese, J.N., Williamson, B., Parker, K., Hattan, S., Khainovski, N., Pillai, S., Dey, S., Daniels, S., *et al.* (2004). Multiplexed protein quantitation in *Saccharomyces cerevisiae* using amine-reactive isobaric tagging reagents. *Mol Cell Proteomics* 3, 1154-1169.
- Rostovtsev, V.V., Green, L.G., Fokin, V.V., and Sharpless, K.B. (2002). A stepwise Huisgen cycloaddition process: copper(I)-catalyzed regioselective "ligation" of azides and terminal alkynes. *Angew Chem Int Ed Engl* 41, 2596-2599.

Sajikumar, S., and Frey, J.U. (2004). Late-associativity, synaptic tagging, and the role of dopamine during LTP and LTD. *Neurobiol Learn Mem.* 82, 12-25.

Salic, A., and Mitchison, T.J. (2008). A chemical method for fast and sensitive detection of DNA synthesis in vivo. *Proc Natl Acad Sci USA.* 105, 2415-2420.

Saxon, E., and Bertozzi, C.R. (2000). Cell surface engineering by a modified Staudinger reaction. *Science.* 287, 2007-2010.

Schenck, A., Bardoni, B., Moro, A., Bagni, C., and Mandel, J.L. (2001). A highly conserved protein family interacting with the fragile X mental retardation protein (FMRP) and displaying selective interactions with FMRP-related proteins FXR1P and FXR2P. *Proc Natl Acad Sci USA.* 98, 8844-8849.

Schmidt, C.J., Ritter, J.K., Sonsalla, P.K., Hanson, G.R., and Gibb, J.W. (1985). Role of dopamine in the neurotoxic effects of methamphetamine *J Pharmacol Exp Ther* 233, 539-544.

Schuman, E.M. (1999). mRNA trafficking and local protein synthesis at the synapse. *Neuron* 23, 645-648.

Scriven, E.F.V., and Turnbull, K. (1988). Azides- their preparation and synthetic uses. *Chem Rev.* 88, 297-368.

Shannon, P., Markiel, A., Ozier, O., Baliga, N.S., Wang, J.T., Ramage, D., Amin, N., Schwikowski, B., and Ideker, T. (2003). *Genome Res.* 13, 2498-2504.

Smeyne, R.J., and Jackson-Lewis, V. (2005). The MPTP model of Parkinson's disease. *Mol Brain Res* 134, 57-66.

Smiley, J.F., Levey, A.I., Ciliax, B.J., and Goldman-Rakic, P.S. (1994). D1 dopamine receptor immunoreactivity in human and monkey cerebral cortex: predominant and extrasynaptic localization in dendritic spines. *Proc Natl Acad Sci USA* 91, 5720-5724.

Smith, W.B., Starck, S.R., Roberts, R.W., and Schuman, E.M. (2005). Dopaminergic stimulation of local protein synthesis enhances surface expression of GluR1 and synaptic transmission in hippocampal neurons. *Neuron* 45, 765-779.

Soellner, M.B., Dickson, K.A., Nilsson, B.L., and Raines, R.T. (2003). Site-specific protein immobilization by Staudinger ligation. *J Am Chem Soc.* 125, 11790-11791.

Sokoloff, P., and Schwartz, J.C. (1995). Novel dopamine receptor half a decade later. *Trends Pharmacol Sci.* 16, 270-275.

Speers, A.E., and Cravatt, B.F. (2004). Profiling enzyme activities in vivo using click chemistry methods. *Chem Biol* 11, 535-546.

Steward, O., and Falk, P.M. (1986). Protein-synthetic machinery at postsynaptic sites during synaptogenesis: a quantitative study of the association between polyribosomes and developing synapses. *J Neurosci.* 6, 412-423.

Steward, O., and Levy, W.B. (1982). Preferential localization of polyribosomes under the base of dendritic spines in granule cells of the dentate gyrus. *J Neurosci.* 2, 284-291.

Sutton, M.A., Wall, N.R., Aakalu, G.N., and Schuman, E.M. (2004). Regulation of dendritic protein synthesis by miniature synaptic events. *Science* 304, 1979-1983.

Swanson-Park, J.L., Coussens, C.M., Mason-Parker, S.E., Raymond, C.R., Hargreaves, E.L., Dragunow, M., Cohen, A.S., and Abraham, W.C. (1999). A double dissociation within the hippocampus of dopamine D1/D5 receptor and beta-adrenergic receptor contributions to the persistence of long-term potentiation. *Neuroscience* 92, 485-497.

Sylvers, L.A., and Wower, J. (1993). Nucleic acid-incorporated azidonucleotides: probes for studying the interaction of RNA or DNA with proteins and other nucleic acids. *Bioconjug Chem.* 4, 411-418.

Szychowski, J., Ngo, J.T., and Tirrell, D.A. (2009). Cleavable reactive biotin probes for the isolation of newly synthesized proteins in bio-orthogonal noncanonical amino acid tagging. *Submitted*.

Tiberi, M., Jarvie, K.R., Silvia, C., Falardeau, P., Gingrich, J.A., Godinot, N., Bertrand, L., Yang-Feng, T.R., Fremeau, R.T., and Caron, M.G. (1991). Cloning, molecular characterization, and chromosomal assignment of a gene encoding a second D1 dopamine receptor subtype: differential expression pattern in rat brain compared with the D1a receptor. *Proc Natl Acad Sci USA* 88, 7491-7495.

tom Dieck, S., Sanmarti-Vila, L., Langnaese, K., Richter, K., Kindler, S., Soyke, A., Wex, H., Smalla, K.H., Kampf, U., Franzer, J.T., *et al.* (1998). Bassoon, a novel zinc-finger CAG/glutamine-repeat protein selectively localized at the active zone of presynaptic nerve terminals. *J Cell Biol* 142, 499-509.

Tornøe, C.W., Christensen, C., and Meldal, M. (2002). Peptidotriazoles on solid phase: [1,2,3]-triazoles by regiospecific copper(I)-catalyzed 1,3-dipolar cycloadditions of terminal alkynes to azides. *J Org Chem.* 67, 3057-3064.

Torre, E.R., and Steward, O. (1992). Demonstration of local protein synthesis within dendrites using a new cell culture system that permits the isolation living axons and dendrites from their cell bodies. *J Neurosci.* 12, 762-772.

Tsien, R.Y. (1998). The green fluorescent protein. *Annu Rev Biochem* 67, 509-544.

- van Hest, J.C.M., Kiick, K.L., and Tirrell, D.A. (2000). Efficient incorporation methionine analogues into proteins in vivo. *J Am Chem Soc.* *122*, 1282-1288.
- Vaughn, C.P., Crockett, D.K., Lin, Z., Lim, M.S., and Elenitoba-Johnson, K.S. (2006). Identification of proteins released by follicular lymphoma-derived cells using a mass spectrometry-based approach. *Proteomics.* *6*, 3223-3230.
- Volkow, N.D., Gur, R.C., Wang, G.J., Fowler, J.S., Moberg, P.J., Ding, Y.S., Hitzemann, R., Smith, G., and Logan, J. (1998). Association between decline in brain dopamine activity with age and cognitive and motor impairment in healthy individuals. *Am J Psychiatry.* *155*, 344-349.
- Wang, Q., Chan, T.R., Hilgraf, R., Fokin, V.V., Sharpless, K.B., and Finn, M.G. (2003). Bioconjugation by copper(I)-catalyzed azide-alkyne [3 + 2] cycloaddition. *J Am Chem Soc* *125*, 3192-3193.
- Wang, L., and Schultz, P.G. (2004). Expanding the genetic code. *Angew Chem Int Edn Engl.* *44*, 34-66.
- Wang, X., Ren, X., Kahen, K., Hahn, M.A., Rajeswaran, M., Maccagnano-Zacher, S., Silcox, J., Cragg, G.E., Efros, A.L., and Krauss, T.D. (2009). Non-blinking semiconductor nanocrystals. *Nature* *459*, 686-689.
- Wang, X.J. (1999). Synaptic basis of cortical persistent activity: the importance of NMDA receptors to working memory. *J Neurosci.* *19*, 9587-9603.
- Waltereit, R., and Weller, M. (2003). Signaling from cAMP/PKA to MAPK and synaptic plasticity. *Mol Neurobiol* *27*, 99-106.
- Washburn, M.P., Ulaszek, R., Deciu, C., Schieltz, D.M., and Yates, J.R., 3rd (2002). Analysis of quantitative proteomic data generated via multidimensional protein identification technology. *Anal Chem* *74*, 1650-1657.
- Washburn, M.P., Wolters, D., and Yates, J.R., 3rd (2001). Large-scale analysis of the yeast proteome by multidimensional protein identification technology. *Nat Biotechnol* *19*, 242-247.
- Wittmann, B.C., Schott, B.H., Guderian, S., Frey, J.U., Heinze, H.J., and Duzel, E. (2005). Reward-related FRMI activation of dopaminergic midbrain is associated with enhanced hippocampus-dependent long-term memory formation. *45*, 459-467.
- Wood, D.A., and Rebec, G.V. (2004). Dissociation of core and shell single-unit activity in the nucleus accumbens in free-choice activity. *Behav Brain Res.* *152*, 59-66.

- Zhang, H., Li, X.J., Martin, D.B., and Aebersold, R. (2003). Identification and quantification of N-linked glycoproteins using hydrazide chemistry, stable isotope labeling and mass spectrometry. *Nat Biotechnol* 21, 660-666.
- Zhang, J., Campbell, R.E., Ting, A.Y., and Tsien, R.Y. (2002). Creating new fluorescent probes for cell biology. *Nat Rev Mol Cell Biol* 3, 906-918.
- Zhang, J., Goodlett, D.R., Quinn, J.F., Peskind, E., Kaye, J.A., Zhou, Y., Pan, C., Yi, E., Eng, J., Wang, Q., *et al.* (2005). Quantitative proteomics of cerebrospinal fluid from patients with Alzheimer disease. *J Alzheimers Dis* 7, 125-133; discussion 173-180.
- Zhong, J., Zhang, T., and Bloch, L.M. (2006). Dendritic mRNAs encode diversified functionalities in hippocampal pyramidal neurons. *BMC Neurosci* 7, 17.
- Zhou, Y., Wang, Y., Kovacs, M., Jin, J., and Zhang, J. (2005). Microglial activation induced by neurodegeneration: a proteomic analysis. *Mol Cell Proteomics* 4, 1471-1479.

APPENDIX

Materials and Methods

Chapter II

Please refer to Dieterich et al. (2007) for complete protocol. It is appended to this thesis.

Chapter III

Reagents

All reagents were ACS grade and purchased from Sigma unless noted otherwise. BDNF was purchased from Promega, and used at a concentration of 50 mg/ml. HPG was purchased from Chiralix (The Netherlands).

Organic Synthesis

AHA and the triazole ligand were prepared as described previously (Link et al., 2007; Wang et al., 2003). TexasRed-PEO₂-Alkyne was prepared by dissolving TexasRed-PEO₂-propionic acid succinimidyl ester (Biotium Inc.) in excess neat propargylamine. After 30 minutes, the solution was added dropwise to diethyl ether. A precipitate was formed and collected by centrifugation. The precipitate was dried and characterized by ion spray MS to confirm the formation of the product with a molecular weight of 802.96 g/mol. The azide-bearing fluorescein tag was synthesized using the amine-reactive 5-carboxyfluorescein-PEO₈-propionic acid succinimidyl ester (Biotium Inc.) and 3-azidopropan-1-amine prepared as described in Carboni et al. (Carboni et al., 1993) to yield a product with a molecular weight of 896.89 g/mol.

Cultured Hippocampal Neuron and Organotypic Hippocampal Cultures

Dissociated hippocampal neurons were prepared and maintained as previously described (Aakalu et al., 2001). Briefly, hippocampi from postnatal day 0 to 2 were dissected out and dissociated by either trypsin or papain and plated at a density of 40,000 cells/cm² onto poly-D-lysine-coated glass-bottom Petri dishes (Mattek). Cultures were maintained in Neurobasal A medium containing B-27 and Glutamax supplements (Invitrogen) at 37°C for 18–24 days before use. Organotypic hippocampal cultures were prepared according to Gogolla et al. (Gogolla et al., 2006), and maintained in culture for three weeks before use.

Acute hippocampal slices

500 µm hippocampal slices are isolated from 22-24 day old male Sprague-Dawley rats using a vibrating microtome (Leica). The slices are maintained in artificial cerebrospinal fluid (aCSF; containing [in mM] 119 NaCl, 2.5 KCl, 1.3 MgSO₄, 2.5 CaCl₂, 1.0 NaH₂PO₄, 26.3 NaHCO₃, 11 glucose [pH 7.2]) in a chamber filled with 95% O₂/5% CO₂. Slices are allowed to recover for 1.5 hours at room temperature (RT) before stimulation and further manipulation.

Immunohistochemistry in acute slices

The 500 µm slices were fixed in 4% paraformaldehyde and 0.2% glutaraldehyde in PBS for 2 hours on ice. Then they were incubated in PBS at 4°C overnight and then mounted in 2.5% agarose and sliced to 50 µm using a vibrating microtome (Leica). The slices were permeabilized in 5% normal goat serum and 0.05% Triton X-100 in PBS overnight at 4°C. Immunocytochemistry was done using rabbit anti-microtubule-associated protein 2

(anti-MAP2) polyclonal (1:800; AB5622; Chemicon) and anti-rabbit Alexa Fluor 488 (1:500; Invitrogen). The slices were then mounted onto Silane-prep glass slides (Sigma) with MOWIOL solution, dried at RT overnight, and kept at 4°C until imaged. Images were acquired using a Zeiss LSM 510 laser scanning confocal microscope with a Plan-Apochromat 10x or 40x/1.3 oil objective.

Copper-Catalyzed [3+2]-Azide-Alkyne-Cycloaddition Chemistry (CuAAC) and Detection of Tagged Proteins

In all culture experiments, growth medium was removed from neuronal cultures and replaced with either HEPES-buffered solution (HBS) (Malgaroli and Tsien, 1992) or methionine-free Hibernate A (HibA) medium (BrainBits LLC.) for 30 minutes to deplete endogenous methionine. For AHA labeling, HBS and HibA were supplemented with 2 mM AHA, 2 mM AHA plus 40 mM anisomycin, or 2 mM methionine. After incubation at 37°C, 5% CO₂, cells were washed with chilled PBS-MC (1mM MgCl₂ and 0.1 mM CaCl₂ in PBS) on ice to remove excess amounts of AHA and methionine followed by immediate fixation with chilled 4% paraformaldehyde, 4% sucrose in PBS-MC for 20 minutes at RT.

For CuAAC, in order to avoid copper bromide-derived precipitates, we used TCEP in combination with copper sulfate to generate the Cu(I) catalyst during the CuAAC reaction (Link et al., 2004). The triazole ligand, TCEP, fluorescent tag (TRA or FLA), and copper sulfate were added to PBS pH 7.6 at 1/1000 dilution. The CuAAC reaction was incubated overnight at RT. The reaction was promptly removed and cells

were washed twice with 0.5 mM EDTA, 1% Tween-20 in PBS pH 7.6, followed by three washes with PBS pH 7.6.

For immunolabeling after AHA-incorporation and cycloaddition, cells were treated sequentially with PBS, blocking solution (0.1% Triton X-100, 2 mg/ml BSA, 5% sucrose, 10% normal horse serum in PBS), primary Ab in blocking solution at 4°C overnight or at RT for 2 hours, PBS-Tx (0.1% Triton X-100 in PBS), Alexa488- or Alexa568-conjugated secondary Ab in blocking solution, PBS-Tx and PBS, and mounted in Gold Prolonged Antifade reagent (Invitrogen) prior to imaging. The following primary antibodies were used: rabbit anti-microtubule-associated protein 2 (anti-MAP2) polyclonal (1:1000; AB5622; Chemicon); mouse anti-bassoon monoclonal (1:1000; VAM-PS003; Stressgen Bioreagents Corp.). For secondary antibodies, we used anti-rabbit or anti-mouse conjugated Alexa Fluor 488, 568, or 647 (1:500; Invitrogen).

Local Perfusion

All local perfusion experiments are performed with an Olympus IX-70 confocal laser-scanning microscope using Plan-Apochromat 40x/0.95 air or 40x/1.0 oil objectives. Alexa 488 was excited with the 488 nm line of an argon ion laser, and emitted light was collected between 510 and 550 nm. For restricted treatment of isolated somata or dendritic segments, we used a dual micropipette local delivery system. The delivery micropipette was pulled as a typical whole-cell recording pipette with an aperture of ~ 0.5 μ m. The area of local perfusion was controlled by a suction pipette, which was used to draw the treatment solution across one or more dendrites and to remove the perfusion solution from the bath. Alexa 488 hydrazide (1 μ g/ml, Invitrogen) was included in the

perfusion solution to visualize the affected area. The stability of the perfusion was monitored periodically throughout the experiment, and only experiments in which the affected area changed by less than 20% were used for analysis. In all local perfusion experiments, the set-up was maintained at 32°C with a closed box-incubator around the microscope. Multiple small water pans were used to keep the system humid. For analysis of local perfusion experiments, dendrites of treated neurons were first linearized using Image J. The size of the treated area for each soma or dendrite was determined based on Alexa 488 fluorescence integrated across all images (typically 6-10) taken during local perfusion.

Chapter IV

Reagents

Azidohomoalanine was prepared as described by Link et al., 2007.

Homopropargylglycine was purchased from Chiralix, Inc. (The Netherlands).

Organic Synthesis

The DST-azide was prepared as described in Szychowski et al., 2009 (submitted). DST-alkyne was synthesized using the same protocol with this small modification: 1-azidopropylamine was replaced by propargylamine; ¹H NMR (500 MHz, CDCl₃), δ (ppm): 6.97 (s, 1H), 6.35 (s, 1H), 5.52 (s, 1H), 4.57-4.44 (m, 1H), 4.33 (dd, *J* = 7.29, 4.87 Hz, 1H), 4.05 (dd, *J* = 5.22, 2.49 Hz, 2H), 3.75 (t, *J* = 5.81, 5.81 Hz, 2H), 3.69-3.60 (m, 16H), 3.56 (m, 4H), 3.44 (dd, *J* = 7.15, 3.78 Hz, 2H), 3.20-3.07 (m, 2H), 3.03-2.97

(m, 2H), 2.91 (dd, $J = 12.80, 4.88$ Hz, 1H), 2.85 (t, $J = 6.51, 6.51$ Hz, 2H), 2.75 (d, $J = 12.76$ Hz, 1H), 2.65 (t, $J = 7.17, 7.17$ Hz, 2H), 2.51 (t, $J = 5.81, 5.81$ Hz, 2H), 2.37-2.16 (m, 4H), 1.82-1.60 (m, 4H), 1.43 (td, $J = 21.27, 7.37, 7.37$ Hz, 2H), 1.25 (s, 1H); ^{13}C NMR (126 MHz, CDCl_3), δ (ppm): 173.5, 172.0, 171.0, 163.9, 80.0, 71.3, 70.2 (m 8C), 67.3, 61.8, 60.2, 55.6, 45.9, 40.6, 39.2, 38.4, 36.9, 36.0, 34.4, 29.1, 28.1, 25.6, 8.6; m/z calcd for $\text{C}_{29}\text{H}_{49}\text{N}_5\text{O}_8\text{S}_3$ $[\text{M}+\text{H}]^+$: 692.2822, MS found: 714.2 (M+Na), HRMS found: 692.2822.

GFP Protein expression and purification

pJS2 (described in Szychowski et al., 2009) was transformed into the methionine auxotrophic *E. coli* strain M15MA/pREP4 and selected for on LB-agar plates containing kanamycin and ampicillin. A single colony was used to inoculate an overnight 5 mL culture in LB containing kanamycin and ampicillin. The following morning, 1 mL of the culture was diluted in 49 mL of M9 minimal medium (M9 salts, 0.2 % glucose, 1 mM MgSO_4 , 0.1 mM CaCl_2 , 25 mg/mL thiamine) and supplemented with 40 mg/L of each of the twenty natural amino acids in addition to kanamycin and ampicillin. Cells were grown until OD_{600} reached 1.0 (4-5 h), pelleted at 2000 g for 10 minutes at 4°C, and washed twice in cold, sterile 0.9% NaCl. Cells were resuspended in M9 (-Met) medium (M9 medium supplemented with 40 mg/L of each of the natural amino acids except methionine). Either homopropargylglycine, azidohomoalanine, or methionine was added to a final concentration of 1 mM. IPTG was added to a final concentration of 1 mM to induce synthesis of GFP. Cells were induced for 4 h at 37°C and pelleted at 2000 g for 10 minutes at 4°C; the supernatant was removed and cells were frozen at -80°C overnight.

The His-tagged GFP was purified by a Qiagen Ni-NTA resin under native conditions according to the manufacturer's recommendations. The purified protein was subjected to buffer exchange into PBS pH 7.8, using GE Healthcare PD10 columns according to the manufacturer's protocol. Glycerol was added to the protein sample at a final concentration of 50%, and the protein was stored in 50% glycerol at -20°C until used.

Click chemistry and alkylation

For alkylation experiments, COS7 cells were grown to 80% confluence in DMEM++ media. Cells were washed and incubated for 30 minutes in HBS pH 7.4, followed by a 2-hour incubation in either 4 mM methionine in HBS, 4 mM AHA in HBS, or 4 mM HPG in HBS. Cells were pelleted and lysate was prepared as described in Dieterich et al., 2007. Cell lysate was reduced in 2% β -mercaptoethanol for 1 hour in the dark at 25°C and then proteins were acetone precipitated. Upon resuspension, proteins were alkylated using 11mM iodoacetamide for 1 hour in the dark at 25°C , then acetone precipitated. After a second resuspension, the click chemistry reaction was assembled as described in Dieterich et al., 2007.

E. coli growth and measurement of GFP fluorescence

In the GFP protein expression described above, OD_{600} was monitored by taking 0.1 mL of the culture media for every time point before and after media shift. All OD_{600} measurements were recorded in triplicates with a Varian Cary 50 Bio spectrometer. At the same time points, 0.5 mL aliquots of the culture were taken and the cells were pelleted at 2000 g for 5 minutes. Following resuspension in 0.5 mL cold, sterile 0.9%

NaCl containing 75 µg/mL of chloramphenicol, the cells were kept at 4 °C for at least 30 minutes to ensure completion of GFP maturation. GFP fluorescence was measured in triplicate using 100 µL using a Tecan Safire² plate reader (excitation: 485 nm, emission: 535 nm, bandwidth: 20 nm).

Chapter V

Transwell culture system

Hippocampi from newborn Sprague-Dawley rat pups (P0) were prepared as described by Aakalu et al. (2001). The neurons were plated at a density of 1×10^6 cells/well onto semiporous polycarbonate membranes sitting in a 6-well format cell culture dishes. The membranes were coated with poly-D-lysine and growth factor reduced Matrigel. The cultures were grown and matured in Neurobasal A growth serum with B27 and GlutaMAX-1 for 18-21 days at 37°C with 5% CO₂ prior to use.

FUNCAT of cultured hippocampal neurons

Dissociated hippocampal cultures (21-24 DIV) were incubated in HibA without methionine (HibA – Met) for 30 minutes, followed by incubation with HibA – Met with 4 mM AHA for 1 hour. Stimulation was achieved with concurrent bath applications of varying concentrations of SKF81297 (Tocris, dissolved in DMSO). The cultures were then incubated for 15 minutes with Hib – Met with 4 mM methionine. They were immediately fixed on ice with 4% paraformaldehyde and 4% sucrose (w/v) in PBS-MC for 15 minutes. FUNCAT and immunocytochemistry were performed as described above in Chapter III.

Microdissection of acute hippocampal slices

500 μm hippocampal slices were isolated from 24-26 day-old male Sprague-Dawley rats using a tissue chopper. The slices were maintained in artificial cerebrospinal fluid (aCSF; containing [in mM] 119 NaCl, 2.5 KCl, 1.3 MgSO_4 , 2.5 CaCl_2 , 1.0 NaH_2PO_4 , 26.3 NaHCO_3 , 11 glucose [pH 7.2]) in a chamber filled with 95% O_2 /5% CO_2 until microdissection. After microdissection, dendritic slices were allowed to recover for 1.5 hours at room temperature before stimulation and further manipulation.

Sample preparation for mass spectrometry

Dendritic slices were incubated for 2.5 hours in aCSF plus 4 mM AHA and 4 mM ^{13}C -Arg in a chamber filled with 95% O_2 /5% CO_2 . Stimulation was achieved by concurrently applying 40 μM SKF81297 to the incubation solution. Slices were immediately flash frozen and stored at -80°C until use. Frozen slices were thawed on ice and prepared as previously described (Dieterich et al., 2007) except for a few changes due to the nature of the DST-alkyne tag that was used. Prior to click chemistry, the lysate was reduced and alkylated as described in Chapter IV. To elute newly synthesized proteins from the NeutrAvidin resin, protein-bound slurry was incubated with 2% β -Me for 1 hour in the dark with agitation. The supernatant was removed and acetone precipitated and processed for mass spectrometry as described in Dieterich et al., 2007. Digested peptides were desalted using an Alliance HPLC (Waters) coupled to a reverse-phase resin macrotrap at the Protein Exploration Laboratory (Caltech). Peptides were eluted from the resin using a

stepwise gradient ranging from 0-85% acetonitrile. Eluted, desalted peptides were subsequently lyophilized for mass spectrometry analysis.

Multidimensional Protein Identification Technology (MudPIT)

A triphasic microcapillary column containing back-to-back reverse phase (RP) resin (5 micron C-18 coated beads), strong cation exchange (SCX) resin, and more RP resin was used. The relative ratios of each resin varied slightly, but the assembly was as described previously (Dieterich et al., 2006).

Mass spectrometry and bioinformatics

We used a ThermoFinnigan LTQ-FT at the Protein Exploration Laboratory at Caltech for data acquisition. Subsequent analysis was performed using the SEQUEST Sorcerer (Eng et al., 1994) and Mascot (Perkins et al., 1999) to execute the database searches.

Determination of AHA or ¹³C-Arg peptides were done using a custom-made parser.

Further analysis was done using the PeptideProphet (Keller et al., 2002) and ProteinProphet (Nesvizhskii et al., 2003) from the Trans-Proteomic Pipeline as well as Scaffold (Proteome Software, Inc.) and Cytoscape, allowing efficient comparison of individual experiments and data mining.

PROTOCOL

Labeling, detection and identification of newly synthesized proteomes with bioorthogonal non-canonical amino-acid tagging

Daniela C Dieterich¹, Jennifer J Lee¹, A James Link^{2,3}, Johannes Graumann^{1,3}, David A Tirrell² & Erin M Schuman¹

¹Division of Biology, Howard Hughes Medical Institute, California Institute of Technology, Pasadena, California 91125, USA. ²Division of Chemistry and Chemical Engineering, California Institute of Technology, Pasadena, California 91125, USA. ³Present address: Department of Chemical Engineering and Institute for Cellular and Molecular Biology, The University of Texas at Austin, Austin, Texas 78712, USA (A.J.L.); Department of Proteomics and Signal Transduction, Max-Planck-Institute for Biochemistry, Martinsried 82152, Germany (J.G.). Correspondence should be addressed to D.C.D. (dieterd@caltech.edu).

Published online 22 March 2007; doi:10.1038/nprot.2007.52

A major aim of proteomics is the identification of proteins in a given proteome at a given metabolic state. This protocol describes the step-by-step labeling, purification and detection of newly synthesized proteins in mammalian cells using the non-canonical amino acid azidohomoalanine (AHA). In this method, metabolic labeling of newly synthesized proteins with AHA endows them with the unique chemical functionality of the azide group. In the subsequent click chemistry tagging reaction, azide-labeled proteins are covalently coupled to an alkyne-bearing affinity tag. After avidin-based affinity purification and on-resin trypsinization, the resulting peptide mixture is subjected to tandem mass spectrometry for identification. In combination with deuterated leucine-based metabolic colabeling, candidate proteins can be immediately validated. Bioorthogonal non-canonical amino-acid tagging can be combined with any subcellular fractionation, immunopurification or other proteomic method to identify specific subproteomes, thereby reducing sample complexity and enabling the identification of subtle changes in a proteome. This protocol can be completed in 5 days.

INTRODUCTION

Cells respond to fluctuations in their environment by changing the ensemble of proteins they express. Alterations in protein synthesis, degradation and post-translational modifications enable cells to adapt to changing environmental conditions. Hence, a major endeavor in biology is the comparison of two or more protein complements in biological systems, for example, the cancerous versus non-cancerous state, the addicted versus non-addicted brain circuit or the physiology of a genetically altered mouse versus a wild-type littermate. Mass spectrometry (MS)-based proteomics has become a vital and versatile technique to characterize the expression and functional modification of proteins, complementing the genomics efforts. Unlike the substrate of genomic research, DNA, proteins are diverse and heterogeneous biomolecules lacking the possibility of amplification, a fact that impedes their characterization and identification in complex mixtures. A cornucopia of biochemical and analytical tools for protein separation, fractionation and modification have been developed and combined to enable proteomic analysis. Resolving techniques such as one- and two-dimensional gel electrophoresis and multidimensional liquid chromatography, work in conjunction with MS to decipher the protein entity of a cell or a whole organism.

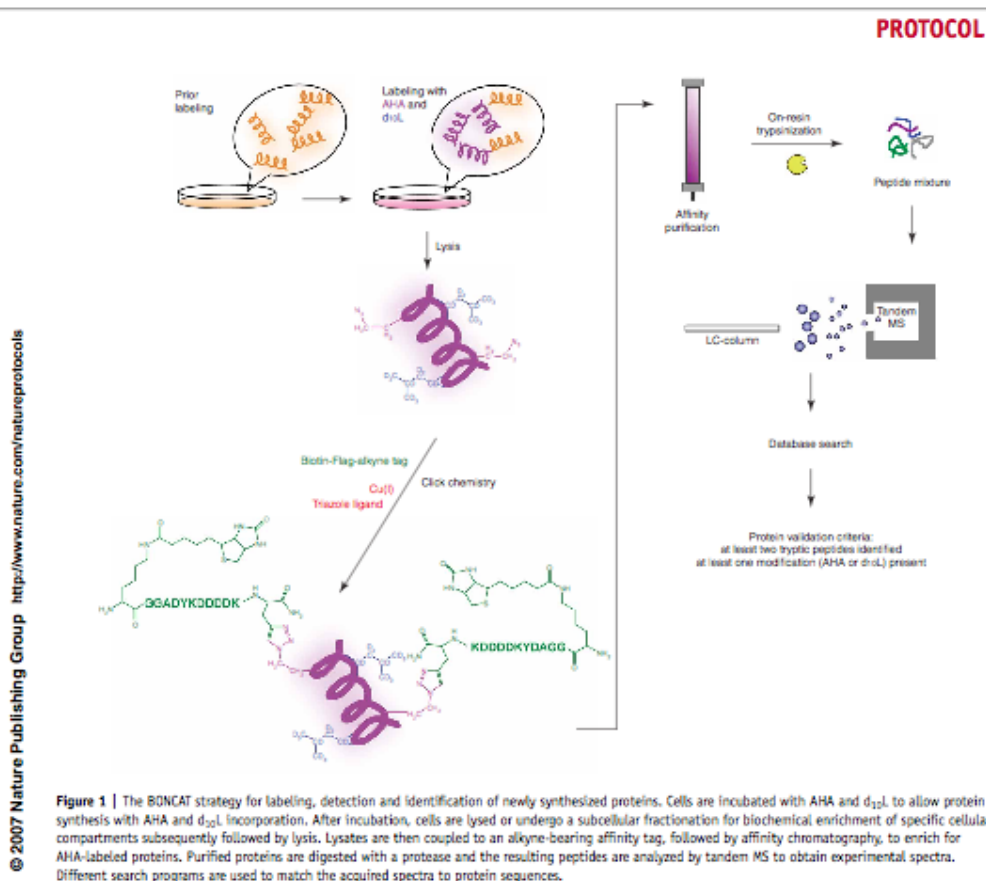
Despite immense technological advances in the last decade, no single proteome of a mammalian cell or lower eukaryotic micro-organism, such as the yeast, has been completely characterized. Facing an estimated number of approximately 10,000 different proteins in a single mammalian cell¹, in-depth identification of a cell's entire proteome, let alone the comparison to another proteome, is a major challenge for modern proteomics. Although today's state-of-the-art MS instruments routinely sequence single purified proteins with subfemtomolar sensitivity, the effective identification of low-abundance proteins is orders of magnitude lower in complex mixtures owing to limited dynamic range and sequencing speed². Copy numbers of proteins from different

mammalian cells and tissues vary with a predicted dynamic range of up to six orders of magnitude, and this number is even several orders of magnitude larger in plasma samples.

Strategies to reduce proteome complexity and to increase the dynamic range of protein identification include fractionation and affinity-purification approaches at both protein and peptide levels before MS analysis. In particular, fractionation methods of whole organelles (mitochondria³ and nucleolus⁴) and compartments, such as the postsynaptic density of neurons^{5,6} as well as affinity-purified protein complexes^{5,7,8}, have been successfully used to enhance proteomic analysis. Furthermore, the combination of MS with affinity purification for different post-translational modifications^{9–13} decreases sample complexity by enrichment of a specific subpopulation of the proteome.

Quantitative knowledge of the particular set of proteins expressed in different cellular locales at different times arguably brings one close to the knowledge of a cell's phenotype. Therefore, special efforts have been dedicated to the development of differential proteomic profiling approaches to compare proteomes with one another and to obtain relative quantification of individual proteins among samples. These methods include differential two-dimensional gel electrophoresis^{14,15}, isotope-coded affinity tags¹⁶ or isobaric tags for relative and absolute quantification¹⁷, quantitative proteomic analysis using samples from cells grown in ¹⁴N or ¹⁵N-media¹⁸ and stable isotope labeling by amino acids in cell culture^{4,19}. Although post-translational modifications such as phosphorylation or ubiquitination readily provide a suitable handle for enrichment of the "phosphoproteome" or for proteins destined for degradation, reducing sample complexity by selectively enriching for newly synthesized proteins is troublesome, as all proteins—old and new—share the same pool of 20 amino acids. Nonetheless, the specific enrichment and identification of recently synthesized proteins would complement the range of differential





© 2007 Nature Publishing Group <http://www.nature.com/natureprotocols>



proteomic profiling methods and deepen our insights into the spatial and temporal dynamics of proteomes.

BONCAT (bioorthogonal non-canonical amino-acid tagging) was developed to specifically identify the subpopulation of newly synthesized proteins²⁰. The core of the BONCAT technique capitalizes on the manifold potential of small bioorthogonal chemo-selective groups (recently reviewed by Prescher and Bertozzi²¹). These groups deliver unique chemical functionality to their target molecules, which subsequently can be tagged with exogenously delivered probes for detection or isolation in a highly selective manner. Among these chemical reporters, azides and alkynes have been used to label proteins^{22–30}, glycans^{27–30} and lipids²³ using the cell's own translation and protein modification apparatus. In the first step of BONCAT, newly synthesized proteins are labeled using the azide-bearing artificial amino acid AHA, endowing them with novel azide functionality, which distinguishes them from the pool of pre-existing proteins (see Fig. 1). Indeed, azides are abiotic in animals with the exception of an azide-metabolite found in unicellular cultures²². Moreover, despite general perception, azides are non-

toxic and stable²². Using the copper-catalyzed azide-alkyne ligation³¹, the reactive azide group of AHA is covalently coupled to an alkyne-bearing biotin-Flag tag in the second step. This tag enables subsequent detection, affinity purification and MS identification of AHA-labeled proteins. The enrichment for newly synthesized proteins decreases the complexity of the sample, fostering the identification of proteins expressed at low levels.

Although we routinely use the biotin moiety for avidin-based affinity purification, the Flag epitope provides sites for trypsin cleavage to allow direct proteolysis of proteins on the affinity matrix, bypassing the need for an elution step. In addition, the Flag epitope can be used as an alternative purification module if native biotinylation of proteins is a concern. After tryptic digestion of avidin-bound proteins, peptides bearing the tryptic remains of tagged AHA can serve as an immediate validation of candidate proteins. In the event of failed tagging, that is, unligated AHA, the mass difference between AHA and methionine marks this peptide as derived from a true newly synthesized candidate protein. To increase the chances of detecting metabolically modified peptides,

PROTOCOL

we colabel cells with tenfold deuterated *l*-leucine ($d_{10}L$), which allows, in conjunction with the modification derived from the introduction of AHA, the validation of candidate proteins. We opted to use $d_{10}L$ in our studies because leucine is the most abundant amino acid (9.83% of all amino-acid residues) in a human protein database as assessed by using the Python script AAEXCLUDE²⁰.

AHA is an effective surrogate for methionine, an essential amino acid, and does not require any (further) manipulations to be accepted as a substrate by the methionyl-tRNA synthetase^{24,25}. Labeling with AHA is very similar to the traditional metabolic labeling with radioactive amino acids (³⁵S-labeled methionine or cysteine) and has been tested in a variety of cell lines, primary neuronal cells as well as organotypic brain slice cultures (unpublished observations). The presence and incorporation of AHA is non-toxic and does not affect global rates of protein synthesis or degradation. A broad range of functionally and biochemically diverse proteins are identified²⁰. The copper-catalyzed azide-alkyne ligation³¹, also known as "click chemistry," can be performed on denatured proteins in the presence of detergents, such as SDS, promoting the likewise identification of diverse classes of proteins, that is, membranous and soluble, acidic and basic as well as high- and low-molecular-weight proteins.

The identification of newly synthesized proteins with BONCAT is limited to proteins that possess at least one methionine residue, excluding the 1.02% of all entries in a human protein database, which do not contain a single methionine. Given that 5.08% of the human proteome possess only a single, N-terminal methionine and that this residue may be subject to removal by post-translational processing, at least 94% of the mammalian proteomes are candidates

for identification by BONCAT²⁰. Interestingly, we found no bias toward methionine-rich proteins in the proteomes we have characterized thus far, as evidenced by our identification of proteins with low methionine content²⁰. Furthermore, the methionine content of candidate proteins was found to be only slightly higher than the methionine content of the comprehensive protein database²⁰.

The core of the BONCAT technique—the chemoselective tagging of AHA-incorporated proteins—is not restricted to the mere identification of newly synthesized proteins in a shotgun proteomics approach. It also offers the possibility to work in combination with other proteomic approaches, such as isotope-coded affinity tags, isobaric tags for relative and absolute quantification or phospho- and glycoproteomic enrichment methods, to directly compare different proteomes in a single MS experiment or to facilitate the identification of even more and more specific subpopulations of the proteome, respectively. In this context, it is noteworthy that researchers may wish to choose any available mass spectrometric identification procedure to adapt to a particular laboratory's individual MS instrumentation environment to pursue identification of BONCAT-derived peptide mixtures. Furthermore, subcellular fractionation and immunopurification of protein complexes can be followed by BONCAT to assess the temporal and spatial dynamics of certain subcellular compartments, organelles and protein-protein interaction networks.

With regard to the specifics of the present protocol, we advise to perform a dot blot analysis mid-way through the procedure on an aliquot of the tagged (biotinylated) protein solution. This is performed to check quickly for the efficiency of the click chemistry reaction as well as to attain a crude estimate of the amount of tagged protein in the sample.

MATERIALS

REAGENTS

- Primary cells or cell lines in culture. Cell should be approximately 90% confluent
- 2× HBS (HEPES-buffered saline): 20 mM HEPES (1 M HEPES buffer; Sigma, cat. no. H0887), 238 mM sodium chloride, 10 mM potassium chloride, 4 mM calcium chloride, 4 mM magnesium chloride and 60 mM glucose, pH 7.35. Store in a refrigerator for up to 1 month after sterile filtration. Prepare 1× HBS freshly as needed
- 10× PBS (phosphate-buffered saline): 1.37 M sodium chloride, 27 mM potassium chloride, 43 mM disodium hydrogen phosphate and 14 mM potassium dihydrogen phosphate, pH 7.5
- Water, molecular biology grade (Sigma, cat. no. W4502)
- AHA (prepared as described previously³¹; alternatively, researchers may obtain AHA via custom synthesis from appropriate organic synthesis companies): 20 mM stock solution in molecular biology grade water, store for up to 1 month at 4 °C; keep powder desiccated at room temperature (RT, 20–24 °C)
- *l*-Leucine- d_{10} ($d_{10}L$; Sigma, cat. no. 492949): 100 mM stock solution in molecular biology grade water, store for up to 1 month at –20 °C
- *l*-Methionine (Sigma, cat. no. M9625): 20 mM stock solution in molecular biology grade water, store for up to 1 month at 4 °C
- 20% (w/v) SDS in molecular biology grade water
- 20% (v/v) Triton X-100 in molecular biology grade water
- Triazole ligand (prepared as described previously³¹): 200 mM stock solution in DMSO ▲ CRITICAL Avoid exposure of the solution to air and water. Aliquot into small volumes and store at –20 °C. Store powder desiccated at RT
- Biotin-Flag-Alkyne (TAP) tag: NH₂-Biotin-GGADYKDDDDK-propargylglycine-CONH₂ (GenScript Corporations; amino acids bold in one-letter code): 25 mM stock solution in 1× PBS, aliquot and store at –20 °C for up to 6 months
- Copper (I) bromide, 99.999% (Aldrich, cat. no. 254185), store desiccated at RT
- Tris-(2-carboxyethyl)phosphine (TCEP; Sigma, cat. no. C4706): 0.5 M in molecular biology grade water, prepare fresh before use

- Iodoacetamide (Sigma, cat. no. I1149): 0.5 M in molecular biology grade water, prepare fresh before use
- Complete EDTA-free protease inhibitor (Roche, cat. no. 1873580)
- Benzonase (Sigma, cat. no. E1014)
- PD-10 columns (Amersham Pharmacia Bioscience, cat. no. 17-0851-01)
- ImmunoPure biotinylated BSA (Pierce, cat. no. 29130)
- Immobilized NeutrAvidin (Pierce, cat. no. 29200)
- Sequencing grade modified trypsin (Promega, cat. no. V5111)
- Endoproteinase Lys-C (Roche, cat. no. 1420429)
- Urea (Sigma, cat. no. U1250)
- Formic acid, 88% (vol/vol), ACS reagent (Sigma, cat. no. 399388)
- 10× TBS (Tris-buffered saline): 200 mM Tris/HCl, 8% (w/v) sodium chloride, pH 7.6
- 4× SDS sample buffer: 1% (w/v) SDS, 40% (v/v) glycerol, 20% (v/v) β-mercaptoethanol, 250 mM Tris/HCl pH 6.8, 0.004% (w/v) bromophenol blue
- Nitrocellulose membrane (such as Protran BA85, 0.45 μm, from Whatman) and PVDF membrane (0.2 μm, such as Immobilon-P from Bio-Rad, ImmobilonP from Millipore)
- Western blotting detection system, such as ECL from GE Healthcare
- Imaging film such as KODAK BioMax XAR Film
- Empty spin columns (such as Handee Spin Columns with screw caps and Luer-Lok adaptors from Pierce, cat. no. 69705)

EQUIPMENT

- Dot blot apparatus (such as Bio-Dot from Bio-Rad, cat. no. 170-6545)
 - Rotisserie-Rotator
 - Temperature-controlled shaker for microcentrifuge tubes (such as Thermomixer from Eppendorf)
 - Electrospray-ionization ion-trap tandem mass spectrometer (e.g., Thermo Finnigan LCQ or LTQ)
- Software tools
- Search algorithms such as SEQUEST³⁴, MASCOT³⁵ and XTandem^{36,37}
 - DTASelect³⁸ or PeptideProphet³⁹ and ProteinProphet⁴⁰



PROTOCOL

REAGENT SETUP

All solutions for click chemistry must be free of EDTA, EGTA and other chelators to avoid inactivation of the copper (I) catalyst.

AHA/d₁₀L-HBS We use 4 mM AHA and 4 mM d₁₀L in 1× HBS (AHA-HBS) for labeling of HEK293, COS7 or primary neuronal cells. However, investigators may wish to determine the optimal concentration of AHA and d₁₀L as well as labeling time individually for metabolic labeling for each cell type on a small-scale first.

Met/d₁₀L-HBS Use same concentration of methionine in experiments as AHA and d₁₀L for the control sample.

PBS-MC 1× PBS supplemented with 1 mM magnesium chloride and 0.1 mM calcium chloride; chill on ice.

PBS-PI 1× PBS supplemented with Complete EDTA-free protease inhibitor, prepare fresh immediately before use according to the manufacturer's instructions; chill on ice until use.

PD-10-column buffer 0.05% (w/v) SDS in 1× PBS.

Biotinylated BSA standard for dot blot analysis Reconstitute ImmunoPure biotinylated BSA as a stock solution of 2 mg ml⁻¹ in water. Prepare biotinylated BSA working solutions of the following concentrations in 1× TBS: 1, 0.5, 0.25, 0.125, 0.0625 and 0.03125 ng μl⁻¹.

TBS-T 0.05% (v/v) Tween 20 (Sigma, cat. no. P1379) in 1× TBS, pH 7.6.

NeutrAvidin-binding buffer 1% (v/v) NP-40 (Nomidet P40 Substitute; Fluka, cat. no. 74385), 0.05% (v/v) SDS and 1× PBS, pH 7.5.

NeutrAvidin wash buffer A (NW-A) 1% (v/v) NP-40 and 1× PBS, pH 7.5.

NeutrAvidin wash buffer B (NW-B) 50 mM ammonium bicarbonate.

PBS-T 0.1% v/v Tween 20 in 1× PBS, pH 7.5.

Polyclonal rabbit biotin antibody (Bethyl Laboratories Inc., cat. no. A150-109A): 1:10,000 in 5% dry milk in PBS-T or TBS-T.

Secondary HRP-conjugated anti-rabbit antibody (Such as from Jackson Immuno Research) in 5% dry milk in PBS-T or TBS-T.

PROCEDURE

Cell labeling ● TIMING 3.5 h

1| Prepare 1× HBS, AHA/d₁₀L-HBS and Met/d₁₀L-HBS (for control samples)—see REAGENTS and REAGENT SETUP—and warm to 37 °C (at least 20 min). You will need 6 ml of each solution for a round 100 mm dish.

2| Rinse cells briefly in 6 ml of 1× HBS and incubate in the same volume of fresh 1× HBS for 30 min in a 37 °C, 5% CO₂ incubator. This preincubation step allows the depletion of amino acids including methionine and leucine.

3| Remove 1× HBS, add 6 ml of AHA/d₁₀L-HBS or Met/d₁₀L-HBS to cells; move cells back to 37 °C, 5% CO₂ incubator for desired incubation time. In our experiments, we found an incubation of 1–2 h to be sufficient. However, shorter and longer incubation times should be selected according to the specific nature of the experiment and the cells used.

4| Place cell dishes on ice and rinse cells briefly in chilled PBS-MC. (Magnesium chloride and calcium chloride are added to PBS in this step to maintain proper ionic strength in the buffer system to preserve membrane integrity. Once the cells are lysed, this is no longer necessary.)

5| Harvest cells in 6 ml of chilled PBS-PI supplemented with 1 mM magnesium chloride and 0.1 mM calcium chloride; transfer the cell suspension to a 15 ml plastic tube, spin down (2,000g, 5 min, 4 °C) and carefully remove all the supernatant from the cell pellet.

■ **PAUSE POINT** Cell pellets can be stored at –80 °C for several months after flash freezing in liquid nitrogen without any harmful effect on click chemistry efficiency. Note that after harvesting the cells, one may proceed to Step 6, or alternatively carry out subcellular fractionation protocols before cell lysis. In either case, we recommend the use of a phosphate buffer system (≥ pH 7.5) for the subsequent click chemistry reaction (see also Step 6).

Click chemistry reaction ● TIMING 18 h; overnight step

6| Lyse cell pellet in 250 μl of 1% (w/v) SDS in PBS (lysis buffer) by vigorous vortexing. Add 1 μl of Benzonase (≥ 500 U) and mix well. Boil samples for 10 min at 96–100 °C to achieve complete lysis and denaturation of proteins; chill on ice.

? TROUBLESHOOTING

7| Adjust samples to 0.1% (w/v) SDS by adding the appropriate amount of PBS (~2,250 μl). Add 25 μl of 20% (v/v) Triton X-100 to a final concentration of 0.2% (v/v).

▲ **CRITICAL STEP** High concentrations of SDS (> 0.2% (w/v)) will decrease the efficiency of the tagging reaction.

8| Spin down at 2,000g for 5 min at 4 °C; transfer the supernatant to a new test tube and allow it to warm up to RT.

9| Thaw TAP tag and triazole ligand; prepare a 10 mg ml⁻¹ copper bromide suspension in molecular biology grade water; transfer 10 mg of copper bromide to a microcentrifuge test tube and add 1 ml of water immediately before use. Vortex vigorously for 20 s. If more than two samples are processed, use multiple fresh copper bromide suspensions.

▲ **CRITICAL STEP** Fresh copper bromide suspensions must be used because of the rapid disproportionation of the catalytically active Cu(I) ion in copper bromide to Cu(0) and Cu(II) in the presence of water.

10| For each 1 ml of the supernatant from Step 8, add 1 μl triazole ligand, 2 μl TAP tag and 10 μl of copper bromide suspension (in the mentioned order). After the addition of the triazole ligand, a light “milky” turbidity of the sample appears, which vanishes after the addition of the TAP tag and the copper bromide suspension.

▲ **CRITICAL STEP** The click chemistry reaction mix has to be set up for each sample separately in the mentioned order without any delay to avoid precipitation of the triazole ligand and disproportionation of the Cu(I) ion. After the addition of each reagent, vortex vigorously for 15–20 s.



PROTOCOL

11| Incubate samples either for 6 h at RT under constant agitation in a rotisserie-rotator, or

■ **PAUSE POINT** Incubate overnight at 4 °C with constant agitation.

12| Spin down at 2,000g for 5 min at 4 °C. A small turquoise pellet should be observed.

? **TROUBLESHOOTING**

13| Transfer the supernatant to a new test tube.

■ **PAUSE POINT** Samples can be stored at –20 °C at this point for short periods of time (1–2 days).

Dot blot analysis ● **TIMING 5 h**

14| Remove excess unreacted tag by gel filtration using PD-10 columns. Equilibrate each column with 25 ml of PD-10-column buffer. Apply 2.5 ml of sample, discard flow-through and elute sample with 3.5 ml of PD-10-column buffer; keep the 3.5 ml sample eluate fractions collected on ice until further use. Columns can be reused for larger sample volumes after washing with 30 ml of water and re-equilibration with 25 ml of PD-10-column buffer.

15| Prepare 200 µl of sample dilutions in 1× TBS. We routinely use 1:200 and 1:100 dilutions of the samples from Step 14.

16| Equilibrate nitrocellulose membrane in 1× TBS and assemble the dot blot according to the manufacturer's recommendation. Before applying the samples and the BSA standards, wash all wells once with 100 µl 1× TBS. Gently remove the buffer from the wells by applying vacuum. Apply to each well 100 µl of biotinylated BSA standard (at different concentrations; see REAGENT SETUP) and 100 µl of sample dilutions in duplicate. Remove the samples from the wells by applying vacuum. Wash all wells once again with 100 µl of 1× TBS.

17| Blocking of nonspecific protein binding to the membrane is achieved by placing the membrane in 5% dry milk in TBS-T for 45 min at RT with gentle agitation on a rocking plate. Blocking reduces "noise" and eliminates false positives in the dot blot. Incubate the membrane with the polyclonal rabbit biotin antibody dilution (1:10,000 in 5% dry milk in TBS-T) for 1 h at RT with gentle agitation. Wash the membrane three times with TBS-T for 5 min each. Incubate the membrane with the secondary antibody dilution (1:10,000 in 5% dry milk in TBS-T) for 45 min at RT with gentle agitation. Wash the membrane three times with TBS-T for 5 min each. Detect biotinylated proteins using a western blotting detection system such as ECL from GE Healthcare in combination with an imaging film such as BioMax XAR film from KODAK according to the manufacturer's instructions. The amount of biotinylated, that is, newly synthesized proteins in the samples is estimated densitometrically by comparing the intensity of the sample dots with the intensity of biotinylated BSA standard dots (see Fig. 2).

? **TROUBLESHOOTING**

NeutrAvidin purification and on-resin trypsinization ● **TIMING 19 h; overnight step**

18| Heat the samples from Step 14 for 3 min at 96–100 °C to bring any SDS precipitates back into solution.

19| Adjust samples to 1% (v/v) NP-40 and 0.05% (w/v) SDS in PBS-PI at an approximate concentration of 25 µg ml⁻¹ of biotinylated proteins. Preserve 30 µl of this sample for subsequent western blot analysis ("input"); immediately add 10 µl of 4× SDS sample buffer and store at –20 °C until further use (1–2 weeks).

20| For each 25 µg of biotinylated proteins, transfer 100 µl of NeutrAvidin resin (provided as a 50% slurry, i.e., 100 µl of the slurry corresponds to approximately 50 µl resin or "bed" volume) to a 15 ml plastic tube. Wash NeutrAvidin resin three times with ten bed volumes of NeutrAvidin-binding buffer.

21| Add the sample solution from Step 19 to the washed NeutrAvidin resin from Step 20.

■ **PAUSE POINT** Allow binding of biotinylated proteins to NeutrAvidin by incubating overnight (12–16 h) at 4 °C with constant agitation.

22| Spin down the resin at 2,000g for 5 min at 4 °C. Remove the supernatant carefully from the resin; preserve 30 µl of the supernatant for subsequent western blot analysis ("supernatant"); immediately add 10 µl of 4× SDS sample buffer and store at –20 °C until further use (1–2 weeks).

23| Wash resin with ten bed volumes of NW-A buffer for 10 min at RT with constant agitation, spin down (2,000g for 5 min at 4 °C) and discard the supernatant; repeat two more times.

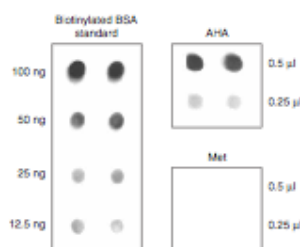


Figure 2 | Dot blot analysis of AHA versus Met-treated samples. Dot blot analysis provides a mid-procedure demonstration of proper copper(I)-catalyzed tagging as well as a crude estimate of the amount of tagged protein in the sample. Duplicates of each condition are shown. The dot blot membrane was probed with an anti-biotin antibody.

PROTOCOL

24] Wash resin two times with NW-B buffer followed by two washes with 1× PBS in the same manner as above.

25] Wash resin two times with 50 mM ammonium bicarbonate as before, then transfer the resin to a microcentrifuge tube using a cut tip with a bigger opening. Spin down the resin (4,000g for 5 min at 4 °C). Carefully remove the supernatant. Note that researchers could alternatively proceed with SDS elution of NeutrAvidin-bound proteins followed by one-dimensional gel electrophoresis and appropriate in-gel trypsinization and tandem MS instead of MudPIT analysis, thus adapting to a particular laboratory's individual MS instrumentation environment.

26] For each initial 100 µl of Neutravidin slurry, resuspend the resin to a total volume of 87 µl in 50 mM ammonium bicarbonate. This "reduced" volume is to compensate for the later volume gain caused by dissolving urea in Step 28.

27] Heat the suspension for 10 min at 70 °C while agitating the beads using the Thermomixer.

28] Immediately, add 18 mg of urea beads for each initial 100 µl of Neutravidin slurry to the suspension and vortex the suspension until the beads have been dissolved. The final concentration of urea should be between 2 and 3 M to facilitate trypsinization of the partially denatured NeutrAvidin-bound proteins. Note that the biotin–NeutrAvidin interaction is stable at urea concentrations as high as 8 M.

29] Allow the suspension to cool down to RT before adding the reducing agent TCEP to a final concentration of 3.125 mM (for each 100 µl suspension, add 0.625 µl of 0.5 M TCEP) to reduce disulfide bonds. Incubate for 30 min at RT with constant agitation.

30] Alkylate reduced cysteine residues by adding iodoacetamide to a final concentration of 11.2 mM (for each 100 µl of suspension, add 2.25 µl of 0.5 M iodoacetamide). Incubate for 30 min at RT in the dark with constant agitation. This alkylation step is necessary for the identification of cysteine-containing peptides, promoting maximal possible sequence coverage of BONCAT-labeled candidate proteins.

31] Transfer a small aliquot (30–50 µl) of the suspension to a microcentrifuge tube for subsequent western blot analysis ("NeutrAvidin-bound proteins"). Spin down, remove the supernatant, add 20 µl of 4× SDS sample buffer and store at –20 °C until further use (1–2 weeks).

32] Add 0.1 µg endoproteinase Lys-C per 100 µl of suspension to initiate proteolysis and incubate for 4 h at 37 °C while agitating the beads. Lys-C cleaves at the C-terminal end of lysine and the resulting peptides are larger than tryptic peptides.

33] Add calcium chloride to a final concentration of 0.1 mM and trypsinize the sample adding 1 µg trypsin per 100 µl of suspension.

■ **PAUSE POINT** Incubate the reaction mixture overnight at 37 °C while agitating the beads.

34] Transfer the suspension to an empty spin column in a microcentrifuge tube. Briefly pulse-spin to separate the supernatant containing the tryptic peptides from the resin. Add formic acid to a final concentration of 5% (v/v) to the peptide solution and store at –20 °C until further use.

■ **PAUSE POINT** Samples can be stored at –20 °C for 1–2 weeks.

35] Transfer the resin back into a microcentrifuge tube and resuspend it in 50 mM ammonium bicarbonate. The total volume of the suspension should be the same as for the proteolytic digestion (see Step 31). Transfer the same aliquot as in Step 31 of this suspension to a microcentrifuge tube for subsequent western blot analysis ("NeutrAvidin after trypsinization"). Spin down, remove the supernatant, add 4× SDS sample buffer and store at –20 °C until further use (1–2 weeks).

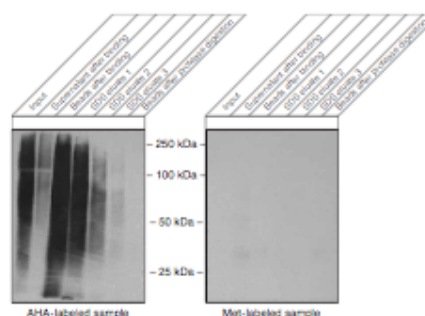


Figure 3 | Western blot analysis of AHA versus Met-treated sample purification fractions. Upon completing the procedure, a western blot analysis of the various collected fractions will reflect the efficiency of the purification and subsequent trypsinization. The western blot membrane was probed with an anti-biotin antibody.

PROTOCOL

36 Perform analysis of the samples collected in Steps 19, 22, 31 and 35 using the standard western blot technique to evaluate the purification and trypsinization efficiency using a biotin antibody. A typical example of western blot is shown in **Figure 3**.

Mass spectrometrical analysis • TIMING 2 days

37 We use MudPIT^{41,42} as a shotgun proteomics approach for the identification of peptides in complex mixtures generated with BONCAT. Alternatively, researchers may wish to use either a gel-based proteomics technique (in which case, NeutrAvidin-bound proteins are eluted from the resin after Step 25) or a separate cation exchange and reverse-phase chromatography. A step-by-step MudPIT protocol has been described in detail elsewhere^{4,30}; therefore, the following section is focusing on the search parameters necessary for the identification of AHA- and d₁₀L-modified peptides.

38 Search the tandem mass spectra against a protein sequence database using the SEQUEST algorithm. The following dynamic modification search parameters should be considered for the methionine residue (see **Figure 4**): After complete tag cleavage, the mass gain of tagged AHA over methionine is 107 AMU (atomic mass unit). In the case of incomplete tag cleavage, the resulting mass gain of tagged AHA over methionine is 695.6 AMU (with no further fragmentation of the tag moiety required), whereas in the event of failed tagging (unligated AHA), the mass loss of AHA over methionine would be 5.1 AMU. A set of stringent search constraints including the fully tryptic status of each peptide, a minimum of two valid peptides per locus and a minimum of one peptide containing an AHA-derived or d₁₀L modification, are required to ensure that identified proteins were translated during the AHA labeling step. Sample spectra can be found as supplementary material of Dieterich *et al.*²⁰ online under <http://www.pnas.org/cgi/content/full/0601637103/DC1>.

• TIMING

Cell labeling

Steps 1 and 2, 1 h

Step 3, Variable, that is, experiment dependent

Steps 4–5, 20 min

Click chemistry reaction

Steps 6–11, 30 min

Step 12, Variable: 6–16 h, depending on incubation temperature

Step 13, 10 min

Dot blot analysis, Steps 14–17, 5 h

Neutravidin purification

Steps 18 and 19, 10 min

Step 20, 20 min

Step 21, 12–16 h (overnight)

Steps 22–25, 2.5 h

On-resin trypsinization

Steps 26–31, 1.5 h

Step 32, 4 h

Step 33, 12–16 h (overnight)

Step 34, 10 min

Step 35, 10 min

Step 36, 8 h

Mass spectrometrical analysis, Steps 37 and 38, 2 days

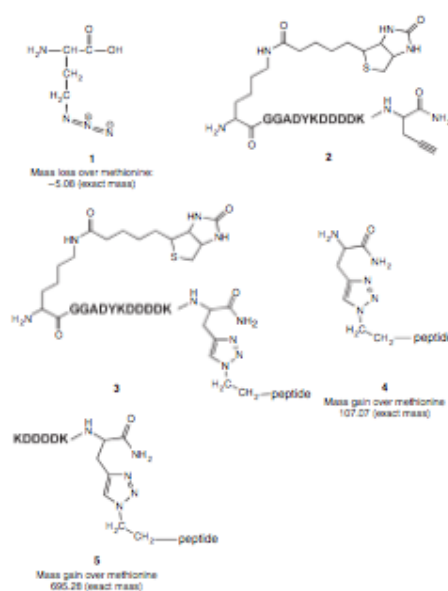


Figure 4 | Structure of AHA-based modifications. (1) Unligated AHA, (2) unligated affinity tag, (3) affinity tag coupled to AHA before trypsinization, (4) remaining moiety after complete trypsinization and (5) remaining moiety after one missed cleavage.

7 TROUBLESHOOTING

Troubleshooting advice can be found in **Table 1**.

TABLE 1 | Troubleshooting table.

Steps	Problem	Possible reason	Solution
6	Incomplete cell lysis	Detergent concentration insufficient Total protein concentration too high Insufficient genomic DNA lysis	Increase detergent concentration up to 2% (w/v) SDS Increase sample volume Use more Benzonase to facilitate lysis of genomic DNA or shear DNA with a syringe and a needle
12	Failed click chemistry reaction	Too much detergent present Ineffective triazole ligand Bad quality of copper (I) bromide suspension pH too low	Lower detergent concentration Prepare fresh triazole ligand Use fresh copper (I) bromide Check pH of the solution and adjust to > pH 7.5
17	Low levels of tagged proteins	Failed click chemistry reaction Labeling time too short	See "Problem Step 12" Increase incubation time with AHA

ANTICIPATED RESULTS

Following a 2 h incubation time with AHA/d₁₀L and using 1.8–2.1 mg of whole mammalian cell lysates, approximately 150–200 µg of biotinylated protein is tagged with BONCAT for subsequent NeutrAvidin purification and tandem MS analysis. From these, about 200 valid candidates containing either AHA- or d₁₀L-based modified peptides can be identified with a Thermo Finnigan LCQ mass spectrometer in a shotgun approach, such as MudPIT. The use of new mass spectrometers with higher sensitivity, faster sequencing speed and higher dynamic range promises to increase the number of identifications. The rate of protein synthesis may vary from cell line to cell line and between cell lines, primary cultures and organotypic slice cultures (unpublished observations).

ACKNOWLEDGMENTS We thank S.A. Kim and E.H. Friedrich for critical reading of the manuscript. This work was supported by the Howard Hughes Medical Institute, the Beckman Institute at the California Institute of Technology and NIH (R2104020589 to E.M.S.), MS analysis was performed at the MS facility of the laboratory of R.J. Deshaies (Howard Hughes Medical Institute, Caltech), which is supported by the Beckman Institute at Caltech and a grant from the Department of Energy to R.J.D. and Barbara J. Wold. D.C.D. is supported by the German Academy for Natural Scientists Leopoldina (BMBF-IP09901/8-95). J.G. was supported by R.J. Deshaies through Howard Hughes Medical Institute funds. A.J.L. was supported by a National Science Foundation Graduate Research Fellowship.

COMPETING INTERESTS STATEMENT The authors declare that they have no competing financial interests.

Published online at <http://www.natureprotocols.com>
Reprints and permissions information is available online at <http://npg.nature.com/reprintsandpermissions>

- Pandey, A. & Mann, M. Proteomics to study genes and genomes. *Nature* **405**, 837–846 (2000).
- de Godoy, L. et al. Status of complete proteome analysis by mass spectrometry: SILAC labeled yeast as a model system. *Genome Biol.* **7**, R50 (2006).
- Mootha, V.K. et al. Integrated analysis of protein composition, tissue diversity, and gene regulation in mouse mitochondria. *Cell* **115**, 629–640 (2003).
- Andersen, J.S. et al. Nucleolar proteome dynamics. *Nature* **433**, 77–83 (2005).
- Collins, M.O. et al. Molecular characterization and comparison of the components and multiprotein complexes in the postsynaptic proteome. *J. Neurochem.* **97** (suppl. 1): 16–23 (2006).
- Schirmpf, S.P. et al. Proteomic analysis of synaptosomes using isotope-coded affinity tags and mass spectrometry. *Proteomics* **5**, 2531–2541 (2005).
- Gavin, A.C. et al. Functional organization of the yeast proteome by systematic analysis of protein complexes. *Nature* **415**, 145–147 (2002).
- Ho, Y. et al. Systematic identification of protein complexes in *Saccharomyces cerevisiae* by mass spectrometry. *Nature* **415**, 180–183 (2002).
- Chang, E.J., Archambault, V., McLachlin, D.T., Knutchinsky, A.N. & Chait, B.T. Analysis of protein phosphorylation by hypothesis-driven multiple-stage mass spectrometry. *Anal. Chem.* **76**, 4472–4483 (2004).
- Garcia, B.A., Shabanowitz, J. & Hunt, D.F. Analysis of protein phosphorylation by mass spectrometry. *Methods* **35**, 256–264 (2005).
- Peters, E.C., Brock, A. & Ficarro, S.B. Exploring the phosphoproteome with mass spectrometry. *Mini Rev. Med. Chem.* **4**, 313–324 (2004).
- Mann, M. & Jensen, O.N. Proteomic analysis of post-translational modifications. *Nat. Biotechnol.* **21**, 255–261 (2003).
- Xu, P. & Peng, J. Dissecting the ubiquitin pathway by mass spectrometry. *Biochim. Biophys. Acta* **1764**, 1940–1947 (2006).
- Freeman, W.M. & Hemby, S.E. Proteomics for protein expression profiling in neuroscience. *Neurochem. Res.* **29**, 1065–1081 (2004).
- Lilley, K.S. & Friedman, D.B. All about DIGE: quantification technology for differential-display 2D-gel proteomics. *Expert Rev. Proteomics* **1**, 401–409 (2004).
- Gygi, S.P. et al. Quantitative analysis of complex protein mixtures using isotope-coded affinity tags. *Nat. Biotechnol.* **17**, 994–999 (1999).
- Ross, P.L. et al. Multiplexed protein quantitation in *Saccharomyces cerevisiae* using amine-reactive isobaric tagging reagents. *Mol. Cell. Proteomics* **3**, 1154–1169 (2004).
- Washburn, M.P., Ulaszek, R., Deciu, C., Schieltz, D.M. & Yates, J.R., 3rd. Analysis of quantitative proteomic data generated via multidimensional protein identification technology. *Anal. Chem.* **74**, 1650–1657 (2002).
- Ong, S.E. et al. Stable isotope labeling by amino acids in cell culture, SILAC, as a simple and accurate approach to expression proteomics. *Mol. Cell. Proteomics* **1**, 376–386 (2002).
- Dieterich, D.C., Link, A.J., Goumann, J., Timell, D.A. & Schuman, E.M. Selective identification of newly synthesized proteins in mammalian cells using bioorthogonal noncanonical amino acid tagging (BONCAT). *Proc. Natl. Acad. Sci. USA* **103**, 9482–9487 (2006).
- Prescher, J.A. & Bertozzi, C.R. Chemistry in living systems. *Nat. Chem. Biol.* **1**, 13–21 (2005).
- Griffin, R.J. The medicinal chemistry of the azido group. *Prog. Med. Chem.* **31**, 121–232 (1994).
- Kho, Y. et al. A tagging-via-substrate technology for detection and proteomics of farnesylated proteins. *Proc. Natl. Acad. Sci. USA* **101**, 12479–12484 (2004).



PROTOCOL

24. Klück, K.L., Saxon, E., Tirrell, D.A. & Bertozzi, C.R. Incorporation of azides into recombinant proteins for chemoselective modification by the Staudinger ligation. *Proc. Natl. Acad. Sci. USA* **99**, 19–24 (2002).
25. Link, A.J. & Tirrell, D.A. Cell surface labeling of *Escherichia coli* via copper(I)-catalyzed [3+2] cycloaddition. *J. Am. Chem. Soc.* **125**, 11164–11165 (2003).
26. Link, A.J., Vink, M.K. & Tirrell, D.A. Presentation and detection of azide functionality in bacterial cell surface proteins. *J. Am. Chem. Soc.* **126**, 10598–10602 (2004).
27. Luchansky, S.J., Goon, S. & Bertozzi, C.R. Expanding the diversity of unnatural cell-surface sialic acids. *ChemBiochem* **5**, 371–374 (2004).
28. Luchansky, S.J. et al. Constructing azide-labeled cell surfaces using polysaccharide biosynthetic pathways. *Methods Enzymol.* **362**, 249–272 (2003).
29. Mahal, L.K., Yarema, K.J. & Bertozzi, C.R. Engineering chemical reactivity on cell surfaces through oligosaccharide biosynthesis. *Science* **276**, 1125–1128 (1997).
30. Saxon, E. et al. Investigating cellular metabolism of synthetic azidosugars with the Staudinger ligation. *J. Am. Chem. Soc.* **124**, 14893–14902 (2002).
31. Rostovtsev, V.V., Green, L.G., Fokin, V.V. & Sharpless, K.B. A stepwise Huisgen cycloaddition process: copper(I)-catalyzed regioselective “ligation” of azides and terminal alkynes. *Angew. Chem., Int. Ed.* **41**, 2596–2599 (2002).
32. Mangold, J.B., Mischke, M.R. & LaVoie, J.M. Azidoalanine mutagenicity in *Salmonella*: effect of homologation and alpha-methyl substitution. *Mutat. Res.* **216**, 27–33 (1989).
33. Wang, Q. et al. Bioconjugation by copper(I)-catalyzed azide-alkyne [3 + 2] cycloaddition. *J. Am. Chem. Soc.* **125**, 3192–3193 (2003).
34. Eng, J., McCormack, A.L. & Yates, A.J. An approach to correlate tandem mass spectral data of peptides with amino acid sequences in a protein database. *J. Am. Soc. Mass Spectrom.* **5**, 976–989 (1994).
35. Perkins, D.N., Pappin, D.J., Creasy, D.M. & Cottrell, J.S. Probability-based protein identification by searching sequence databases using mass spectrometry data. *Electrophoresis* **20**, 3551–3567 (1999).
36. Craig, R. & Beavis, R.C. TANDEM: matching proteins with tandem mass spectra. *Bioinformatics* **20**, 1466–1467 (2004).
37. Fenyo, D. & Beavis, R.C. A method for assessing the statistical significance of mass spectrometry-based protein identifications using general scoring schemes. *Anal. Chem.* **75**, 768–774 (2003).
38. Tabb, D.L., McDonald, W.H. & Yates, J.R., 3rd. DTASelect and contrast: tools for assembling and comparing protein identifications from shotgun proteomics. *J. Proteome Res.* **1**, 21–26 (2002).
39. Keller, A., Nesvizhskii, A.I., Kolker, E. & Aebersold, R. Empirical statistical model to estimate the accuracy of peptide identifications made by MS/MS and database search. *Anal. Chem.* **74**, 5383–5392 (2002).
40. Nesvizhskii, A.I., Keller, A., Kolker, E. & Aebersold, R. A statistical model for identifying proteins by tandem mass spectrometry. *Anal. Chem.* **75**, 4646–4658 (2003).
41. Link, A.J. et al. Direct analysis of protein complexes using mass spectrometry. *Nat. Biotechnol.* **17**, 676–682 (1999).
42. Washburn, M.P., Wolters, D. & Yates, J.R., 3rd. Large-scale analysis of the yeast proteome by multidimensional protein identification technology. *Nat. Biotechnol.* **19**, 242–247 (2001).
43. Schieltz, D.M. & Washburn, M.P. Analysis of complex protein mixtures using multidimensional protein identification technology (MuDPIT). *Cold Spring Harbor Protocols* 2006 (doi:10.1101/pdb.prot4555).

